ALKALI ACTIVATION AND NATURAL FIBER REINFORCEMENT OF TERMITE MOUND SOIL FOR SUSTAINABLE, LOW COST AND ENVIRONMENTALLY FRIENDLY CONSTRUCTION MATERIALS

Dissertation

Submitted to the Department of Materials Science and Engineering
African University of Science and Technology, Abuja- Nigeria
in Partial Fulfillment of the Requirements for the
Award of the Degree of
Doctor of Philosophy

in the Department of Materials Science and Engineering
African University of Science and Technology, Abuja- Nigeria

ASSIA ABOUBAKAR MAHAMAT (ID No: 70156)

MATERIALS SCIENCE AND ENGINEERING

April 2021

ALKALI ACTIVATION AND NATURAL FIBER REINFORCEMENT OF TERMITE MOUND SOIL FOR SUSTAINABLE, LOW COST AND ENVIRONMENTAL-FRIENDLY CONSTRUCTION MATERIALS

By

Assia ABOUBAKAR MAHAMAT

A THESIS APPROVED BY THE DEPARTMENT OF MATERIALS SCIENCE AND ENGINEERING

RECOMMENDED: …… ……

Supervisor: Prof. Holmer SAVASTANO Jr.

…… ……

Co-Supervisor: Dr. Salifu Tahiru AZEKO,

……

Head of the Department of the Material Science and Engineering, AUST.

Approved: .....

Vice President, Academics

Date: .....

ABSTRACT

In the construction field, development of green, sustainable and renewable materials is the main focus of research. In that direction, alkali activation technique has attracted a lot of attention in the past few years. The alkali activation technique consists of activating aluminosilicates materials under alkaline conditions. To limit the risk of toxicity or exposure to high alkaline solution and eco-friendly concerns, One-part alkali activation is considered in this study. Besides, the application of this technique to optimize earth-based materials implies the production of robust earth-based bio-composites. However, termite mound soil is an earth-based material which has not been investigated sufficiently as a construction material. This study provides enlightenment on the application of one-part alkali activation of termite mound soil. The effects of the activator's concentration, curing conditions, curing temperature on the specimens were appraised. The bio-composite was manufactured through mechanical compaction technique to obtain closely packed specimens. Fiber reinforcement was used as a strengthening and toughening process. The physical, macro-microstructural and mechanical properties were investigated to correlate between the microstructure and bulk properties. Results have shown improved mechanical properties after the alkaline activation. Furthermore, the dimensional stability of the specimens after the alkaline activation was satisfactory compared to the inactivated termite mound soil. Inclusion of the natural fiber impacted positively the mechanical properties of the bio-composite via crack propagation's limitations within the termite mound soil-based matrix as the compressive strength increased after fiber's inclusion. Furthermore, the Machine Learning techniques used to predict the compressive strength of the alkali activated termite mound soil based were successful confirming the right selection of the factors affecting the compressive strength. These Machine Learning approaches would reduce cost and time for the laboratory experiments and also predict the desired properties based on the mixtures required. The implications of these results are considered for the development of low-cost housing. Especially in regions with high housing demand but without accessibility to conventional building materials. Moreover, the results are analyzed as eco-friendly, renewable and sustainable prospective construction materials requiring effortless techniques to be replicated at the industrial scale. This investigation has demonstrated the feasibility of transforming termite mound soil and natural waste into sustainable construction materials to be easily industrialized.

Keywords: Termite mound soil, Borassus fruit natural fiber, one-part alkali activated termite mound soil, natural fiber reinforced termite mound soil-based bio-composite.

DEDICATION

This thesis is dedicated to Aboubakar Mahamat Tideye's family for their numerous efforts in my academic career and especially to my husband Prof. Moussa Mahamat Boukar. May Allah (SWT) continue to strengthen us (Ameen).

ACKNOWLEDGEMENTS

I would like to express my gratitude to the World Bank, The African Development Bank (AfDB), African Centers of Excellence (ACE) Program, the Nelson Mandela Institution, the Pan African Materials Institute (PAMI) and the African University of Science and Technology (AUST), Abuja, for financial support.

I would like to thank my supervisor Prof. Holmer Savastano Jr. for his guidance and educative comments. I also want to thank my committee members Prof. Peter Azikiwe Onwualu, Prof. Ali Nordine Leklou and Dr. Salifu Tahiru Azeko for their enlightening comments.

I also extend my sincere acknowledgement to the Multifunctional Materials Research Group at the African University of Science and Technology, Abuja-Nigeria, the staff of the civil engineering laboratory of the Nile University of Nigeria, Abuja-Nigeria and the staff of the Institut de Recherche en Génie Civil et Mécanique (GeM) équipe de recherche Interactions Eau-Géomatériaux (IEG), Saint Nazaire-France for their care and useful suggestions.

Finally, I would like to thank singularly my husband Prof. Moussa Mahamat Boukar for his support and encouragements. To my children for their patience during the whole program and to my parents, brothers and sisters for believing in my ability to complete this program.

PREFACE

This dissertation is an original intellectual property of Assia Aboubakar Mahamat containing work done from the period of June 2018 to April 2021 for the fulfillment of Doctor of Philosophy degree in the Department of Materials Science and Engineering at the African University of Science and Technology, Abuja-Nigeria.

I was the lead investigator, and the related activities were accomplished by me. Those activities including concept formation, data collection, experiments, data analysis as well as manuscript preparation and were executed under the supervision of Prof. Holmer Savastano Jr.

In this work, the mechanical properties of termite mound soil were presented. The termite mound soil is a local earth-based material that's abundantly available, henceforth collected to design bio-composite sustainable building units. The bio-composite is comprised of the termite mound soil and natural Borassus fruit fiber. They were produced using the concept of alkaline activation technology.

At the time this dissertation was submitted, two of its chapters (3 and 4) were published in the Buildings-MDPI journal and Heliyon-Elsevier journal respectively. The chapter 5 is under review in Applied science journal from MDPI, while chapter 6 is in the manuscript write up process.

TABLE OF CONTENT

Table of Contents

LIST OF FIGURES

LIST OF TABLES

Peer Review Publications in PhD Focus

1. **Mahamat, A. A**.; Bih, N.L.; Ayeni, O.; Onwualu, P.A.; Savastano Jr., H.; Soboyejo, W.O. "Development of Sustainable and Eco-friendly Materials from Termite Hill Soil Stabilized with Cement for Low-Cost Housing in Chad". *Buildings* **2021**, *11*, https://doi.org/ 10.3390/buildings11030086
2. **Assia Aboubakar Mahamat**, Ifeyinwa Ijeoma Obianyo, Blasuis Ngayakamo, Numfor Linda Bih, Olugbenga Ayeni, Salifu T. Azeko, Holmer Savastano, "Alkali activation of compacted termite mound soil for eco-friendly construction materials".Heliyon,Volume7,Issue3,2021,https://doi.org/10.1016/j.heliyon.2021.e06597.
3. Linda Bih,N; **Aboubakar Mahamat, A**. Hounkpe Bidossessi,J.; Azikiwe Onwualu,P. ; Boakye,E.E.. "the effect of polymer waste addition on the compressive strength and water absorption of geopolymer ceramics. Appl. Sci. 2021, 11, 3540. https://doi.org/10.3390/app11083540
4. Machine Learning approaches for prediction of the compressive strength of alkali activated termite mound soil (under review).
5. Obianyo, I.I.; **Mahamat, A.A**,; Anosike-Francis, E. N.; Stanislas, T.T.; Onyelowe, K.C.; Onwualu, A.P.; Soboyejo, A.B.O. "Performance of lateritic soil stabilized with combination of bone and palm bunch ash for sustainable building applications". Cogent Eng, (Accepted on the 3rd February 2021). https://doi.org/10.1080/23311916.2021.1921673.

List of Conference Proceedings/Book of Abstract

1. Mahamat, A. A.; Bih, N.L., Savastano Jr . Optimization of termite mound soil through alkali activation and cement stabilisation for sustainable and eco-friendly construction materials. 1st International Conference on Multidisciplinary Engineering and Applied Science (ICMEAS2021), Abuja, Nigeria.

1.0 Chapter One: Introduction

1. Introduction

This chapter briefly outlines the advantages of the using of earth-based material especially termite mound soil in construction. These advantages are observed in terms of eco-friendliness, availability, durability, strength and low cost. It focuses also on the binding technologies namely the alkali activation used to efficiently improve the binding mechanisms of the termite mound soil. The fiber reinforcement used to improve its mechanical properties is also discussed in this chapter. Unanswered questions originated from the use of the optimization's technologies are examined. The objectives and thesis's set up are presented at the end of this chapter.

2. Motivations and unresolved issues

According to estimates by UN-Habitat, approximately 238 million people lived in slums or informal settlements in Sub-Saharan Africa (SSA) only in 2018[1]. These figures indicate the precarious conditions in some regions. Subsequently, the low-life expectancy, poor heath indices, low indices of wellbeing in these regions are affected because housing is a major fundamental need for humans, and it constitutes the main factor for its survival and its development.

Globally, the construction field is facing major concerns about the carbon emissions in the atmosphere. These emissions are associated with the production of cement which is typically used for construction of buildings across the world [2], constituting about 7% of global CO_2 emissions [3][4]. In addition, conventional construction materials are very expensive and almost inexistent in some regions. For instance, in some regions limitations such as geographical constraints and scarcity of manufacturing industries make conventional construction materials very inaccessible hence very costly. Hence, effort must be directed towards the development of alternative building materials that are eco-friendly and cost effective[5] [6] and can reduce the overall use of cement in buildings [2][7], eco-friendly and available locally at low cost. The efforts must be developed to attain the global sustainable development goals (SDGs), goal 11 being the target. Within this context, earth-based materials are "green" materials that can reduce carbon emissions[8] that are associated with the construction materials. Earth based materials possess attractive mechanical properties, henceforth, their production as construction materials requires low

amount of energy and their maintenance during their life service doesn't require high amount of energy either. The use of earth-based materials in construction is old as the beginning of mankind [9]. However, cost [10], availability[11] and performances[12] (Strength, toughness and hygroscopicity) are the fundamental requirements for construction materials selection for construction applications. Hence, a deep understanding of termite mound soil's fundamentals is required to examine the binding mechanism making it a suitable construction material.

Presently, considerable progress has been made in terms of application of fiber reinforcement in earth-based materials[13]–[17] but very insufficient in the case of the termite mound soil[18]–[20]. Most of the studies carried out on the termite mound soil examined its application as stabilisation or partial replacement to cement without correlating its microstructure to its bulk properties. On the other hand, studies focused on using the termite's secretions as binder earthen road construction[21], [22]. Some commercialized products have been manufactured and are already in the market. However, to the author's knowledge there is not any existing literature on the use of one-part alkali activation of termite mound soil reinforced with Borassus fruit natural fiber.

3. Objectives

Termite mound soil is an earth-based material that has not been fully investigated but used empirically. The science underlying its binding mechanism would lead to its use efficiently as a construction material. This is because; it allows us to understand the effect of each variable on the desired bulk properties. This study explored the development of novel palmyra natural fiber reinforcement termite mound soil-based bio-composite by benefiting from the alkali activation of the termite mound soil to manufacture the specimens. The effect of the processing on the novel designed bio-composite was appraised through mechanical compaction technique. The investigation involved experimental and computer-based prediction techniques. These computer-based techniques implied the use of Artificial Intelligence methods for the predictions of the mechanical properties of alkali activated termite mound soil. This investigation is aimed to:

- Gain clear understanding of termite mound soil properties, as these properties define its performances. The targeted properties are the microstructural

(mineralogy, morphology and binding mechanism), physical and macrostructural (mechanical) properties.

- Apprehend the termite mound soil's microstructure to enable engineering other aluminosilicates into materials similar to the termite mound soil in regions where there are no termite hills.
- Examine the effect of factors such as initial curing temperature, curing conditions, activator concentration on the examined properties of the alkali activated termite mound soil.
- Evaluate the effect of fiber content on the physical, microstructural and macrostructural behavior of the compacted alkali activated termite mound soil.
- The development of low cost and environmentally friendly materials for sustainable construction from agricultural waste (palmyra natural fiber) plus termite mound soil through optimisation technologies that are cost friendly and easily performed. Therefore, the strengthening and toughening technologies used in these investigations don't require expensive instruments to be produced at large scale.
- Artificial Intelligence techniques were used to predictions the performances of the composite under variations of factors affecting the mechanical properties.
- The study was carried out in the sub-Saharan African region and could be replicated in most tropical climates worldwide. As based on that the techniques were carefully selected to not restrict the investigation to only one specific region. Henceforth, the feasibility of the investigation worldwide. The industrial manufacturing of the designed Bio-composite will reduce the numbers of people living in slums therefore it will increase productivity, welfare and create local jobs.

This study focuses on the development of low cost, eco-friendly and sustainable construction materials using sub-Saharan African as a case study. The results have shown the possibilities to replicate these techniques worldwide.

4. Thesis layout

The thesis is subdivided into seven (7) chapters that are mainly focused on papers that have been published or submitted to peer review journals.

Chapter two presents the literature review with a focus on termite mound soil and palmyra ethiopium natural fiber. It provides a brief description of the techniques of characterizations used alkali activation and natural fiber reinforcement.

Chapter three provides the properties of the termite mound soil from the microstructure to the macrostructure confirming its utilization as an ecofriendly and low-cost construction material.

Chapter four resolves the effect of natural potash used as alkaline activator. The effects of the natural potash on the termite mound soil were investigated based on alkali activation under various temperatures.

Chapter five presents the Artificial Intelligence techniques used for the prediction of the mechanical properties of the alkali activated termite soil. The prediction is aimed to ease the understanding of the alkali activated termite soil under various conditions.

Chapter six presents the palmyra ethiopium natural fiber reinforcement of one-part alkali activated termite mound soil-based bio-composite. The natural fiber was used as reinforcement in the one-part alkali activated termite mound based-soil bio-composite to assess its effect on the mechanical properties of the bio-composite.

Lastly, chapter seven presents the focal conclusions emerged from the investigation in addition to focusing on the suggestions for future work.

References

[1] United Nations Statistics Division (UNSD) and Division of the Department of Economic and Social Affairs (DESA)., "Make cities and human settlements inclusive, safe, resilient and sustainable," Accessed: Nov. 06, 2020. [Online]. Available: https://unstats.un.org/sdgs/report/2019/goal-11/.

[2] M. R. Karim, M. M. Hossain, M. N. N. Khan, M. F. M. Zain, M. Jamil, and F. C. Lai, "On the utilization of pozzolanic wastes as an alternative resource of cement," *Materials*, vol. 7, no. 12, pp. 7809–7827, 2014, doi: 10.3390/ma7127809.

[3] T. Kim, S. Tae, C. U. Chae, and K. Lee, "Proposal for the evaluation of eco-efficient concrete," *Sustainability (Switzerland)*, vol. 8, no. 8, Jul. 2016, doi: 10.3390/su8080705.

[4] H. Zhang *et al.*, “Air pollution and control action in Beijing,” *Journal of Cleaner Production*, vol. 112. Elsevier Ltd, pp. 1519–1527, Jan. 20, 2016, doi: 10.1016/j.jclepro.2015.04.092.

[5] R. Pode, “Potential applications of rice husk ash waste from rice husk biomass power plant,” *Renewable and Sustainable Energy Reviews*, vol. 53. Elsevier Ltd, pp. 1468–1485, Jan. 01, 2016, doi: 10.1016/j.rser.2015.09.051.

[6] M. Bediako, “Pozzolanic potentials and hydration behavior of ground waste clay brick obtained from clamp-firing technology,” *Case Studies in Construction Materials*, vol. 8, pp. 1–7, Jun. 2018, doi: 10.1016/j.cscm.2017.11.003.

[7] K. H. Mo, U. J. Alengaram, M. Z. Jumaat, S. P. Yap, and S. C. Lee, “Green concrete partially comprised of farming waste residues: A review,” *Journal of Cleaner Production*, vol. 117. Elsevier Ltd, pp. 122–138, Mar. 20, 2016, doi: 10.1016/j.jclepro.2016.01.022.

[8] S. A. Memon, I. Wahid, M. K. Khan, M. A. Tanoli, and M. Bimaganbetova, “Environmentally friendly utilization of wheat straw ash in cement-based composites,” *Sustainability (Switzerland)*, vol. 10, no. 5, May 2018, doi: 10.3390/su10051322.

[9] R. Eires, A. Camões, and S. Jalali, “Ancient materials and techniques to improve the earthen building durability,” in *Key Engineering Materials*, 2015, vol. 634, pp. 357–366, doi: 10.4028/www.scientific.net/KEM.634.357.

[10] A. A. Mahamat, N. Linda Bih, O. Ayeni, P. Azikiwe Onwualu, H. Savastano, and W. Oluwole Soboyejo, “Development of Sustainable and Eco-Friendly Materials from Termite Hill Soil Stabilized with Cement for Low-Cost Housing in Chad,” *Buildings*, vol. 11, no. 3, p. 86, Feb. 2021, doi: 10.3390/buildings11030086.

[11] “Climate Change Science: A Modern Synthesis.”

[12] W. O. Soboyejo, *Mechanical properties of engineered materials*. Marcel Dekker, 2003.

[13] E. B. Ojo *et al.*, “Mechanical performance of fiber-reinforced alkali activated un-calcined earth-based composites,” *Construction and Building Materials*, vol. 247, Jun. 2020, doi: 10.1016/j.conbuildmat.2020.118588.

[14] A. Megalingam, M. Kumar, B. Sriram, K. Jeevanantham, and P. Ram Vishnu, “Borassus fruit fiber reinforced composite: A review,” *Materials Today: Proceedings*, Mar. 2020, doi: 10.1016/j.matpr.2020.02.750.

[15] Z. Li, L. Wang, and X. Wang, “Cement composites reinforced with surface modified coir fibers,” *Journal of Composite Materials*, vol. 41, no. 12, pp. 1445–1457, Jun. 2007, doi: 10.1177/0021998306068083.

[16] H. Savastano, A. Turner, C. Mercer, and W. O. Soboyejo, “Mechanical behavior of cement-based materials reinforced with sisal fibers,” in *Journal of Materials Science*, Nov. 2006, vol. 41, no. 21, pp. 6938–6948, doi: 10.1007/s10853-006-0218-1.

[17] K. Mustapha, E. Annan, S. T. Azeko, M. G. Zebaze Kana, and W. O. Soboyejo, “Strength and fracture toughness of earth-based natural fiber-reinforced composites,” *Journal of Composite Materials*, vol. 50, no. 9, pp. 1145–1160, 2016, doi: 10.1177/0021998315589769.

[18] A. van Huis, “Cultural significance of termites in sub-Saharan Africa,” *Journal of Ethnobiology and Ethnomedicine*, vol. 13, no. 1, Jan. 2017, doi: 10.1186/s13002-017-0137-z.

[19] T. Nwakonobi, C. Anyanwu, and L. Tyav, “Effects of rice husk ash and termite hill types on the physical and mechanical properties of burnt termite clay bricks for rural housing,” *Global Journal of Pure and Applied Sciences*, vol. 20, no. 1, p. 57, 2015, doi: 10.4314/gjpas.v20i1.9.

[20] R. K. Kandasami, R. M. Borges, and T. G. Murthy, “Effect of biocementation on the strength and stability of termite mounds,” *Environmental Geotechnics*, vol. 3, no. 2, pp. 99–113, Apr. 2016, doi: 10.1680/jenge.15.00036.

[21] A. A. R. Corrêa, L. Bufalino, T. de Paula Protásio, M. X. Ribeiro, D. Wisky, and L. M. Mendes, “Evaluation of mechanical properties of adobe chemically stabilized with ‘synthetic termite saliva,’” in *Key Engineering Materials*, 2014, vol. 600, pp. 150–155, doi: 10.4028/www.scientific.net/KEM.600.150.

[22] O. B. Faria, R. A. G. Battistelle, and C. Neves, “Influence of the addition of ‘synthetic termite saliva’ in the compressive strength and water absorption of compacted soil-

cement," *Ambiente Construído*, vol. 16, no. 3, pp. 127–136, Sep. 2016, doi: 10.1590/s1678-86212016000300096.

2.0 Chapter Two: Literature review

1. Introduction

In this section, the hypothesis on the development of termite mound soil is briefly introduced. The engineering properties of termite mound soil and its limitations as a construction material are the focal points of this investigation. Consequently, modern and ecofriendly technologies have been used to improve its major limitations[1]. Hence, attention is given to these technologies namely alkali activation and fiber reinforcement to strengthen and toughen the termite mound soil[2]. A brief description of the characterization techniques used in the examination of the various modifications made from the optimizations technologies is presented. Computer based tool are preferably used to predict accurately the properties of the termite mound soil under various mixtures [3]. This is achieved in the aim of reducing time and cost during the experimental stages to minimize error. Therefore, Artificial Intelligence (AI) approaches used during the study to predict some of the key properties based on given other properties is explored.

2. Why termite mound soil?

Termite Mound Soil (TMS) is the soil obtained from the pile of earth (commonly called termite's hill) produced by mound-building termites [4]. Termites are the dominant species in the tropical ecosystem where they can make up to 95% of the total quantity of soil insect in the ecosystem. Termites are considered “ecosystem engineers” because they modify the environment by creating biogenic structures, which change the soil’s properties and can build the most complex structures by construction enormous and very strong mounds.

Termites use their salivary secretions to process soil. Also their filth is rich in organic matter; organic carbon, phosphorus, potassium, magnesium, nitrogen [5].Due to the high content of organic matter[6], the pH increases nutrient and their ability to mix the soil and organic matter from different horizons used in Agriculture [7], [8]. Their gut is formed by compartments that present rising gradients of pH and different status of oxygen and hydrogen. These characteristics are certainly important and may effectively contribute to soil chemical and physical modifications. However, Clay content in termite mounds is usually 20% higher than in nearby soils[9].

A study on the Pozzolanic potentials of the calcined ant mound clay was carried by A.U. Elinwa, it was focused on investigating the pozzolanic potentials of this material and the effects of the calcined ant mound clay on cement mortar and concrete properties[10]. Therefore, they considered the physical repercussions of ant mound clay on the hydration process of cement and on mortar's compressive strength and its repercussions on the flexural and splitting tensile strength. They concluded by classifying the termite mound soil as a natural pozzolana.

Omofunmi reported that the termite mound clay is a better material in terms of moulding than ordinary clay [11]. TMS predominant component is clay whose plasticity has been improved by secretions from the termites during the construction of the mound. However, Minjinyawa et al. (2012) demonstrated that TMS showed good resistance to weather, abrasion and penetrations of liquids compared to ordinary clay [4]. In the other hand, the results obtained from Ricardinho et al. (2015) indicated the considerable effect of termites on tropical latosol's properties exists. That effect is associated with the termite's role in nutrient cycling and renewal of mineral soil [12].

Additionally, some studies evaluated the effects of Synthetic Termite Saliva incorporation into adobe. M.Gandia et al. (2019), analysed the physical, mechanical and thermal properties of synthetic termite saliva stabilised soil[13]. They reported an insignificant increase in bulk density with the addition of synthetic termite saliva.

Results from previous studies have shown that the use of the TMS in construction as well as in the soil doesn't require sintering during manufacturing and the strong binding mechanism present in the termite mound soil [14]. Besides displaying these attractive properties, the termite mound is a renewable source. Study carried out showed the feasibility of reproducing termite hill in a controlled environment [15]. The abundance of the termite mound soil has been shown in work [16]

3. Evaluation of the Microstructure

Scanning Electron Microscopy-Energy Dispersive Spectroscopy (SEM-EDX), Fourier Transform infrared (FTIR) and X-ray Ddiffraction (XRD) were the key implements used to perform microstructural characterization, bonding mechanism and crystal phases identification. In this section a brief description of these techniques is presented.

a. Morphological/chemical content analysis

Scanning Electron Microscopy-Energy Dispersive Spectroscopy (SEM-EDX) is the most commonly morphological characterization technique. This technique was used to illuminate and examine the microstructure of the TMS and alkali activated termite mound soil in order to understand the strengthening mechanism[17]. The SEM is an electron microscope, designed for directly studying the surfaces of objects. Also, it utilizes a beam of focused electrons of relatively low energy as an electron probe that is scanned in a regular manner over the specimen. Hence, SEM scans a focused electron beam over a surface to create an image. The electrons in the beam interact with the sample, producing various signals that can be used to obtain information about the surface topography and composition[18]. In SEM's detection mode details of 1-5nm can be visualized, therefore detection of new phases can be confirmed.

b. Diagnosis of functional group

Fourier Transform Infrared (FTIR) is one of the major spectroscopic methods utilized in the exploration of alkali activated binders. In this method chemical bonds enclosed by a material can be identified through infrared absorption spectrum as the method observes molecular bond vibrations at various infrared frequencies. Additionally, FTIR spectroscopy can be used to provide information on the transition of vibrations arising from small structural changes. With alkali activated clays, it can be used to evaluate the connectivity within Si-O-(Si,Al) frameworks through shifts in the peak associated with asymmetric stretch of that bond [17].

c. Crystalline phases identification

X-ray Ddiffraction (XRD) analysis is one of the most powerful methods used to provide information about used for quantification, phase analysis, crystal structures, and crystallite size and stacking sequences. X-ray diffraction is based on Bragg's law of diffraction, $n\lambda = 2d \sin \theta$ [18] where λ is the wavelength of the incident radiation (Cu radiation), d is the spacing between the (hkl) planes, n is an integer, and θ is the angle between the incident beam and the scattering planes. XRD is very useful for the detection of structural changes in order to detect any significant modification in the structure's mineralogy of the alkaline activated binder.

4. Binding mechanism of termite mound soil

The binding mechanism is the factor governing the strength and durability of materials. Therefore, to strengthen and toughen a construction material evaluation and understanding of the binders are key features. In earth-based materials, cement and lime are the mostly used binders. However, apart from these two traditional binders there is the non-traditional stabilisers, chemical stabilizers and by-product stabilisers[19]. Most of the binders used vary in terms of the formation of new compounds and hydrophobicity. The discussion in this section will focus on the potential pozzolanic characteristic of the TMS, the binding mechanisms during alkaline activation and mechanical compaction.

a. Pozzolanic characteristic of termite mound soil

Pozzolanic reactions are secondary reactions related to the calcium-based binders. By definition a pozzolan is a siliceous or siliceous and aluminous material that in itself possesses little or no cementitious value but when divided into fine form and in the presence of moisture will chemically react with calcium hydroxide at ordinary temperatures to form compounds having cementitious properties[20]. Investigation was carried out on the pozzolanic behavior of termite mound soil [10], from the results of that investigation the termite mound soil was classified as natural pozzolana.

b. Alkali activation

Any binder system derived by the reaction of an alkali metal source (solid or dissolved) with a solid silicate powder is classified as alkali activation[21]. The reaction of an alkali source with an alumina- and silica-containing solid precursor as a means of forming a solid material comparable to hardened Portland cement was first patented by German cement chemist and engineer Kühl in 1908[22]. The alkali sources used can include alkali hydroxides, silicates, carbonates, sulphates, aluminates or oxides essentially any soluble substance which can supply alkali metal cations, raise the pH of the reaction mixture and accelerate the dissolution of the solid precursor[23]. Alkali activation technology also provides the opportunity for the utilisation of waste streams that may not be of significant benefit in ordinary Portland cement-blending applications[24]. This may indicate that the binder structures formed with a lower calcium and higher aluminosilicate content could provide advantages in terms of binder stability over extended time periods or may be

related to incompatibility in material (chemical and mechanical) properties between the existing and new materials if the repair material is not well selected[25].

From the synthesis alkali activated binders are classified as high calcium and low calcium binders. Based on that classification, alkali activated TMS can be classified as low calcium binder. In this class of binder, the alkaline activation needs to be performed with the presence of higher alkaline source with curing temperatures ranging from 60-200°C[26].

Correlation between geopolymer's microstructure and mechanical properties have been investigation Duxson et al. (2007) the authors reported that the variation in the microstructure affects significantly the young modulus. Therefore, the young's modulus of geopolymers is determined by the microstructure rather than the composition as assumed [27].

Conventional alkali activated materials (AAMs) or two-part alkali activated binders are generally conducted with aluminosilicates with SiO_2+Al_2O_3 content higher than 80 wt.% [28]. Therefore, the intensive use of metakaolin as precursor in alkaline activation[29]. However, issues related with shrinkage in alkali activated binders constitute a key component [30] during alkali activation. Consequently, fiber reinforcement can be used to remedy the shrinkage-related issues [31], [32]. There is the need to explore alternative synthesis routes of alkali activated binders resulting in more eco-friendliness of the process.

c. Soil Compaction

Soil compaction is defined as the process of packing soil particles closely together by mechanical manipulation. This results in increasing the dry density or dry unit weight of the soil[33]. Generally, this process refers to a reduction in the air voids under a loading[34]. Study of soil compaction is important as it enables us to engineer the strength of the TMS to the desired strength[35]. Compactive effort, along with optimum water content is an effective tool to strengthen the termite mound soil used in construction.

5. Natural fibers

Natural fibers have gained a lot of interest in earth-based matrix reinforcement. In addition to their biodegradability[36], renewability and eco-friendly[37] features, natural fibers

possess good tensile properties. Straw, sisal, coir, bagasse, jute, hemp are the natural fibers commonly used as reinforcements in earth-based composites.

a. Physical properties, Mechanical Properties and Chemical treatment

Diameter, length, morphology and chemical content of fibers constitute the main characteristics defining the natural fibers performances. Their tensile properties are often improved by chemical treatment which results in removing unwanted component, increasing binding between the reinforcement and matrix interface.

b. Hygroscopic properties

Hygroscopicity defines the natural fiber's ability to absorb water resulting in swelling. Swelling induces hygral stresses as the earth-based matrix does not expand freely due to the presence of the natural fiber [38]. On the other hand, thermal properties of the natural fibers are related to shrinkage of the earth-based matrix in dry environment. Resulting in more interstices or voids within that matrix consequently failing to reinforce the matrix. The hygrothermal properties of natural fibers are important as the earth-based matrix is sensitive to both dry and wet environment.

6. Mechanical properties of Natural fibers reinforced earth- based materials bio-composite

a. Compressive strength evaluations

Compressive strength represents an important characteristic in designing load bearing structures. Therefore, it has acquired a lot of attention in the development of unconventional construction materials[39]. However, there are no standard describing the testing procedures of unconventional materials, subsequently the testing procedures of conventional construction materials are applied. Generally, the compressive strength of earth-based materials is dependent on the production techniques and curing conditions because earth-based materials displayed the highest resistance to axial loads in the dry state. Hence, the variability in compressive strength of earth-based materials.

b. Flexural strength evaluations

Flexural strength designates the property of a material to withstand transversal or bending loading. It represents the highest yield stress within a material. For earth-based materials,

the flexural strength is not commonly examined as earth-based materials are often used under compression loading. However, the flexural strength often follows the trend of compressive strength. In addition to the fiber's reinforcement that increases the flexural strength, as the fibers limit the propagation of cracks within the matrix[40]. Resulting in higher induced ductility in these brittle materials.

7. Artificial Intelligence Techniques

Artificial intelligence (AI) designate the simulation of human intelligence in machines. These machines are programmed to mimic humans' actions such as learning and problem-solving. AI has the ability to rationalize and take actions to obtain efficient manner of achieving a specific goal[42]. Machine Learning (ML) is a subset of AI which refers to the concept of computer programs to learn and adapt automatically new data without assistance.

In recent years, machine learning (ML) based models have been used extensively in construction materials and other areas [43]. The outputs could be predicted accurately by using the appropriate inputs even without knowing their relationship. This is due to the high efficiency performances to process data by the models which can reduce time and money consuming experiments[44]. Also, the ML models can help in achieving the desired mechanical properties of materials based on various mixture design but without any knowledge of the relationship between the inputs and outputs. Therefore, the advantage of using ML models for the prediction of compressive strength.

References

[1] R. Eires, A. Camões, and S. Jalali, "Ancient materials and techniques to improve the earthen building durability," in *Key Engineering Materials*, 2015, vol. 634, pp. 357–366, doi: 10.4028/www.scientific.net/KEM.634.357.

[2] C. A. Fapohunda and D. D. Daramola, "Experimental study of some structural properties of concrete with fine aggregates replaced partially by pulverized termite mound (PTM)," *Journal of King Saud University - Engineering Sciences*, 2019, doi: 10.1016/j.jksues.2019.05.005.

[3] I. C. Ezema, *Materials*. Elsevier Inc., 2019.

[4] B. B. Mujinya *et al.*, “Clay composition and properties in termite mounds of the lubumbashi area, D.R. congo,” *Geoderma*, vol. 192, no. 1, pp. 304–315, 2013, doi: 10.1016/j.geoderma.2012.08.010.

[5] Y. Millogo, M. Hajjaji, and J. C. Morel, “Physical properties, microstructure and mineralogy of termite mound material considered as construction materials,” *Applied Clay Science*, vol. 52, no. 1–2, pp. 160–164, 2011, doi: 10.1016/j.clay.2011.02.016.

[6] P. Jouquet, S. Traoré, C. Choosai, C. Hartmann, and D. Bignell, “Influence of termites on ecosystem functioning. Ecosystem services provided by termites,” *European Journal of Soil Biology*, vol. 47, no. 4, pp. 215–222, Jul. 2011, doi: 10.1016/j.ejsobi.2011.05.005.

[7] I. L. Ackerman, W. G. Teixeira, S. J. Riha, J. Lehmann, and E. C. M. Fernandes, “The impact of mound-building termites on surface soil properties in a secondary forest of Central Amazonia,” *Applied Soil Ecology*, vol. 37, no. 3, pp. 267–276, Nov. 2007, doi: 10.1016/j.apsoil.2007.08.005.

[8] P. Jouquet, N. Guilleux, R. R. Shanbhag, and S. Subramanian, “Influence of soil type on the properties of termite mound nests in Southern India,” *Applied Soil Ecology*, vol. 96, pp. 282–287, Nov. 2015, doi: 10.1016/j.apsoil.2015.08.010.

[9] M. A. Arshad, M. Schnitzer, and C. M. Preston, “Characterization of humic acids from termite mounds and surrounding soils, Kenya,” *Geoderma*, vol. 42, no. 3–4, pp. 213–225, 1988, doi: 10.1016/0016-7061(88)90002-X.

[10] A. U. Elinwa, “Experimental characterization of Portland cement-calcined soldier-ant mound clay cement mortar and concrete,” *Construction and Building Materials*, vol. 20, no. 9, pp. 754–760, Nov. 2006, doi: 10.1016/j.conbuildmat.2005.01.053.

[11] O. E. Omofunmi and O. I. Oladipo, “Assessment of termite mound additive on soil physical characteristics,” *Agricultural Engineering International: CIGR Journal*, vol. 20, no. 1, pp. 40–46, 2018.

[12] T. S. Sarcinelli *et al.*, “Chemical, physical and micromorphological properties of termite mounds and adjacent soils along a toposequence in Zona da Mata, Minas Gerais State, Brazil,” *Catena*, vol. 76, no. 2, pp. 107–113, 2009, doi: 10.1016/j.catena.2008.10.001.

[13] R. M. Gandia, A. A. R. Corrêa, F. C. Gomes, D. B. Marin, and L. S. Santana, “Physical, mechanical and thermal behavior of adobe stabilized with ‘synthetic termite saliva,’”

Engenharia Agricola, vol. 39, no. 2, pp. 139–149, Mar. 2019, doi: 10.1590/1809-4430-Eng.Agric.v39n2p139-149/2019.

[14] A. A. R. Corrêa, L. Bufalino, T. de Paula Protásio, M. X. Ribeiro, D. Wisky, and L. M. Mendes, "Evaluation of mechanical properties of adobe chemically stabilized with 'synthetic termite saliva,'" in *Key Engineering Materials*, 2014, vol. 600, pp. 150–155, doi: 10.4028/www.scientific.net/KEM.600.150.

[15] B. Jean-Pierre *et al.*, "Spatial distribution and Density of termite mounds in a protected habitat in the south of Cote d'Ivoire: case of national floristic center (CNF) of UFHB of Abidjan," vol. 11, no. 3, 2015.

[16] B. E. Society and A. Ecology, "The Abundance of Large Termite Mounds in Uganda in Relation to Their Environment Author (s): D . E . Pomeroy Source : Journal of Applied Ecology , Vol . 15 , No . 1 (Apr ., 1978), pp . 51-63 Published by : British Ecological Society Stable URL : http:," vol. 15, no. 1, pp. 51–63, 2009.

[17] "SYNTHESIS AND CHARACTERIZATION OF EXTRUDED ALKALI ACTIVATED EARTH-BASED COMPOSITES FOR SUSTAINABLE BUILDING CONSTRUCTION," 2019.

[18] Jr. William D. Callister, *Materials Science and Engineering An Introduction*, Seventh. New York, : John Wiley & Sons, Inc., 2007.

[19] G. B. P. M. Claudio Finocchiaroa, "FT-IR study of early stages of alkali activated materials based on pyroclastic deposits (Mt. Etna, Sicily, Italy) using two different alkaline solutions," *Construction and Building Materials* , vol. 262, 2020, doi: https://doi.org/10.1016/j.conbuildmat.2020.120095.

[20] S. A. Memon and M. K. Khan, "Ash blended cement composites: Eco-friendly and sustainable option for utilization of corncob ash," *Journal of Cleaner Production*, vol. 175, pp. 442–455, Feb. 2018, doi: 10.1016/j.jclepro.2017.12.050.

[21] A. Bahurudeen and M. Santhanam, "Influence of different processing methods on the pozzolanic performance of sugarcane bagasse ash," *Cement and Concrete Composites*, vol. 56, pp. 32–45, 2015, doi: 10.1016/j.cemconcomp.2014.11.002.

[22] M. Torres-Carrasco and F. Puertas, "Alkaline activation of different aluminosilicates as an alternative to Portland cement: alkali activated cements or geopolymers La activación

alcalina de diferentes aluminosilicatos como una alternativa al Cemento Portland: cementos activados alcalinamente o geopolímeros," 2017. [Online]. Available: www.ricuc.cl.

[23] Hans Kuhl, "Slag cement and process of making the same. United States patent office," New York, Oct. 1908.

[24] J. L. Provis, "Alkali-activated materials," *Cement and Concrete Research*, vol. 114. Elsevier Ltd, pp. 40–48, Dec. 01, 2018, doi: 10.1016/j.cemconres.2017.02.009.

[25] J. L. Provis, A. Palomo, and C. Shi, "Advances in understanding alkali-activated materials," *Cement and Concrete Research*, vol. 78. Elsevier Ltd, pp. 110–125, Dec. 01, 2015, doi: 10.1016/j.cemconres.2015.04.013.

[26] H. Ye and A. Radlińska, "Shrinkage mechanisms of alkali-activated slag," *Cement and Concrete Research*, vol. 88, pp. 126–135, Oct. 2016, doi: 10.1016/j.cemconres.2016.07.001.

[27] P. Duxson, A. Fernández-Jiménez, J. L. Provis, G. C. Lukey, A. Palomo, and J. S. J. van Deventer, "Geopolymer technology: The current state of the art," *Journal of Materials Science*, vol. 42, no. 9, pp. 2917–2933, May 2007, doi: 10.1007/s10853-006-0637-z.

[28] P. Duxson, J. L. Provis, G. C. Lukey, S. W. Mallicoat, W. M. Kriven, and J. S. J. van Deventer, "Understanding the relationship between geopolymer composition, microstructure and mechanical properties," *Colloids and Surfaces A: Physicochemical and Engineering Aspects*, vol. 269, no. 1–3, pp. 47–58, Nov. 2005, doi: 10.1016/j.colsurfa.2005.06.060.

[29] A. Mobili, F. Tittarelli, and H. Rahier, "One-part alkali-activated pastes and mortars prepared with metakaolin and biomass ash," *Applied Sciences (Switzerland)*, vol. 10, no. 16, 2020, doi: 10.3390/app10165610.

[30] P. Duxson, S. W. Mallicoat, G. C. Lukey, W. M. Kriven, and J. S. J. van Deventer, "The effect of alkali and Si/Al ratio on the development of mechanical properties of metakaolin-based geopolymers," *Colloids and Surfaces A: Physicochemical and Engineering Aspects*, vol. 292, no. 1, pp. 8–20, Jan. 2007, doi: 10.1016/j.colsurfa.2006.05.044.

[31] H. Ye, C. Cartwright, F. Rajabipour, and A. Radlińska, “Understanding the drying shrinkage performance of alkali-activated slag mortars,” *Cement and Concrete Composites*, vol. 76, pp. 13–24, Feb. 2017, doi: 10.1016/j.cemconcomp.2016.11.010.

[32] E. B. Ojo *et al.*, “Mechanical performance of fiber-reinforced alkali activated un-calcined earth-based composites,” *Construction and Building Materials*, vol. 247, Jun. 2020, doi: 10.1016/j.conbuildmat.2020.118588.

[33] L. M. Murillo, S. Delvasto, and M. Gordillo, “A study of a hybrid binder based on alkali-activated ceramic tile wastes and portland cement,” in *Sustainable and Nonconventional Construction Materials using Inorganic Bonded Fiber Composites*, Elsevier Inc., 2017, pp. 291–311.

[34] P. Jongpradist, P. Jamsawang, and W. Kongkitkul, “Equivalent void ratio controlling the mechanical properties of cementitious material-clay mixtures with high water content,” *Marine Georesources and Geotechnology*, vol. 37, no. 10, pp. 1151–1162, Nov. 2019, doi: 10.1080/1064119X.2018.1539534.

[35] A. W. Bruno, D. Gallipoli, C. Perlot, and J. Mendes, “Effect of very high compaction pressures on the physical and mechanical properties of earthen materials,” *E3S Web of Conferencese3sconf/20160914004*, 2016, doi: DOI: 10.1051/e3sconf/20160914004.

[36] R. Illampas, I. Ioannou, and D. C. Charmpis, “Adobe bricks under compression: Experimental investigation and derivation of stress-strain equation,” *Construction and Building Materials*, vol. 53, pp. 83–90, Feb. 2014, doi: 10.1016/j.conbuildmat.2013.11.103.

[37] A. Megalingam, M. Kumar, B. Sriram, K. Jeevanantham, and P. Ram Vishnu, “Borassus fruit fiber reinforced composite: A review,” *Materials Today: Proceedings*, Mar. 2020, doi: 10.1016/j.matpr.2020.02.750.

[38] P. Sudhakara *et al.*, “Studies on Borassus fruit fiber and its composites with Polypropylene,” *Composites Research*, vol. 26, no. 1, pp. 48–53, Feb. 2013, doi: 10.7234/kscm.2013.26.1.48.

[39] K. K. Chawla, *Composite materials: Science and engineering, third edition*. Springer New York, 2012.

[40] J. E. Aubert, P. Maillard, J. C. Morel, and M. al Rafii, “Towards a simple compressive strength test for earth bricks?,” *Materials and Structures/Materiaux et Constructions*, vol. 49, no. 5, pp. 1641–1654, May 2016, doi: 10.1617/s11527-015-0601-y.

[41] Jaap Schijve, *Fatigue of Structures and Materials*, Second edition., vol. 25. Netherlands : Elsevier, 2009.

[42] J. M. Marangu, “Prediction of Compressive Strength of Calcined Clay Based Cement Mortars Using Support Vector Machine and Artificial Neural Network Techniques,” *Journal of Sustainable Construction Materials and Technologies*, vol. 5, no. 1, pp. 392–398, Apr. 2020, doi: 10.29187/jscmt.2020.43.

[43] H. Anysz, Ł. Brzozowski, W. Kretowicz, and P. Narloch, “Feature importance of stabilised rammed earth components affecting the compressive strength calculated with explainable artificial intelligence tools,” *Materials*, vol. 13, no. 10, May 2020, doi: 10.3390/ma13102317.

[44] D. van Dao, H. B. Ly, H. L. T. Vu, T. T. Le, and B. T. Pham, “Investigation and optimization of the C-ANN structure in predicting the compressive strength of foamed concrete,” *Materials*, vol. 13, no. 5, pp. 1–17, 2020, doi: 10.3390/ma13051072.

3.0 Chapter Three: Termite mound soil cement stabilized synthesis for low cost and environmental-friendly construction materials

1. Introduction

In the last decades, the construction field is facing major concerns about the carbon emissions associated with production of cement which is typically used for construction of buildings across the world [1]. Since these emissions are responsible for about 7% of global CO_2 emissions [2,3], there is a need to explore alternative building materials that will reduce the overall amount of CO_2 emissions. This has stimulated significant research efforts into alternative building materials [4,5] that can reduce the overall use of cement in buildings [1,6]. Within this context, earth-based materials are "green" materials that can reduce the carbon emissions [7] that are associated with the construction of buildings. Compared to conventional cement-based [8] building materials [9], earth-based materials are cheap [10], environmental-friendly [11,12] and available [13] globally. They can also have attractive combinations of mechanical properties [14,15] while consuming lower amounts of energy during their production [16,17]. However, according to estimates by UN-Habitat, approximately 238 million people lived in slums or informal settlements in Sub-Saharan Africa (SSA) in 2018 [18]. These slums are generally considered to be sub-standard housing. They also contribute to low-life expectancy, poor heath indices and low indices of well- being because housing is a major fundamental need for human being and constitutes the main factor for its survival and its development. Therefore, adequate housing contributes to physical development, moral health and social stabilization. All these factors affect immensely individual ability and productivity, thus the low productivity of SSA. In SSA, some countries have easy access to conventional building materials as is the case of Nigeria compared to others SSA countries, for instance Chad. In Nigeria, the construction industry is directed towards development of sustainable materials from wastes [5,13] and earth- based [19] and recycled materials [12] through environmental-friendly technologies [6]. In Chad, transformation of local materials into sustainable construction materials have not been promoted, hence the region's dependence on cement. Despite that, Chad's access to conventional building materials is problematic because of geographical constraints and scarcity of manufacturing industries. In fact, in Chad, construction materials are principally imported from Nigeria as the few local manufacturing industries are not reliable [20,21]; consequently, these imported materials

are very expensive. In addition, the construction field is dependent on the borders movement as it witnesses shortages that paralyze this field. Chad is one of the central African countries that has experienced massive growth of slums with immense decrease of productivity in the last decades. In Chad, the gross domestic product is estimated at 728 USD per citizen and the general debt rate is evaluated at 334 USD per citizen [22], for a population of 15 million in 2018. Additionally, from the World Bank report an adult in Chad is 71% less productive than a person benefiting from appropriate basic needs services [23] (health, housing and education). It is noteworthy that the cost of a standard house is about 1000 USD per m^2 [24]. From these statistics, affording an adequate house is really difficult for a low-income citizen, but in reality, it is almost impossible. Hence, the first step in addressing the problem of housing in Chad can be the partial replacement of cement with natural pozzolanas or similar in the production of blocks. This could solve the challenge of cost, however, the challenges related to the brittle failure can be addressed by addition of natural fibers as reinforcement. In most cases, the structural applications of earth-based materials [11] require the use of cement as a stabilizer [25] or reinforcement with natural and [26]/synthetic [27] fibers. In any case, the underlying strengthening and toughening mechanisms associated with the stabilization of earth-based materials have not been studied using the mechanistic approaches that have been applied to the study of natural fiber-reinforced earth-based composites [15]. Termite hills are classified as earth-based materials, they are very abundant in Chad but do not serve any economic value, so they are often demolished. In contrast, our basic understanding of termite hill soil composition, formation and bonding is still very limited. Termite hill soil or (termite mound soil, TMS) is obtained from termite hills that are produced by mound-building termites [28]. Termites are the dominant species in the tropical ecosystem, where they constitute up to 95% of the total quantity of soil insect in the ecosystem. They are considered as “ecosystem engineers” because they bind the soil with their secretions (saliva) to produce complex and robust termite mounds. They also egest and excrete organic matter and elements such as phosphorus, potassium, magnesium and nitrogen, which can be mixed with the soil for applications in agriculture [29]. Hence, termite mound soils contain relatively high contents of organic matter. Their relatively high pH values also increase their ability to mix with nearby soils. Furthermore, the guts of termites have been shown to contain compartments that present rising gradients of pH and different status of oxygen and hydrogen [30], which may contribute ultimately to the chemistry and

structure of termite mound soils. In any case, the resulting termite mounds contain soils with clay contents that are 20% greater than those in nearby soils [28].

Prior work by Elinwa [31] has explored the potential to use TMS as pozzolanic materials in mixtures of calcined ant mound clay and cement mortar. Their work explored the effects of ant mound clay on the hydration process (in cement), as well as the resulting compressive strength, and its repercussions for the flexural and splitting tensile strength. They concluded that their ant mound clay was a weak pozzolanic material. Previous work reported that termite mound clay is a better molding material than ordinary clay [32]. The improvements in the molding characteristics of the termite mound soil were attributed to the effects of saliva secretions (from termites) during the construction of termite mounds. Minjinyawa et al. [30] have also shown that termite mounds have good resistance to erosion, abrasion and penetrations of liquids, compared to ordinary clay. Other researchers have also suggested that the improved mechanical properties of TMS (compared to those of nearby soils) can be attributed to the effects of termite secretions [32]. Researchers have suggested that termites can also have a significant effect on nutrient cycling and the renewal of mineral soil [33]. Gandia et al. [29] have also studied the effects of mixing synthetic termite saliva with adobe. The resulting materials exhibited a modest increase in the bulk densities of adobe with mixtures of saliva. Synthetic termite saliva products have emerged from prior studies on TMS [34]; they play the role of stabilizer due to the formation of organo-mineral compounds (that are present in the soil) that bind clay particles together. The products obtained from termite saliva are also ecologically sustainable, hydrophobic, water soluble, resistant to oxidation, resistant to microorganisms, applicable as low viscosity and cost efficient [35]. Subsequently, TMS presents the characteristic of a sustainable and renewable alternative to conventional building materials except for the few problems that can be solved through stabilization among other techniques. From the American Society for Testing and Materials (ASTM), stabilization is a technique to increase the soil strength by enhancing its load-bearing capacity, improving its permeability, resistance, solving swelling and damping problems [36]. Boga et al. carried out studies on the spatial distribution and density of termites in an artificial botanic forest. They found out that over 26 termites' mounds were inactive out of 165 mounds [37]. Based on these results, it can be deducted that the quantity of inactive termite mounds may be higher in the natural environment.

In any case, our current understanding of the effects of stabilizers on strength and fracture behavior of termite mound soils is limited. Therefore, the current study will explore the effects of cement stabilizers [38] on the strength and fracture toughness of controlled mixtures of termite mound soil and cement. This study is a first in terms of examining the fracture mechanism in soil-based termite mound mixtures. It is anticipated that the partial replacement of cement with TMS could reduce the effective cost of building materials that are used in sustainable construction. It could also reduce the overall gas emissions associated with the production of mortars that are used for the stabilization of earth-based materials. It is noteworthy to recall that in this study abandoned (or inactive termites') mounds have been used.

2. Materials and Methods

a. Materials

The TMS that was used in this study was collected from mounds in N'djamena, Chad. The particle sizes of the soils extracted from the 10-15-year-old deserted mounds were determined via sieving in accordance with the British Standard BS 1377:2 code [39], revealing that 85% of particles were finer than 800 μm. Atterberg limits for the TMS were determined in accordance with BS 1377:2. The moisture content of the TMS was also determined in accordance with BS 1377:2, while the specific gravity was determined using the ASTM D854—14 code [40]. Energy dispersive spectroscopy (EDX) was used to obtain semi-quantitative estimates of the chemical compositions of the TMS during scanning electron microscopy (SEM). This was done using a Carl Zeiss scanning electron microscope that was instrumented with a Model EVO LS10 EDX system (Carl Zeiss, Pleasanton, CA, USA). The physical properties and the chemical composition of the TMS are summarized in Table 1.

Table 3.1 Termite mound soil physical and chemical characteristics.

Physical Properties	
Particle size distribution	85% smaller than 800μm
Moisture content	3.85%
Specific gravity	2.60
Dry density	0.458g/cm^3

Optimum moisture content	15%
Liquid limit	35.17%
Plastic limit	20.80%
Plasticity index	14.37%
Chemical Composition (main elements only) wt.%	
SiO_2	19.376
Al_2O_3	9.154
Fe_3O_4	7.534
K_2O	1.865

Portland cement produced by Dangote Portland Limestone Cement Industry (Abuja, Nigeria) from their depot at the Federal Capital Territory, Nigeria. The Portland cement was used as a stabilizer in this study. The cement used is the Portland cement type I following the ASTM requirements for general construction purpose [41] with fairly high tricalcium silicate C3S. The ordinary Portland cement contains about 75 wt% of calcium silicate minerals with fine particles of 70 μm according to the supplier.

In the sample preparation order, TMS/cement mixtures with 0, 5, 10, 15 and 20 wt% of Portland cement were mixed in a laboratory mixer for 5–10 min before addition of water. The resulting mixtures were then poured into metallic cubic molds with dimensions of 50 mm × 50 mm × 50 mm for the fabrication of compression testing, whereas molds with dimensions of 200 mm × 100 mm × 50 mm were used for bend specimens or determination of flexural strengths. For the determination of fracture toughness, molds with dimensions of 200 mm × 100 mm × 50 mm with single edge notch were used. The specimens were cured at room temperature (27 ◦C) for 7, 14 and 28 days before testing, and a minimum of 3 samples were produced for each formulation and each testing. All the mix designs were produced under the same conditions, but not on the same day.

b. Materials Characterizations

X-ray diffraction (XRD) was used to determine the crystal structures of the minerals that were present in the mixtures of TMS at the different replacement level of Portland cement. This was done using a Thermo Scientific X-ray Fluorescence (XRF) Epsilon Spec- trometer (model ARL quant'x XRD, Rotkreuz, Switzerland) that was

operated within a 2θ range of 3–65◦, a wavelength of 1.5406 Å and an angular velocity of 3 ◦/min. The XRD samples were prepared by grinding the TMS and the mixture (with a pestle and a mortar) to a fine homogeneous powder. The ground powder was poured onto an aluminum specimen holder prior to XRD analysis.

A Thermo Scientific Nicolet iS5 FTIR system (Thermo Scientific Nicolet, Worcester, MS, USA) was used for the characterization of bonds that were present in the powder mixtures of TMS and Portland cement with volume ratios of 100:0, 95:5, 90:10, 85:15 and 80:20. Prior to FTIR analysis, the different mixtures were blended with potassium bromate (KBr) in a ratio of 5:1. This was done in a ceramic mold before compacting the mixed powders to form pellets that were placed on specimen holders for the FTIR analysis.

SEM was used to characterize the cured microstructures of the TMS and Portland ce- ment structures. This was done using a Carl Zeiss Model EVO LS10 (Carl Zeiss, Pleasanton, CA, USA) that was instrumented with an EDX system that can detect elements between sodium (Na, Z = 11) and uranium (U, Z = 92) with high resolution. Prior to SEM imaging, the samples were embedded in silver containing a polymer/metal mixture, ground, polished and coated with gold, to facilitate the imaging of the surfaces using SEM.

c. Mechanical Properties measurements

For the compression deformation, compressive strength testing was carried out on the specimens for each composition of TMS and Portland cement with volume ratios of 100:0, 95:5, 90:10, 85:15 and 80:20. Three samples were produced for each composition and were cured at room temperature (27 ˚C) for 7, 14 and 28 days, prior to mechanical testing. The specimens were then loaded monotonically in an electromechanical testing machine UTM7001 Model 4002 (Utest, Ankara, Turkey) at a loading rate of 1.2 kN/s. Prior to testing, the actual dimensions of the specimens were measured using Vernier calipers. The compressive strengths were obtained usingthe following expression:

$$\sigma c = \frac{Fi}{Ai} \qquad (1)$$

where σc is the compressive strength in megapascal (MPa), Fi is the force at the onset of failure in newton (N) and Ai is the initial cross-sectional area in millimetre square (mm^2). The flexural tests were conducted on specimens of 200 mm × 100 mm × 50 mm; for each formulation three samples were produced and cured in the laboratory environment at room temperature (27 °C) for 7, 14 and 28 days. Hence, a total number of 45 specimens were produced for the flexural tests. The specimens were subjected to the same conditions before being loaded under a three-point bending regime in a hydraulic universal testing machine UTM7001 Model 4002 (Utest, Ankara, Turkey) at a loading rate of 1.2 KN/s. The flexural strength was calculated from the following equation:

$$\sigma f = \frac{3FL}{bd^2} \qquad (2)$$

where σf is the flexural strength in MPa, F is the load at the onset of failure in N, L is the distance between the support points in m, b is the breadth in m of the specimen and d is the width of the specimen in m. Three specimens were tested for each composition. To study the fracture toughness, the resistance-curve method was used. Experiments were carried out on single edge notched bend (SENB) [33]; the specimens were molded in metallic molds with a notch to width ratio (a_0/w) of 0.4. The specimens were subjected to three-point bend loading in an electromechanical testing machine UTM7001 Model 4002 (Utest, Ankara, Turkey) as seen in Figure 1. The resistance-curve experiments were carried out on specimens left in the laboratory environment at a temperature of 27 ◦C for 7 days, 14 days and 28 days. The specimens were loaded at a ramp rate of 1.2 N/s to examine the possible crack propagation; this was achieved with a probe scope video monitoring system. The video obtained from the probe scope was analyzed with the scientific imaging software

"image J 2", which was used to investigate the crack/microstructure interactions that resulted in the resistance-curve behavior. Loading was carried out until the specimens broke into two or more pieces. The critical stress intensity factors were then calculated using the following expression:

$$K = \frac{PSf(a/w)}{\sqrt{BW}} \qquad (3)$$

where K is the critical stress intensity factor in MPa·m 12 , a is the crack length in m, F(a/w) is the specimen compliance, P is the applied load in N, S is the span in mm, B is the specimen thickness in mm and W is the specimen width in mm. SEM was used to examine the crack/microstructure interactions associated with stable crack growth, prior to the onset of catastrophic failure.

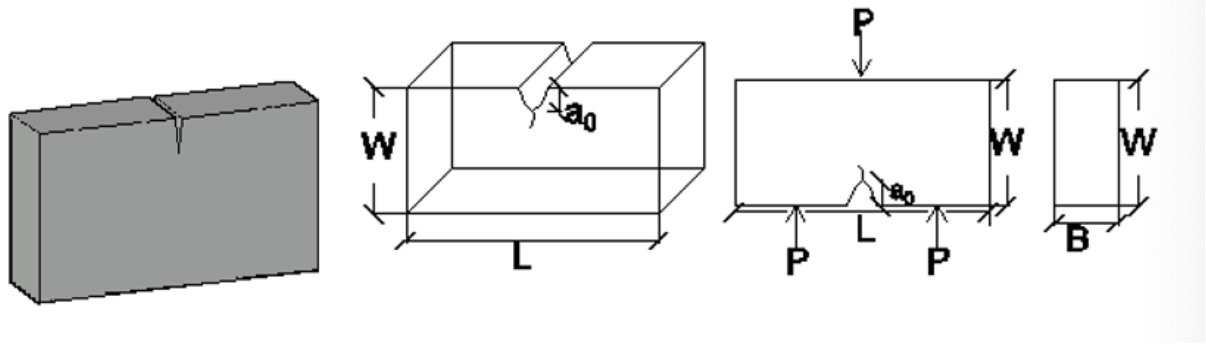

L	Specimen Length	200
W	Specimen Width	100
B	Specimen thickness	50
a0	Notch length	20

Figure 1. Detailed schematics for single edge notched bend (SENB) specimens.

d. Statistical analysis

Data analysis was conducted on the different mechanical properties to analyze the effect of the stabilization variation on the mechanical behavior from the early curing age until 28 days. One-way analysis of variance (ANOVA) tests was used to detect the existence of variations between the population means. The null hypothesis (Ho) suggests that the different curing days do not have any effect on the mechanical properties (fracture toughness, compressive and flexural strength) meaning that the average results for all curing conditions are equal. While the alternative hypothesis (Ha) suggests that at least one average result is different in other terms:

H_0: $\mu_1 = \mu_2 = \mu_3$ and Ha: at least one average of the mechanical properties is different

where μ_1, μ_2 and μ_3 are population means corresponding to the mechanical properties (compressive-flexural strengths and fracture toughness) at different curing days for the stabilized and unstabilized TMS. A confidence degree of 95% was selected for this study

3. Results and Discussions

a. Effect of the TMS Partial Replacement on the Microstructural Properties

i. Morphological and chemical component analysis

SEM Micrographs for the initial TMS presented in Figure 2. SEM Micrographs for the initial TMS presented in Figure 2.

Figure 3 shows heterogeneous microstructures with various particles sizes and shapes. It is also interesting to note that microcracks, highly interconnected particles with some superficial pores, were observed abundantly in the unstabilized samples, whilst they tend to decrease in the stabilized mixtures with Portland cement, as shown.

Presence of new minerals namely Sr, Kr and Ra can be noticed. This can be attributed to the manufacturing process because these minerals do not appear in any other specimens. A possible explanation is that during the specimen's fabrication, the materials might have been contamined with a foreign material containing these minerals.

The SEM-EDX analysis shows that the TMS is rich in silicate and alumina; these results are similar to the ones obtained from Ajiboye's work. In his work, the termite soil was classified as natural pozzolanas [28]. The overall silicate and alumina contents of the TMS/Portland cement mixtures have increased upon the replacement of TMS with Portland cement. The Calcuim (Ca) present in the cement reacts with the water and the environing air to form calcium hydroxide $CaO\ (s) + H_2O\ (l) \rightarrow Ca\ (OH)_2(s)$ [10]. The increase in the silicate and alumina content is attributed to the formation of di-calcium and tri-calcium silicates, which imparts strength to the cement. The alumina supplied by the TMS behaves as a flux when mixed in the cement. Furthermore, the iron oxide present in the initial TMS forms tri-calcium alumina-ferrite [42] by reacting with the calcium supplied by the cement, which results in improved strength and hardness. Thus, the TMS provides sources of Si and Al_2O_3 for additional hydration reaction with the Ca apported by the cement to impart the strength of the mixtures.

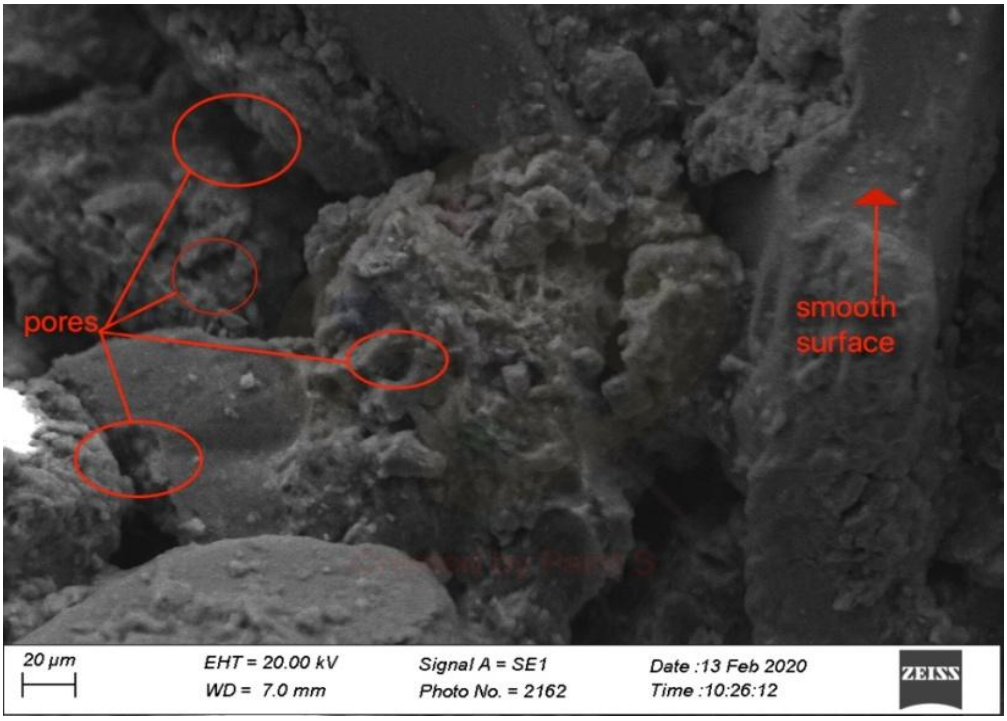
pores
smooth
surface
20 µm
EHT = 20.00 kV
WD = 7.0 mm
Signal A = SE1
Photo No. = 2162
Date :13 Feb 2020
Time :10:26:12
ZEISS

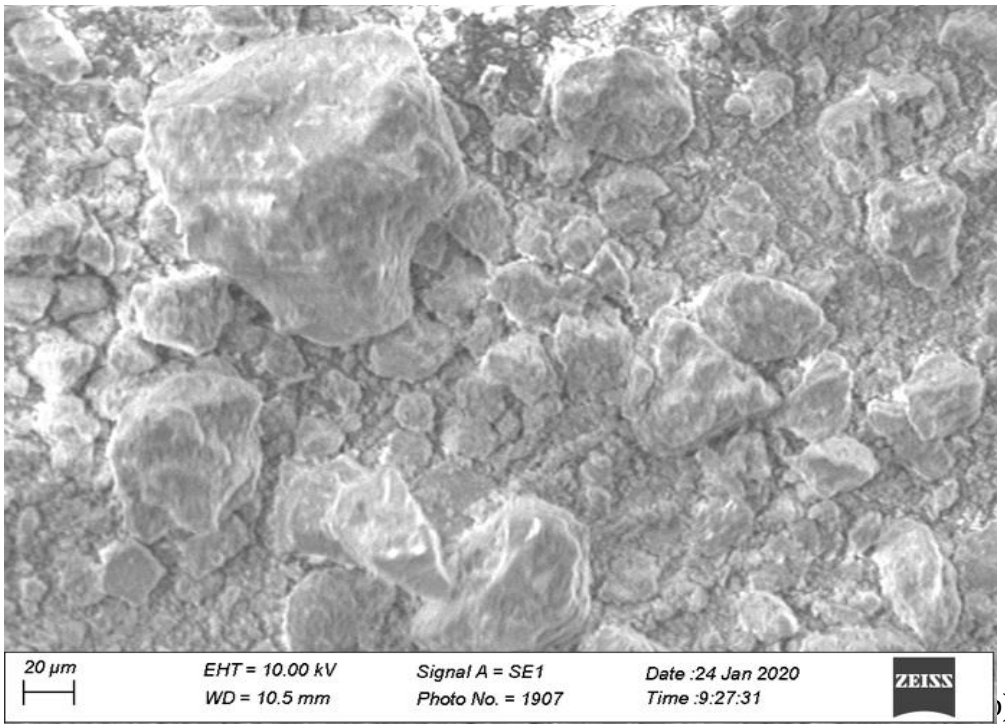
20 µm
EHT = 10.00 kV
WD = 10.5 mm
Signal A = SE1
Photo No. = 1907
Date :24 Jan 2020
Time :9:27:31
ZEISS

)

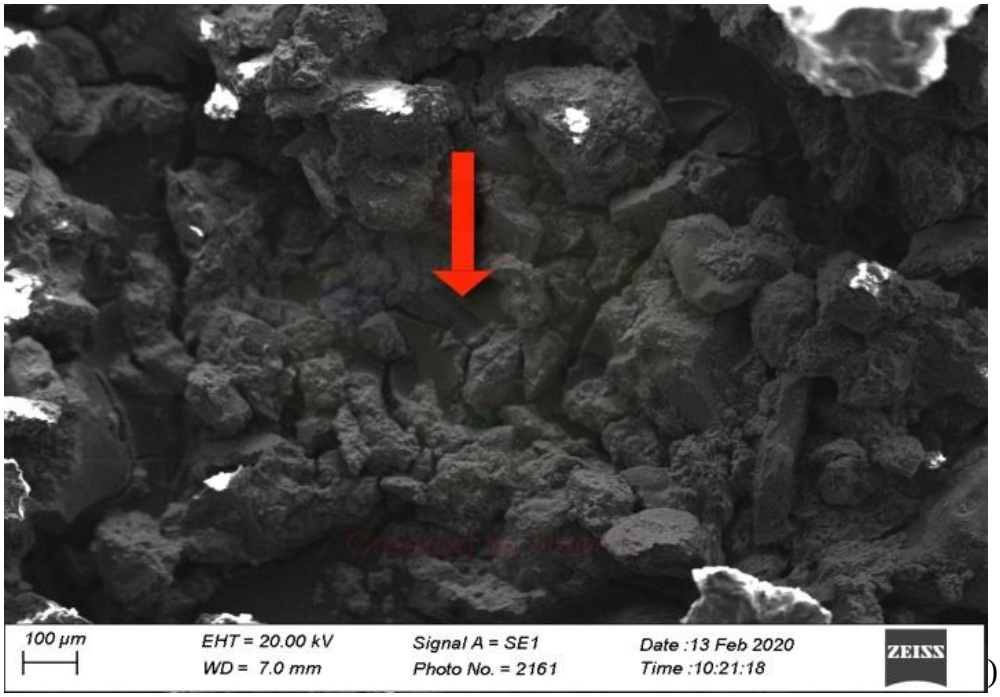
100 µm
EHT = 20.00 kV
WD = 7.0 mm
Signal A = SE1
Photo No. = 2161
Date :13 Feb 2020
Time :10:21:18
ZEISS

)

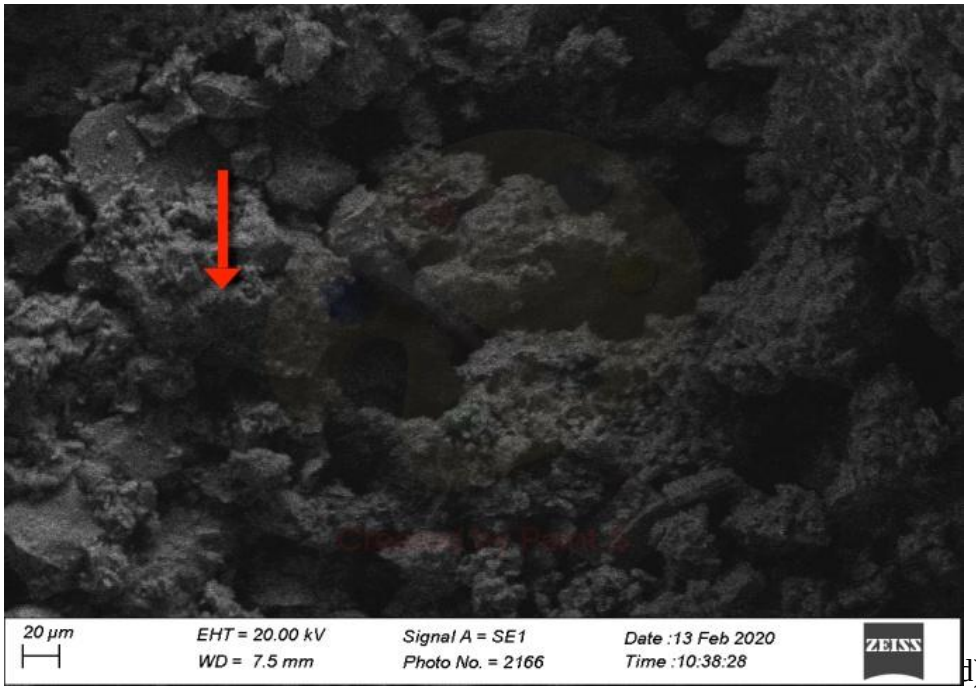
20 µm
EHT = 20.00 kV
WD = 7.5 mm
Signal A = SE1
Photo No. = 2166
Date :13 Feb 2020
Time :10:38:28
ZEISS

d)

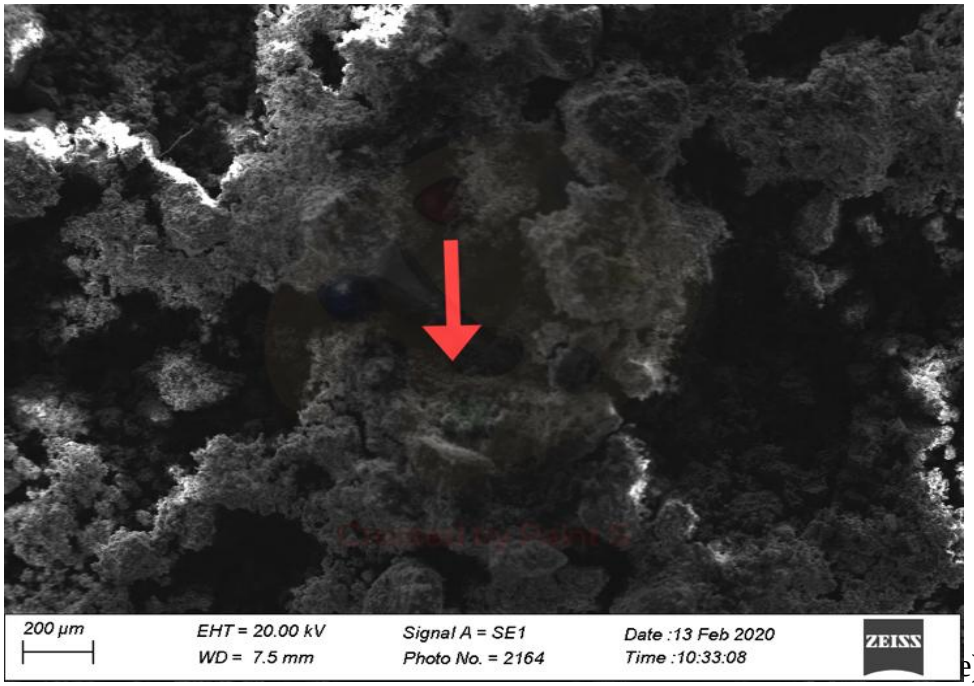

e)

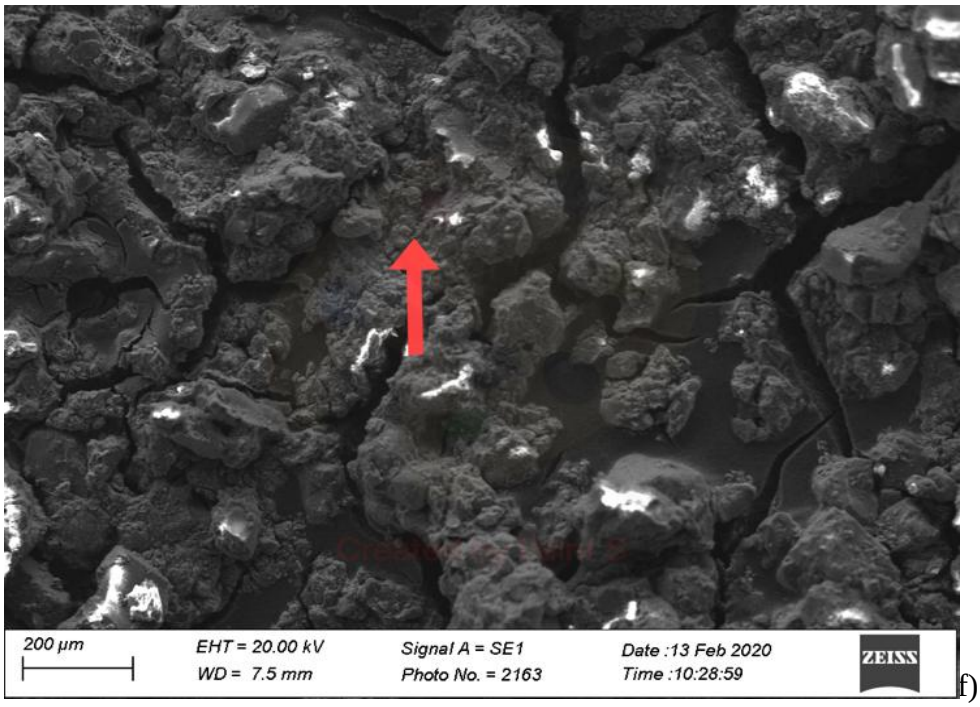

f)

Figure 3.1 SEM micrographs of: **a**) unstabilised termite mound soil; **b**) Ordinary Portland Cement (OPC); **c**) specimens containing 5wt% of OPC; **d**) specimens containing 10wt% of OPC; **e**) specimens containing 15wt% of OPC; **f**) specimens containing 20wt% of OPC.

Figure 3 shows heterogeneous microstructures with various particles sizes and shapes. It is also interesting to note that microcracks, highly interconnected particles with some

superficial pores, were observed abundantly in the unstabilized samples, whilst they tend to decrease in the stabilized mixtures with Portland cement, as shown.

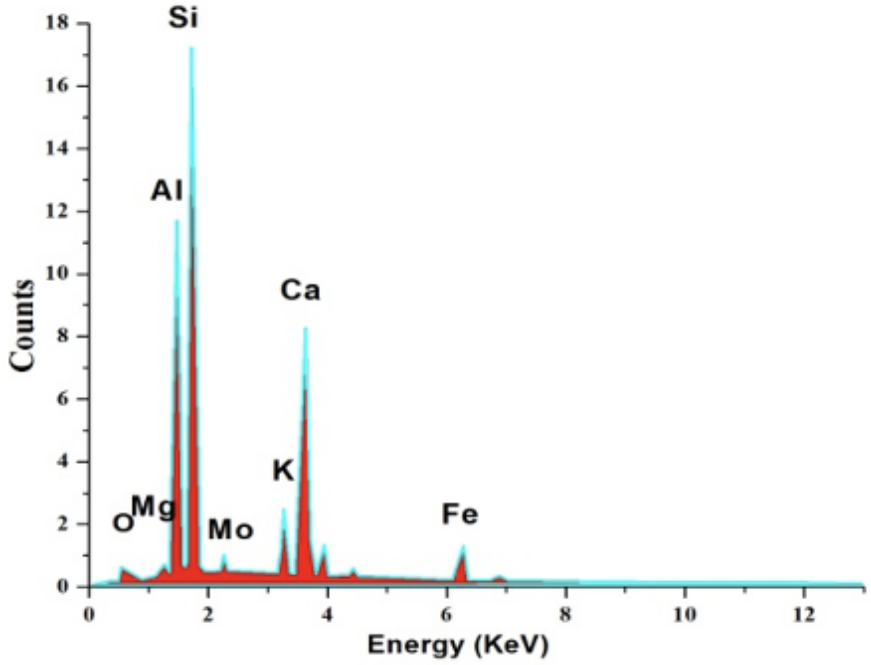

a)

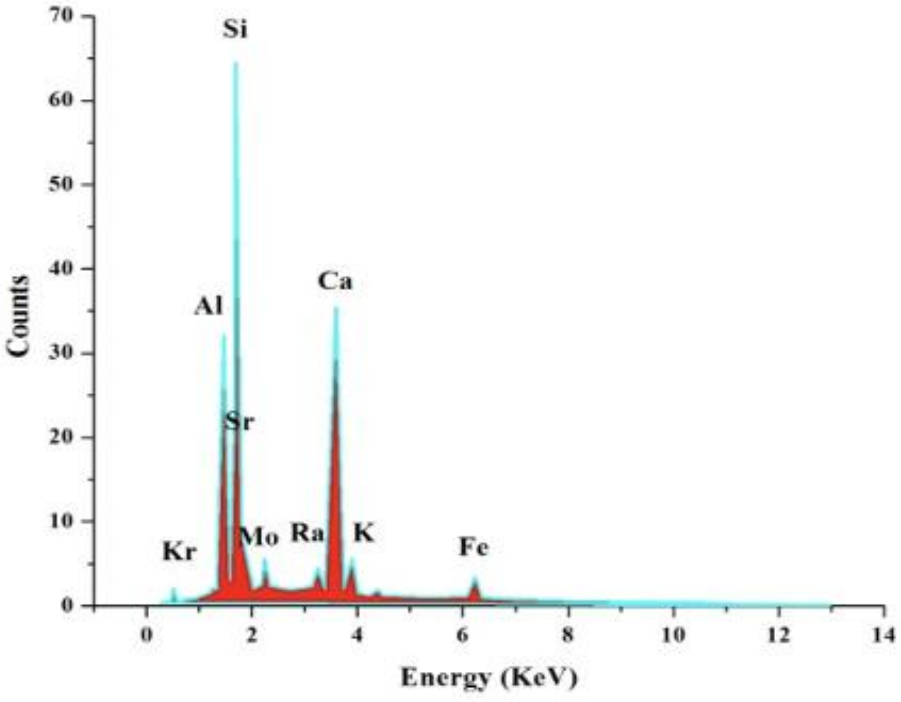

b)

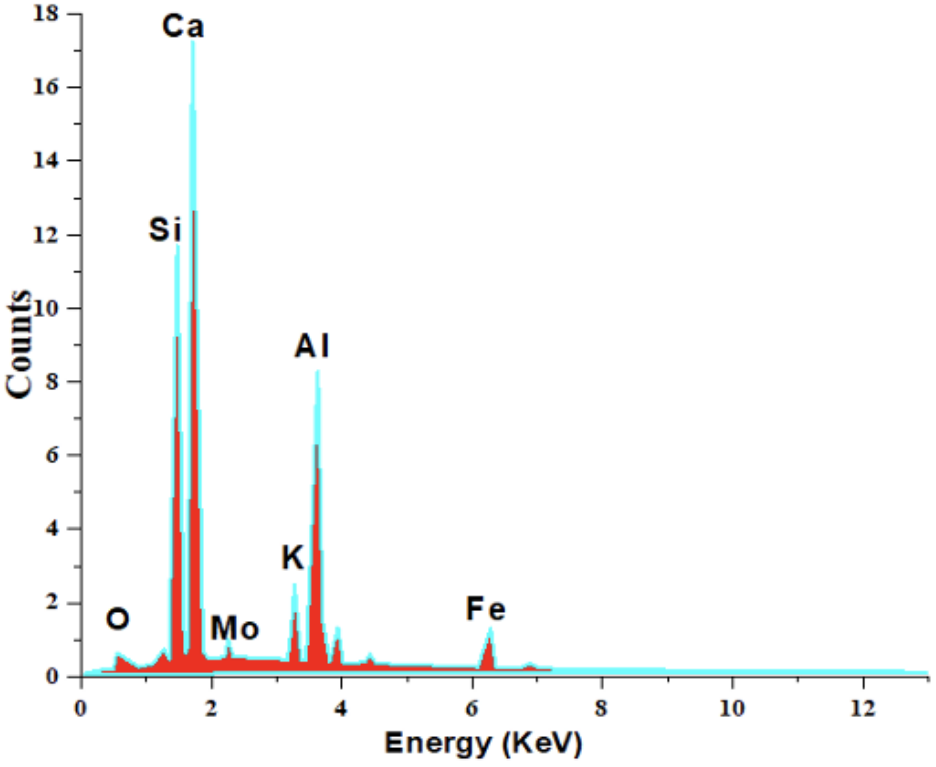
Ca
Si
Al
K
O
Mo
Fe
Counts
Energy (KeV)

c)

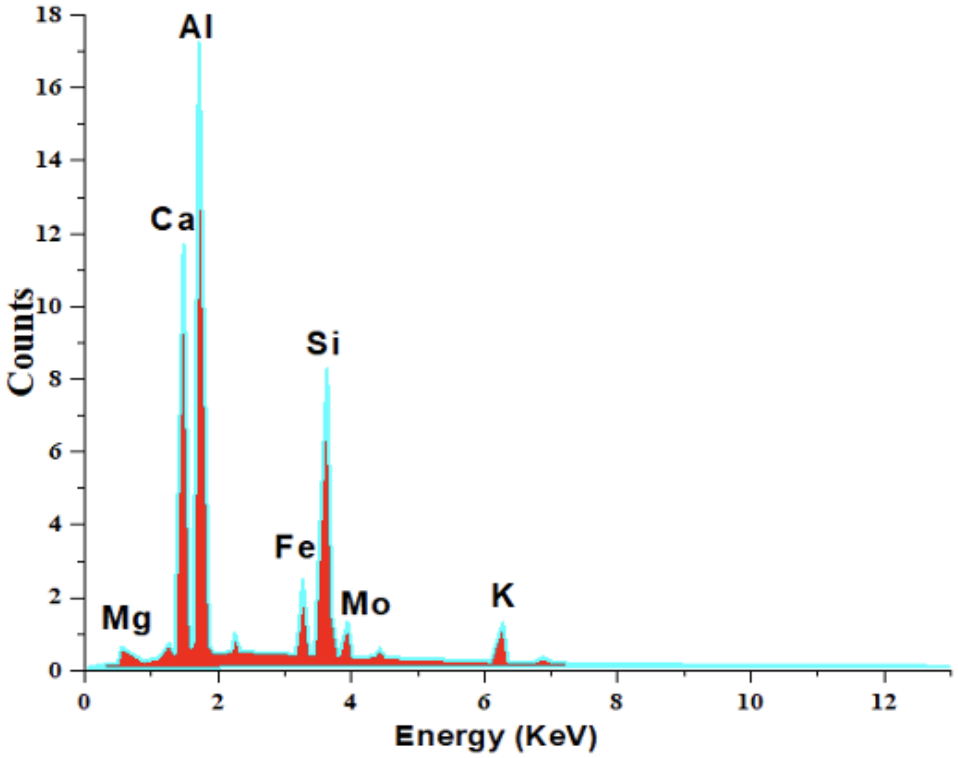
Al
Ca
Si
Fe
Mo
K
Mg
Counts
Energy (KeV)

d)

Figure 3.2 EDX micrographs of: a) specimens containing 5wt% of stabilisation; b) specimens containing 10wt% of stabilisation; c) specimens containing 15wt% of stabilisation; d) specimens containing 20wt% of stabilisation.

The presence of new minerals namely Sr, Kr and Ra can be noticed. This can be attributed to the manufacturing process because these minerals do not appear in any other specimens. A possible explanation is that during the specimen's fabrication, the materials have been mistakenly polluted with a foreign material containing these minerals.

The overall silicate and alumina contents of the TMS/Portland cement mixtures have increased upon the replacement of TMS with Portland cement. The Ca present in the cement reacts with the water and the environing air to form calcium hydroxide $CaO\ (s) + H_2O\ (l) \rightarrow Ca\ (OH)_2(s)$ [10]. The increase in the silicate and alumina content is attributed to the formation of di-calcium and tri-calcium silicates, which imparts strength to the cement. The alumina supplied by the TMS behaves as a flux when mixed in the cement. Furthermore, the iron oxide present in the initial TMS forms tri-calcium alumina-ferrite by reacting with the calcium supplied by the cement, which results in improved strength and hardness. Thus, the TMS provides sources of Si and Al_2O_3 for additional hydration reaction with the Ca apported from the cement to impart the strength of the mixtures.

Furthermore, the mineralogical analysis conducted by Faria [43] showed that the predominant clay-mineral is kaolinite, hence the similarities with our present results but with some differences. These differences can be attributed to the variations in the location from where the TMS is collected, because locally available clays are used to construct the termite mounds therefore their composition varies from one location to the other. However, each component plays a role in the particles bonding in terms of chemical reactions and physical structure. In any case, the current EDX results show that the partial replacement of TMS with cement increased the amount of calcium (Ca) considerably. This can explain the increase in strength as the replacement level increases. However, this is true only up to some percent replacement; as the replacement level increases the strength decreases. A possible explanation is that the reactions between the elements from the TMS and cement are no longer contributing to the mixture's mechanical behavior.

ii. Crystalline Phases Analysis

The XRD spectra are presented in Figure 4. It presents the mineralogical analysis diffractograms of the specimens at different stabilization levels. From the various graphs it can be concluded that the predominant element is quartz (SiO_2); this confirms the previous EDX results presented in Figure 3. It is interesting to note that the initial crystalline phases observed within the TMS changed considerably after the stabilization. Meanwhile, the change of the peak intensity was not considerable.

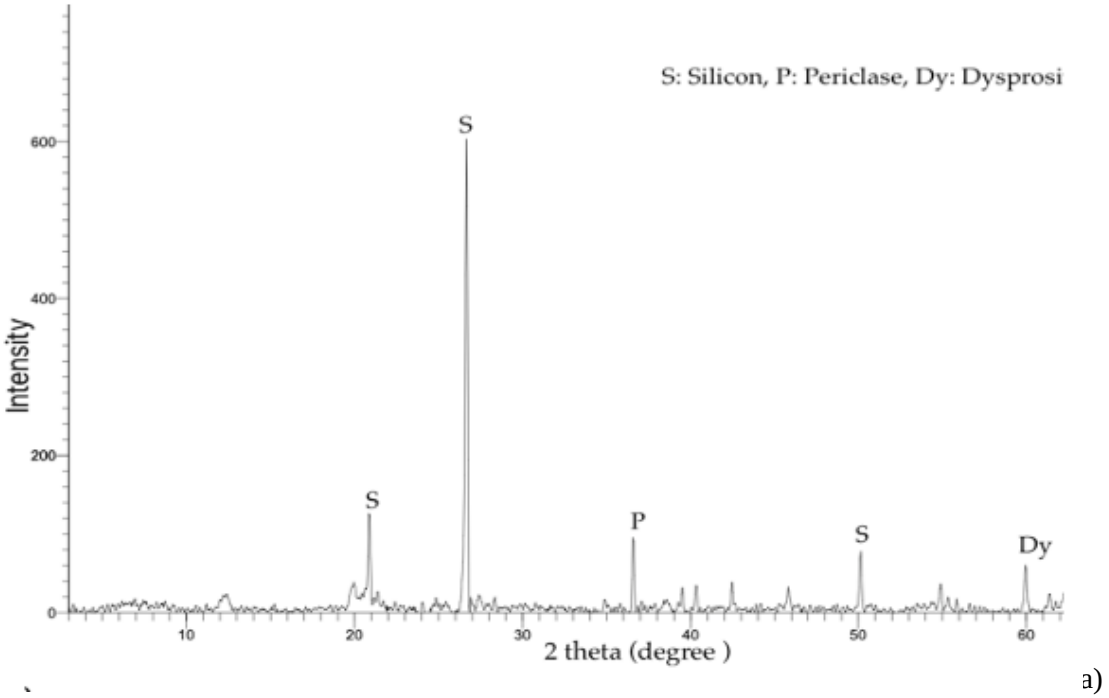

a)

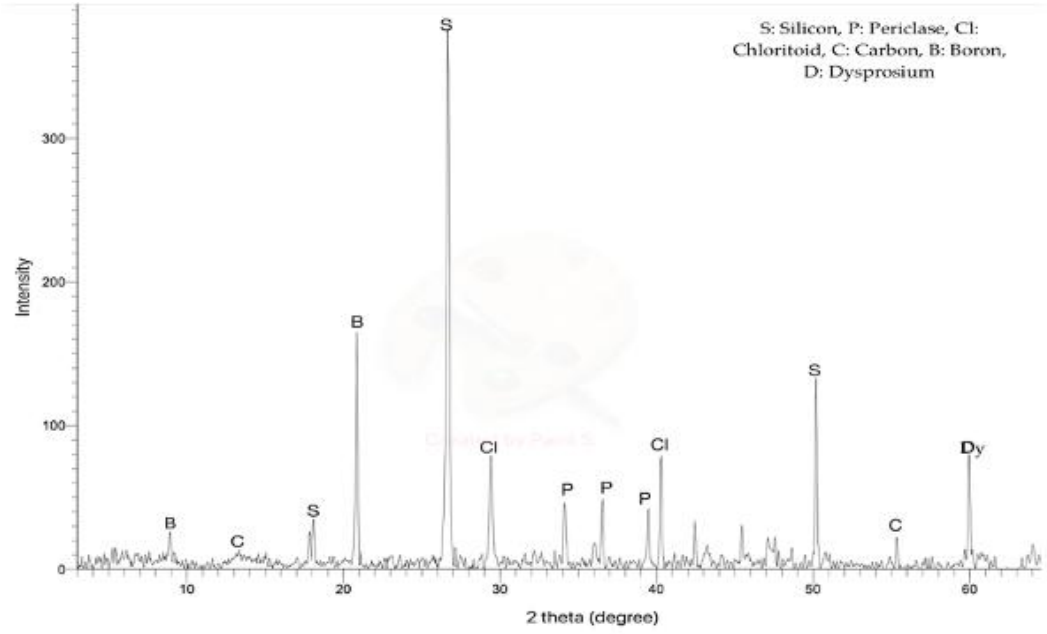
S: Silicon, P: Periclase, Cl:
Chloritoid, C: Carbon, B: Boron,
D: Dysprosium
Intensity
2 theta (degree)
B
C
S
B
S
Cl
P
P
P
Cl
S
C
Dy

b)

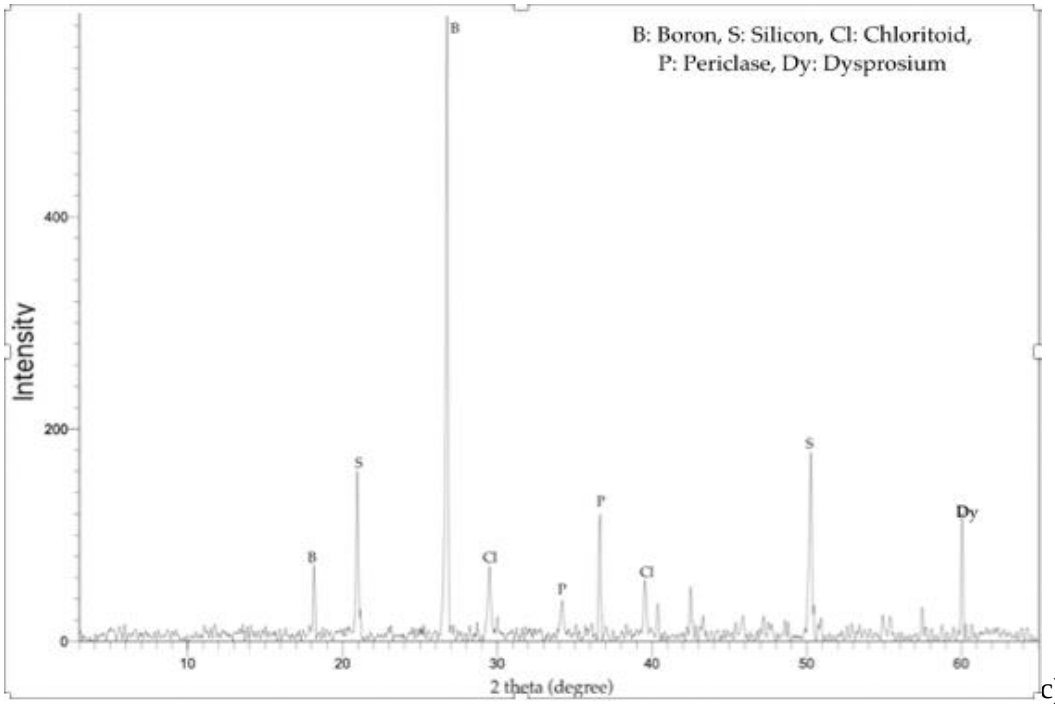
B: Boron, S: Silicon, Cl: Chloritoid,
P: Periclase, Dy: Dysprosium
Intensity
2 theta (degree)
B
S
B
Cl
P
P
Cl
S
Dy

c)

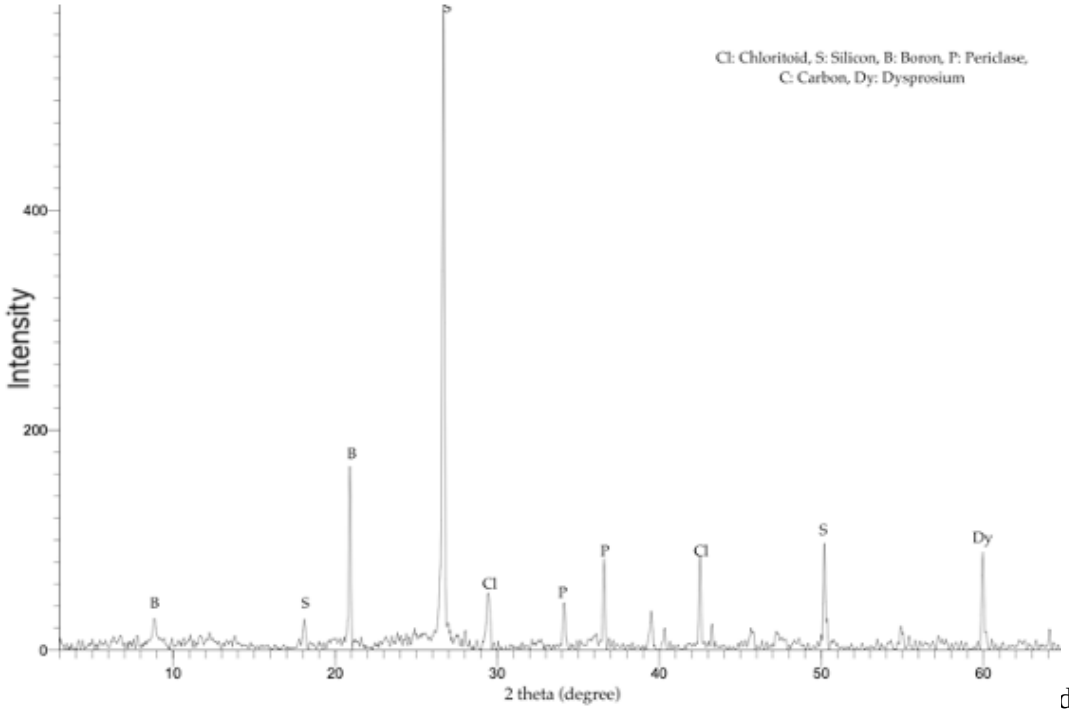
Cl: Chloritoid, S: Silicon, B: Boron, P: Periclase,
C: Carbon, Dy: Dysprosium
Intensity
2 theta (degree)
B
S
B
Cl
P
P
Cl
S
Dy

d)

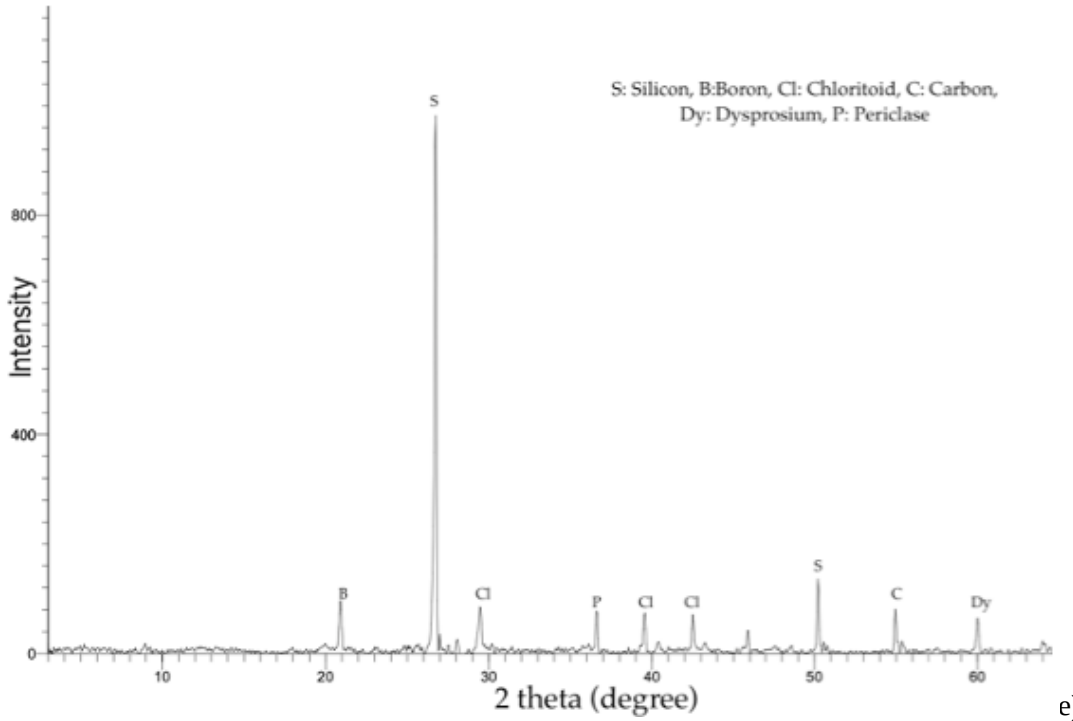
S: Silicon, B:Boron, Cl: Chloritoid, C: Carbon,
Dy: Dysprosium, P: Periclase
Intensity
2 theta (degree)
S
B
Cl
P
Cl
Cl
S
C
Dy

e)

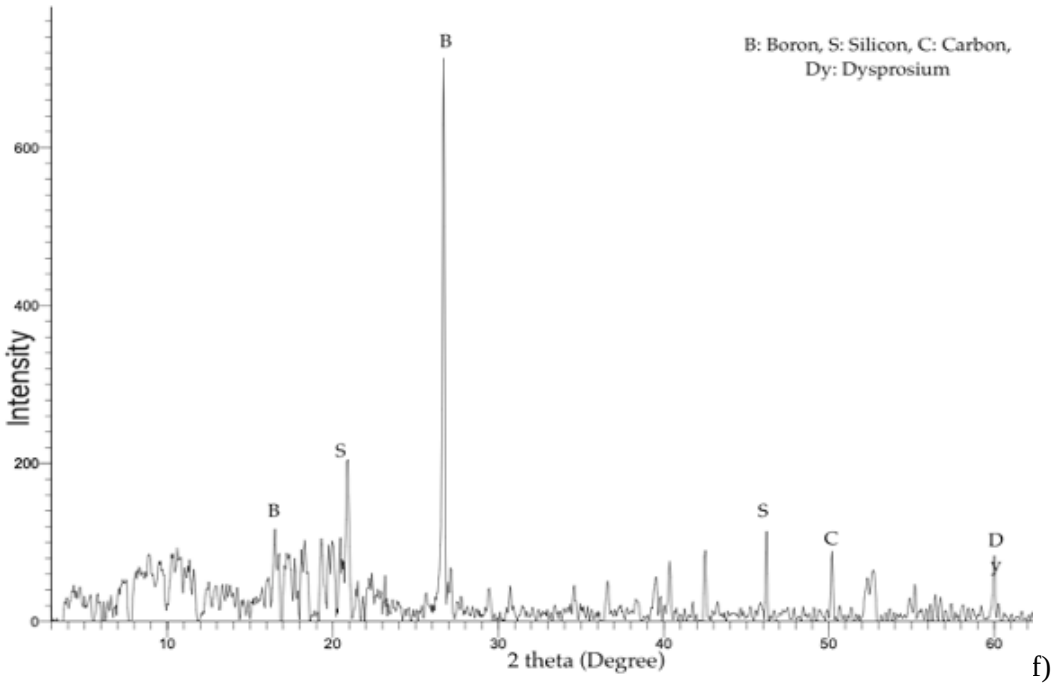

f)

Figure 3.3 XRD spectra of: a) unstabilised termite mound soil; b) Ordinary Portland Cement; **c**) specimens containing 5wt% of OPC; **d**) specimens containing 10wt% of OPC; **e**) specimens containing 15wt% of OPC; **f**) specimens containing 20wt% of OPC.

However, at 5 and 10 wt% there was not any change in the present minerals and the results show that the spectra are dominated by C–C–C bending, O–H stretching- their peaks remained intact too. Nevertheless, some peaks became slightly stronger in the bending and O–Si–O bending bands. In the stabilized mixtures, these bands remained the various stabilization levels showing the formation of cementation compounds as affirmed same, with some displacement. This can be explained by the evident substitution of some components from the EDX results. These changes observed in the spectra of the mixtures, especially for 2θ values were located at around 0–10° and 30–40°. These changes can be interpreted by the formation of new phases (chloritoid and carbon were observed in the stabilized specimens while absent in the initial termite mound soil) as a result of the hydration reaction.

iii. Fourier Transform Infra-red (FTIR) Characterization

The results show that the spectra are dominated by C–C–C bending, O–H stretching-bending and O–Si–O bending bands. In the stabilized mixtures, these bands remained the same, with some displacement. This can be explained by the evident substitution of the Si–

O bounds by Si–O–Al, resulting in the dissolution of the reactive phases (silicon, aluminum) [42].

The existence of network formation after the stabilization of TMS with Portland cement was displayed after the stabilization. This validates the SEM-EDX results where there was some insignificant formation of new phases, but mostly an increase in the number of existing phases was perceived as shown in Table 2. The stretching and bending vibrational absorption peaks of O–H shows the chemical bond of water in the stabilized TMS with cement. The hydration reaction generates calcium hydroxide from the calcium oxide which reacts with the carbon dioxide in the air. However, the carbonation reaction increases the bonding between the soil's particles resulting in compressive strength improvement due to the formation of C–S–H (calcium silicate hydrate) [10]. Figure 3.4 shows the details of the different absorption bands in the FTIR results.

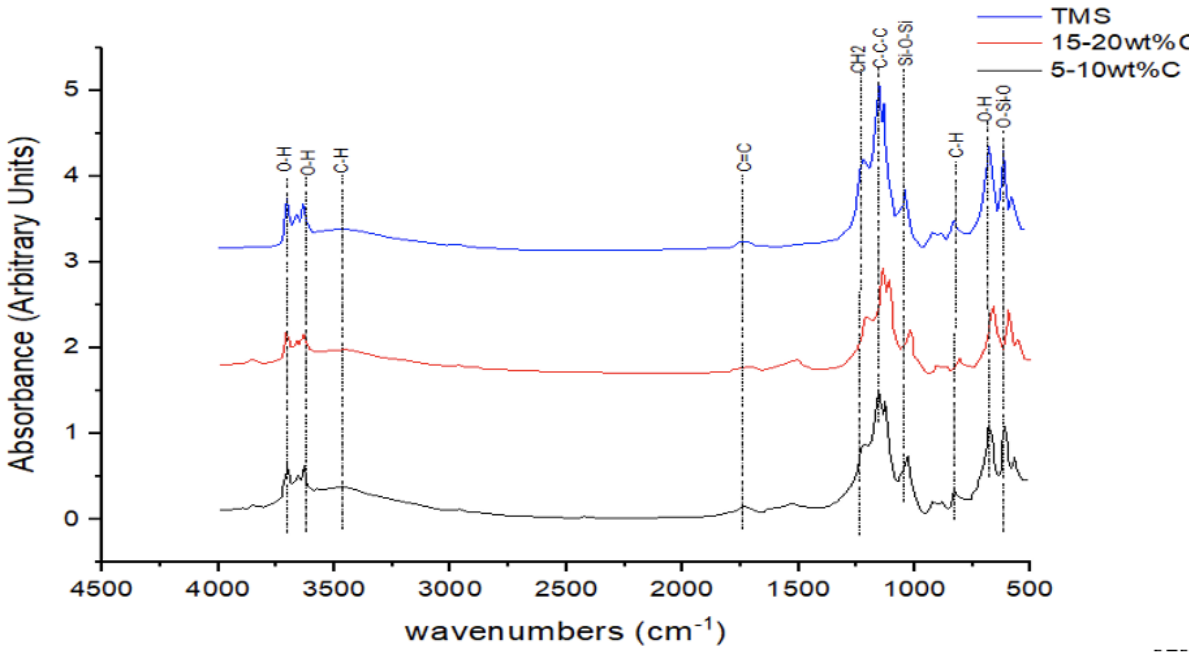

Figure 3.4 FTIR spectra of the unstabilised termite mound soil and the various stabilisation level (5wt%, 10wt%, 15wt% and 20wt%).

Table 3.2 Peaks and functional groups present in the various samples. Termite mound soil (TMS), termite mound soil 95%- cement 5% and termite mound soil 90%- cement 10% (TMS95C5 and TMS90C10), termite mound soil 85%- cement 15% and termite mound soil 80%- cement 20% (TMS85C15 and TMS80C20).

TMS (cm^{-1})	TMS5C95 & TMS	TMS15C85 &	Functional group

	10C90 (cm^{-1})	TMS 20C80 (cm^{-1})	
3854, 3695, 3650, 3620	3695, 3645, 3619	3851, 3695,3647, 3618	O-H stretching
1654	1652	1652	C=C stretching
-	1418	1418	CH_2 & CH_3 bending
1101,1032,1008	1032	1101	C-C-C bending
-	1070	1032,1007	Si–O–Si stretching
913	912	913	C-H bending
795, 694	753, 694	795, 694	O-H bending
538, 469	530, 469	538, 470	O–Si–O bending

b. Effect of Cement Stabilization on the Macrostructure (Compressive and Flexural Strengths, Fracture Toughness)

i. Compressive Strength

The results obtained from the compressive tests are presented in Figure 3.5**.** These show that the compressive strengths increased from the curing age of 7 days to 28 days for all the samples with the exception of the 5 wt% stabilization. The highest compressive strength obtained in this study was 13.91 MPa at 5 wt% replacement. Prior work by Elinwa [31] on calcined TMS showed that the highest compressive strength obtained was 25.9 MPa at 10% replacement. The variation of the results between the previous and present work may be attributed to the effect of calcination in the later work which increased the active elements within the TMS. However, in this current study the highest compressive strength met the minimum compressive strength required by the American Society of Testing Materials (ASTM) for a non-load bearing masonry unit.

Our results also show that the curing duration affected the compressive strengths. As the curing period increases, cementation compounds and reactions such as flocculation and reduction in plasticity may take place affecting the soil's strength from that point on. At 5wt% replacement of TMS by cement, higher crystallinity was observed than in the other mixtures; as load increases the particles tend to be denser, which results in filling the pores, subsequently increasing the compressive strength. The increase of compressive strength can also be attributed to the cementitious reaction taking place between the siliceous and aluminous components of the TMS and the calcium from the Portland cement. During the testing, the samples failed due to formation of almost-vertical surface cracks and

disintegration of sideways (Figure 3.5 b and c). This is an indication of the plastic deformation of the samples into a triangle-like shape causing the disintegration of the sides. Regardless of the disintegration of the sides, the central part remained intact although the samples experienced deformation and cracking before failure. The developed cracks were parallel to the loading direction.

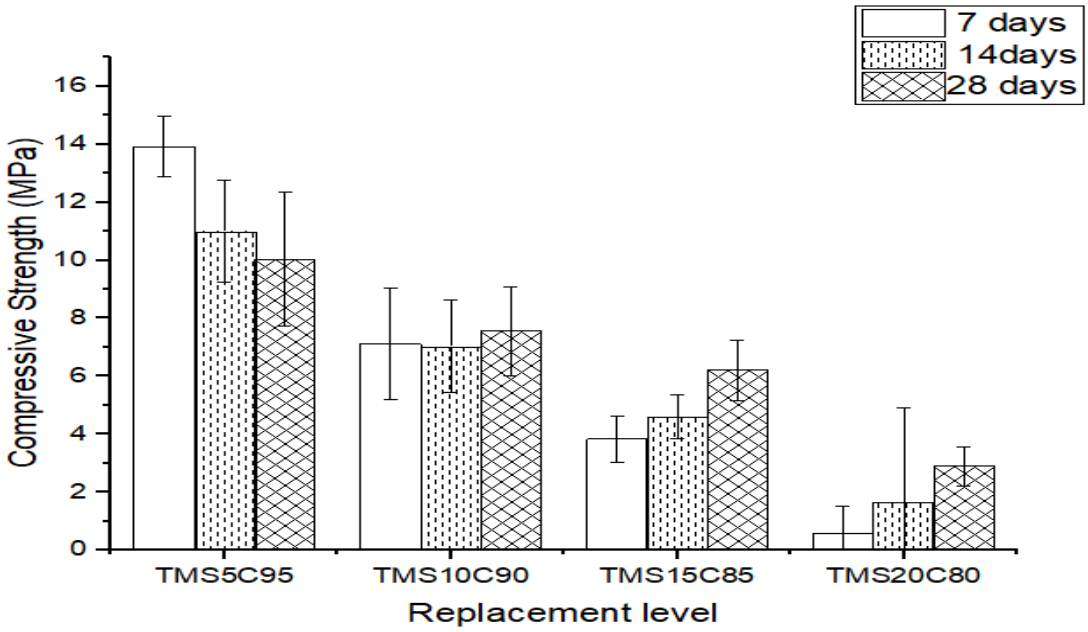

a)

b)


c)

Figure 3.5 a) Compressive strength of the samples at 5, 10, 15 and 20% stabilizations designated as TMS5C95, TMS10C90, TMS15C85 and TMS20C80 respectively at the different curing ages (7, 14 and 28 days), b) specimen failing under compression, c) specimen's failure under 3 points bending test.

ii. Flexural Strength

The results for the flexural strength tests are presented in Figure 3.6**.** The flexural strength increased proportionally to the curing time; from the early time of 7 days to 24 days, the flexural strength for all the samples increased. The unstabilized specimens and the specimens with 20 wt% of cement did not display any flexural strength at 7 days. The highest flexural strength was 10.25 MPa for 5 wt% replacement. However, in the study carried out by Elinwa [31] the stabilization of calcined soil and mound clay into cement had a greater effect on the flexural strength and the highest flexural strength was 7.2 MPa for 10 wt% for 28 days. The differences may be attributed to the soil mineralogy and chemical composition as they are not a "fits all" for all the termite mound soil; it is flexible and mainly dependent on the region where the termite mound is located. The results of the flexural strength followed the direction of the compressive strength; this confirms the relationship between the compressive and tensile strength established by Ajiboye in the case of partial replacement of powdered termite soil in concrete [28]. During the testing, it was observed that the initial crack was generated at the mid-span opposite to the loading

plane before failure as the applied load increased. The specimens underwent brittle failure. The tensile strength development also reflects the formation of the products from the hydration process in water over the curing age.

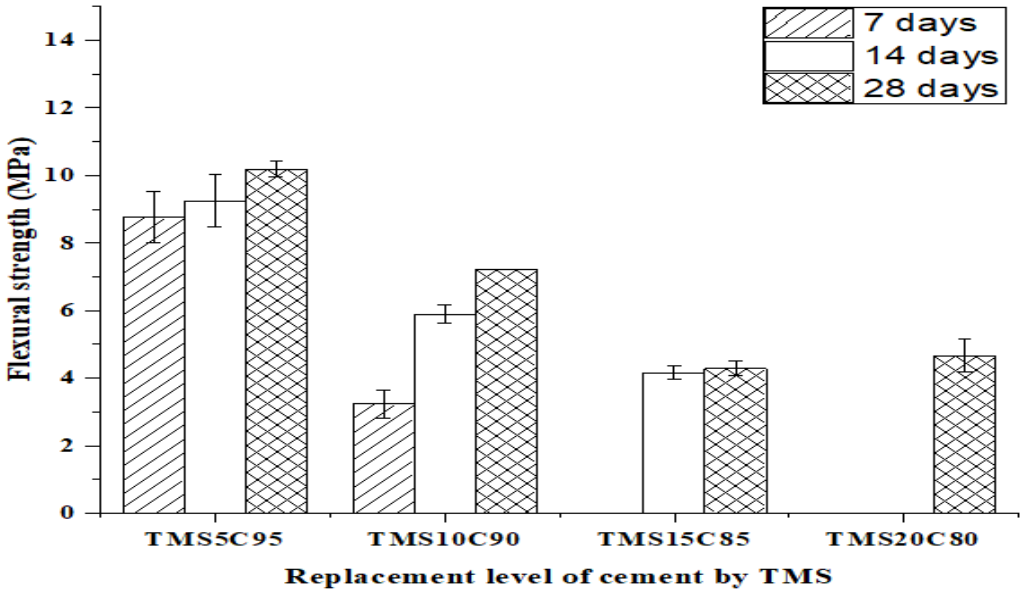

Figure 3.6 Flexural strength of the various samples with 5, 10, 15 and 20% stabilizations designated as TMS5C95, TMS10C90, TMS15C85 and TMS20C80 respectively at the curing ages of 7, 14 and 28 days

iii. Fracture toughness

The results for the fracture toughness tests are presented in Table 3. In this study, three-point bending tests were carried out on SENB specimens made from stabilized and unstabilized TMS in order to understand the mechanical behavior and crack propagation mechanism in the material to ascertain the cement stabilization's effect on the toughness of the TMS. The resistance curve obtained in Figure 3.7 gives the main information about initial and final stress intensity factors (K_0 and K respectively) and the ratio between the crack length and the specimen depth (a_0/W) obtained from the R-curves of individual samples tested for the different curing days (7, 14 and 28 days). The SENB technique allowed us to plot the R-curve as a function of crack propagation Δa; the evolution of cracks follows three stages [44]:

- If $\Delta a=0$ the crack propagation stops.
- If $0< \Delta a< \Delta a_c$ the crack propagation is stable.
- If $\Delta a> \Delta a_c$ the crack propagation is unstable.

Table 3.3 Information obtained from the R-curves of unstabilized and stabilized TMS.

Series	Samples	7 DAYS			14 DAYS			28 DAYS		
		K (MPa.m½)	a/W	P max load (KN)	K (MPa.m½)	a/W	P max load (KN)	K (MPa.m½)	a/W	P max load (KN)
Stabilized TMS	S1	0.0003	0.4	0.0001	0.0013	0.4	0.0005	0.00117	0.4	0.000451
	S2	0.0007	0.5	0.00025	0.0021	0.5	0.00069	0.00148	0.5	0.000506
	S3	0.0009	0.6	0.00027	0.0026	0.55	0.00075	0.00254	0.55	0.000796
	S4	0.0012	0.7	0.00032	0.0037	0.6	0.000975	0.00321	0.6	0.00094
	S5	-	-	-	0.0040	0.65	0.000998	0.00352	0.65	0.000956
Unstabilized TMS	U2	0	0.4	0	0	0.4	0	0	0.4	0
	U3	0	0.5	0	0	0.65	0	0	0.55	0
	U4	0	0.6	0	0	0.7	0	0	0.6	0

It can be observed that the initial crack was generated at the notch, which is at the opposite loading plane of the sample, and it propagates until failure occurs. The stabilized TMS displayed crack propagation mechanisms comporting stable propagation and unstable propagation. At the beginning of the loading, the crack propagation was stable, while it changed to unstable propagation as the loading increased. However, the stable propagation mechanism was considerably more important than the unstable propagation. At the early curing age of 7 days the samples did not show any resistance as they failed at loading of 0 KN. Nevertheless, the samples exhibited some toughness at the late curing age of 28 days: a stress intensity factor of 0.00352 MPa. √m and a/W = 0.65. The specimens are expected to acquire more toughness over a long curing period. The unstabilized TMS showed no toughness for all the curing days, although the crack propagation mechanism was stable. The unstabilized TMS specimens contained remarkable surface cracks; these surface cracks give rise to the stable growth.

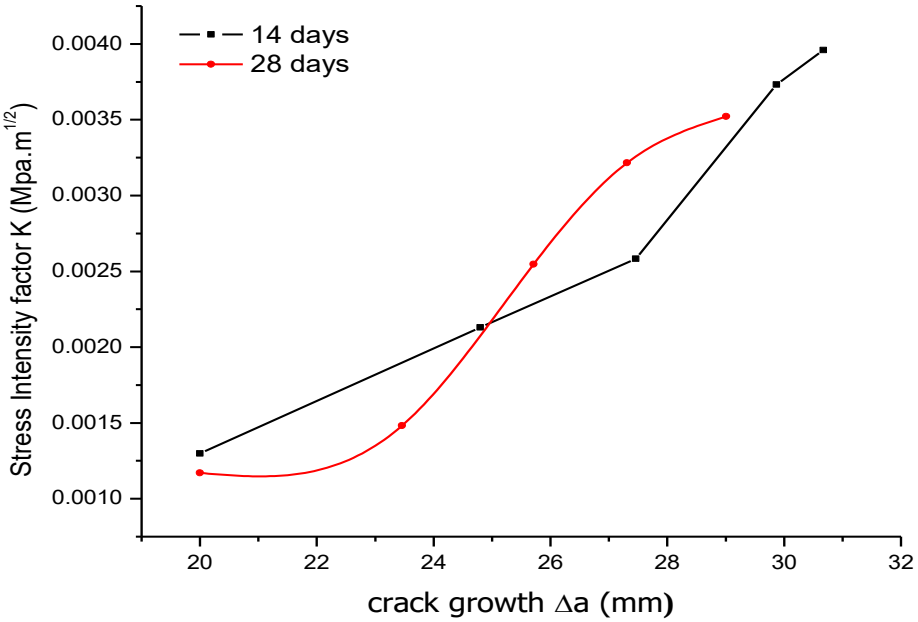

Figure 3.7 Fracture toughness of the 5 wt% stabilization after curing for 14 and 28 days.

iv. Statistical analysis of the mechanical properties

From the statistical analysis of the mechanical properties, it is observed that the unstabilized and stabilized TMS had no significant difference in the means of compressive strength for all curing days. At the 95% confidence level, the means of the flexural strength at 7, 14 and 28 days of curing are not significantly different for the stabilized TMS, while for the unstabilized TMS, the means of flexural strength were significantly different for all curing ages. Finally, for the fracture toughness, the statistical analysis showed a significant difference in the stress intensity factor over the crack growth for the stabilized TMS for all the curing days.

4. Conclusions

This aspect of the work presented the experimental investigation of the strengths (compressive and flexural) and fracture toughness of unstabilized and stabilized TMS. Indeed, the utilization of termite hill soil is aimed to produce eco-friendly materials in construction-related fields to address the problem of housing in the central African region, precisely in Chad. TMS stabilization with cement was used with the aim of obtaining an easily replicable engineering technique for that region, where termite hills are very

abundant but considered as natural waste. In fact, the stabilization of TMS was done by replacing partially the TMS (5 wt%, 10 wt%, 15 wt% and 20 wt%) using Portland cement to ascertain the effect of the cement as stabilizer and also to reduce the amount of cement required in construction. This implies a reduction of the total housing cost. Salient conclusions deduced from the study are presented below.

- The stabilization of TMS with 5% Portland cement showed good interactions between the two phases (cement and TMS) from the microstructural level to the macrostructures (mechanical behavior). Initially, the unstabilized TMS displayed some pozzolanic properties, thus the partial replacement by cement demonstrated very good bonding in addition to the hydration process products. Thus, the stabilization enhanced the TMS strengths due to the development of a greater bond between the soil and cements' particles for all the replacement levels.

- The highest compressive strength was obtained for 5 wt% stabilization. That compressive strength development is high due to the cement stabilization through the formation of a new strong network.

- The flexural strength development followed the compressive strength direction. However, the highest flexural strength observed was 10.25 MPa at 28 days for 5 wt% stabilization. This flexural strength is significantly greater than the results obtained from the calcined termite mound soil [31];

- The various stabilization levels (10, 15 and 20 wt%) did not display any toughness to fracture. Only the 5 wt% displayed some toughness despite its characteristics of crack propagation (stable and unstable). It exhibited the highest stress intensity factor 3.52 kPa. √m at a/W = 0.65 at 28 days.

References

1. Karim, M.R.; Hossain, M.; Khan, M.N.N.; Zain, M.F.M.; Jamil, M.; Lai, F.C. On the Utilization of Pozzolanic Wastes as an Alternative Resource of Cement. *Materials* **2014**, *7*, 7809–7827. [CrossRef] [PubMed]
2. Kim, T.; Tae, S.; Chae, C.U.; Lee, K. Proposal for the Evaluation of Eco-Efficient Concrete. *Sustainability* **2016**, *8*, 705. [CrossRef]
3. Zhang, H.; Wang, S.; Hao, J.; Wang, X.; Wang, S.; Chai, F.; Li, M. Air pollution and control action in Beijing. *J. Clean. Prod.* **2016**, *112*, 1519–1527. [CrossRef]
4. Pode, R. Potential applications of rice husk ash waste from rice husk biomass power plant. *Renew. Sustain. Energy Rev.* **2016**, *53*, 1468–1485. [CrossRef]

5. Bediako, M. Pozzolanic potentials and hydration behavior of ground waste clay brick obtained from clamp-firing technology. *Case Stud. Constr. Mater.* **2018**, *8*, 1–7. [CrossRef]
6. Mo, K.H.; Alengaram, U.J.; Jumaat, M.Z.; Yap, S.P.; Lee, S.C. Green concrete partially comprised of farming waste residues: A review. *J. Clean. Prod.* **2016**, *117*, 122–138. [CrossRef]
7. Memon, S.A.; Wahid, I.; Khan, M.K.; Tanoli, M.A.; Bimaganbetova, M. Environmentally Friendly Utilization of Wheat Straw Ash in Cement-Based Composites. *Sustainability* **2018**, *10*, 1322. [CrossRef]
8. Xu, W.; Lo, Y.T.; Ouyang, D.; Memon, S.A.; Xing, F.; Wang, W.; Yuan, X. Effect of rice husk ash fineness on porosity and hydration reaction of blended cement paste. *Constr. Build. Mater.* **2015**, *89*, 90–101. [CrossRef]
9. Olotuah, A.O. Recourse to earth for low-cost housing in Nigeria. *Build. Environ.* **2002**, *37*, 123–129. [CrossRef]
10. Obianyo, I.I.; Onwualu, A.P.; Soboyejo, A.B. Mechanical behaviour of lateritic soil stabilized with bone ash and hydrated lime for sustainable building applications. *Case Stud. Constr. Mater.* **2020**, *12*, e00331. [CrossRef]
11. Memon, S.A.; Khan, M.K. Ash blended cement composites: Eco-friendly and sustainable option for utilization of corncob ash. *J. Clean. Prod.* **2018**, *175*, 442–455. [CrossRef]
12. Sadh, P.K.; Duhan, S.; Duhan, J.S. Agro-industrial wastes and their utilization using solid state fermentation: A review. *Bioresour. Bioprocess.* **2018**, *5*, 1. [CrossRef]
13. Olorunnisola, A.O. Development of Sustainable Building Materials from Agro-Industrial Wastes in Nigeria. In *Sustainable Construction and Building Materials*; IntechOpen: London, UK, 2019.
14. Ojo, E.B.; Bello, K.O.; Ngasoh, O.F.; Stanislas, T.T.; Mustapha, K.; Savastano, H.; Soboyejo, W. Mechanical performance of fiber-reinforced alkali activated un-calcined earth-based composites. *Constr. Build. Mater.* **2020**, *247*, 118588. [CrossRef]
15. Ojo, E.B.; Mustapha, K.; Teixeira, R.S.; Savastano, H. Development of unfired earthen building materials using muscovite rich soils and alkali activators. *Case Stud. Constr. Mater.* **2019**, *11*, e00262. [CrossRef]
16. Park, J.; Tae, S.; Kim, T. Life cycle CO2 assessment of concrete by compressive strength on construction site in Korea. *Renew. Sustain. Energy Rev.* **2012**, *16*, 2940–2946. [CrossRef]
17. Bahurudeen, A.; Santhanam, M. Influence of different processing methods on the pozzolanic performance of sugarcane bagasse ash. *Cem. Concr. Compos.* **2015**, *56*, 32–45. [CrossRef]
18. Daniel, K. Make cities and human settlements inclusive, safe, resilient and sustainable. *UN Chron.* **2015**, *51*, 26–27. [CrossRef]
19. Onyelowe, K.; Van, D.B.; Igboayaka, C.; Orji, F.; Ugwuanyi, H. Rheology of mechanical properties of soft soil and stabilization protocols in the developing countries-Nigeria. *Mater. Sci. Energy Technol.* **2019**, *2*, 8–14. [CrossRef]
20. H. Foundation. Chad Economy. Available online: https://www.heritage.org/index/country/chad. (accessed on 15 December 2020).
21. Idris, M.K.; Boukar, M.M.; Adeshina, S.A. Analysis of Bad Roads Using Smart phone. In Proceedings of the 15th International Conference on Electronics,

Computer and Computation (ICECCO), Abuja, Nigeria, 12 December 2019; pp. 1–4. [CrossRef]
22. Indicateurs Économiques et Sociodémographiques. Available online: https://fr.countryeconomy.com/pays/tchadHighlight. (accessed on 22 October 2020).
23. World Bank in Chad—Overview. Available online: https://www.worldbank.org/en/country/chad/overview (accessed on 12 October 2020).
24. Ministère des Infrastructures et des Transports. Available online: http://www.mit-tchad.org/index.php/fr/. (accessed on 15 October 2020).
25. Awotera, P.O.; Akinwumi, I.I. Compressive Strength Development for Cement, Lime and Termite-hill Stabilised Lateritic Bricks. *Int. J. Eng. Sci.* **2014**, *3*, 37–43.
26. Mustapha, K.; Annan, E.; Azeko, S.T.; Kana, M.G.Z.; Soboyejo, W. Strength and fracture toughness of earth-based natural fiber-reinforced composites. *J. Compos. Mater.* **2015**, *50*, 1145–1160. [CrossRef]
27. Azeko, S.T.; Mustapha, K.; Annan, E.; Odusanya, O.S.; Soboyejo, W. Recycling of Polyethylene into Strong and Tough Earth-Based Composite Building Materials. *J. Mater. Civ. Eng.* **2016**, *28*, 04015104. [CrossRef]
28. Fapohunda, C.A.; Daramola, D.D. Experimental study of some structural properties of concrete with fine aggregates replaced partially by pulverized termite mound (PTM). *J. King Saud Univ. Eng. Sci.* **2020**, *32*, 484–490. [CrossRef]
29. Gandia, R.M.; Corrêa, A.A.R.; Gomes, F.C.; Marin, D.B.; Santana, L.S. PHYSICAL, MECHANICAL AND THERMAL BEHAVIOR OF ADOBE STABILIZED WITH "SYNTHETIC TERMITE SALIVA". *Engenharia Agrícola* **2019**, *39*, 139–149. [CrossRef]
30. Mujinya, B.; Mees, F.; Erens, H.; Dumon, M.; Baert, G.; Boeckx, P.; Ngongo, M.; Van Ranst, E. Clay composition and properties in termite mounds of the Lubumbashi area, D.R. Congo. *Geoderma* **2013**, *192*, 304–315. [CrossRef]
31. Elinwa, A. Experimental characterization of Portland cement-calcined soldier-ant mound clay cement mortar and concrete. *Constr. Build. Mater.* **2006**, *20*, 754–760. [CrossRef]
32. Omofunmi, O.E.; Oladipo, O.L. Assessment of termite mound additive on soil physical characteristics. *Agric. Eng. Int. CIGR J.* **2018**, *20*, 40–46.
33. Sarcinelli, T.S.; Schaefer, C.E.G.; Lynch, L.D.S.; Arato, H.D.; Viana, J.H.M.; Filho, M.R.D.A.; Gonçalves, T.T. Chemical, physical and micromorphological properties of termite mounds and adjacent soils along a toposequence in Zona da Mata, Minas Gerais State, Brazil. *Catena* **2009**, *76*, 107–113. [CrossRef]
34. Corrêa, A.A.; Bufalino, L.; Protásio, T.D.P.; Ribeiro, M.X.; Wisky, D.; Mendes, L.M. Evaluation of Mechanical Properties of Adobe Chemically Stabilized with "Synthetic Termite Saliva". *Key Eng. Mater.* **2014**, *600*, 150–155. [CrossRef]
35. Kandasami, R.K.; Borges, R.M.; Murthy, T.G. Effect of biocementation on the strength and stability of termite mounds. *Environ. Geotech.* **2016**, *3*, 99–113. [CrossRef]
36. Legget, R.F. American Society for Testing and Materials. *Nat. Cell Biol.* **1964**, *203*, 565–568. [CrossRef]
37. Jean-Pierre, B.; Moise, A.A.A.; Mauricette, S.-W.O.-N.; Sylvain, T.C.; Philippe, K.K.; Yao, T.; Ahouda, Y. Spatial distribution and density of termite mounds in a protected habitat in the south of cote d'ivoire: Case of national floristic center (cnf) of ufhb of Abidjan. *Eur. Sci. J.* **2015**, *11*, 241–259.

38. Firoozi, A.A.; Olgun, C.G.; Baghini, M.S. Fundamentals of soil stabilization. *Int. J. Geo Eng.* **2017**, *8*, 26. [CrossRef]
39. *British Standard Methods of Testing for Soil for Civil Engineering Processes*; British Standards Institution: London, UK, 1990; BS 1337: Part 2.
40. ASTM. *ASTM D854 Standard Test Methods for Specific Gravity of Soil Solids by Water Pycnometer*; ASTM Int.: Washington, DC, USA, 2002; Volume 4, pp. 1–9.
41. ASTM. *ASTM C 150 Standard Specification for Portland Cement*; ASTM Int.: Washington, DC, USA, 2005. [CrossRef]
42. Ayobami, A.B.; Bamidele, A.; Oluwanifemi, A. Influence of water repellent chemical additive and different curing regimes on dimensional stability and strength of earth bricks from termite mound-clay. *Heliyon* **2019**, *5*, 01182. [CrossRef]
43. Faria, O.B.; Battistelle, R.A.G.; Neves, C. Influence of the addition of "synthetic termite saliva" in the compressive strength and water absorption of compacted soil-cement. *Ambiente Construído* **2016**, *16*, 127–136. [CrossRef]
44. Soboyejo, W. *Mechanical Properties of Engineered Materials*; CRC Press: Boca Raton, FL, USA, 2002.

4.0 Chapter Four: physico-mechanical characterization and water sensibility analysis of Alkali activation of termite mound soil based on a natural alkaline activator

1. Introduction

Globally, the building and construction industry plays a major role to the accumulation of greenhouse gas emissions. This industry alone produces approximatively 30% of greenhouse gas emissions worldwide. It accounts for 40% of worldwide energy, 25% of worldwide water and 40% of worldwide resources (UNEP (2014). Cement is the most conventional used material in the construction industry. In 2019, cement production was approximately 4.2 billion tons per year making it the second-high volume commodity after water [1]. The Greenhouse gas emissions related to cement are largely from the energy consumption during the manufacturing of the raw materials to building's demolition. Cement utilization is extremely connected with depletion of mineral reserves particularly in regions where cement consumption rate is higher than the natural resources available.

Financial constraints, available resources would be the primary factors controlling a construction material's choice. On that account, green building technologies have overtaken the construction industry in the last decades. These green building technologies consist of the implementation of constructing using environmental-friendly processes in all the parts of the building's life [2]. The advantages of green buildings are environmental-friendly, natural resources and energy efficiency[3], low cost, and sustainability as a result increasing residents productivity [4]. Among the green buildings' materials, earth-based materials are the most commonly used historically. The use of earth-based materials in construction application is as old as mankind itself. Earth-based materials can be divided into minerals, rocks, soil and water. They constitute the raw material obtained on the earth crust. Nevertheless, not all earth-based materials can be used in construction; their utilization as building materials depends principally on their properties. TMS is the soil obtained from the termite's hill. During the construction of their nest (hill), termites use their salivary secretions and faeces to modify the surrounding soil through biological processes [5] making it a stronger material that can resist erosions over decades. But Kandasami et Al. found that the Atterberg limits (which are commonly used as signatures of clay mineralogy) were not different between the termite's mound soil and the surrounding soil)[5] confirming that termites are not effecting any changes in clay

mineralogy of the mound soils, contrary to what has been suggested by some researchers[6].

Termite's Mounds are spread throughout the tropics. Pomeroy investigated the abundance of termite mounds in Uganda [7], while in Nigeria, Ackerman studied their spread and effect on the environment [8][9] and Jean-Pierre B. studied the spatial distribution of termite's mounds soil in a protected environment in ivory coast [10]. The use of the TMS as a construction material is empirical and traditional without clear scientific explanation behind its usage, despite many studies carried on the termite's mounds soil a clear understanding has not come forth. Elinwa investigated the pozzolanic potential of the calcined termites' mounds, the addition of the calcined termites' mounds clay significantly advanced the initial and final setting times thus they classify it as an accelerator[11]. It's noteworthy that from their chemical analysis the calcined termites' mounds were predominantly composed of SiO_2, Al_2O_3, Fe_2O_3 with a near-neutral pH (7.5). In the termite's mounds, temperature and gases appear to be regulated therefore the interest of engineering these soil structures for sustainable and green construction. Investigations carried by [12] on termite's mounds clay showed that the use of water-repellent chemical contributed to reducing the water absorption level. In their investigation they used hydrated lime and silane/siloxane as additive to the Termites mounds clay. The inclusion of water-repellent admixture prevented thickness swelling of the samples and produced reduction in voids causing high compressive strength. While Kandasami examined the physical attributes of the termite's mound to analyze the internal network of the galleries and tunnels. They concluded that the porosity of the termite mound soil varied with the porosity increasing from the base to the top of the termite's mound, proving the effect of erosion on the top region of the mound [5]. Those applications of the termite mound soil from the literature show the benefits of TMS as a construction material; the main advantage is its natural pozzolanic features. The usage of TMS in construction is restricted due to its sensibility for water; the problem of elevated moisture contents remains unresolved. Thus, Kandasami suggests that TMS can be restricted only to drier climatic zones or those where rainfall spells are not prolonged. The product can waterproof and join the soil components. Gandia studied the physical, mechanical and thermal properties of adobe stabilized with the "synthetic termite saliva"[13]. The incorporation of the "synthetic termite saliva" into the soil, presented greater clay mineral particle cohesion and high hydrophobicity. But the use of "synthetic termite saliva" negatively interfered with

compressive strength. Hence, stabilization is a treatment used to improve the durability, strength of soils, also properties such as reduced plasticity and swelling potential are expected to be improved after the stabilisation [14]. There are many types of stabilizations, from mechanical to chemical. One type of chemical stabilisation is the Alkali activation. Alkali activated material encompasses any binder derived from the reaction of an alkali source with an aluminosilicate solid precursor [15] forming a solid material comparable to hardened Portland cement [16]. The use of an alkaline activating solution does improve the soils stability and reintroduce Greenhouse. Alkali activation technology offers the opportunity to utilize local naturally occurring raw materials as precursor TMS and activators (potash) with performances as good as cement, the termites mound used is an aluminosilicate-rich precursor subsequently it's desirable to use an alkali hydroxides source [17] subsequently the choice of potassium hydroxides. For Alkali Activated Materials (AAM), the gas emission was calculated to be lower than cement by 80 to 30% [18], the depletion of natural reserves is less because the Alkali activation technology allows to use waste ashes[19] and slags [20] into valuable materials by reducing heavy metals emission to the environment. Alkali activated materials are resistance to high temperature and fire, resistance to acid and chemical attack, volumetric stability after hardening, low thermal conductivity, low permeability and low cost [15]. The alkaline nature of the stabilizer affects greatly the pH of the soil by increasing it. However, in some cases the alkalinity will start decreasing at late curing ages because of the decrease in calcium ions as the hydration reaction progresses. That consumption of alkalinity indicates the occurrence of bonds formation and strengthening of soils [14]. The degradation of Alkali activated materials is much lower than the modern cement degradation as demonstrated by the Roman structures' resistance to degradation over the time.

Alkali activation has been proved to be a very friendly technique for mechanical improvement of aluminosilicates. Subsequently, the difference of this study from previous literature is to link the microstructure to the macrostructural responses. To achieve that, a better understanding of the alkali activation's effect on the termite's soil is required. It's foreseen that the alkali activation will greatly affect the mechanical behavior and dimensional stability of the termite's soil as a building material. This technique can reduce the CO_2 emission related with conventional building materials and the technique is easily practicable everywhere without very high energy consumption required thus breaking down the cost of sustainable housing.

The development of green, renewable and sustainable materials from termite mound soil through alkaline activation by the utilization of natural potash is aimed in this investigation. The derived objectives will increase standard housing accessibility in regions where the termite soil is abundant and doesn't represents any economic value (specifically in the sub-Saharan region).

2. Materials and Methods

a. Materials

The TMS in this study was obtained from deserted and inhabited mounds in Abuja, Nigeria. The soil was crushed manually and sieved prior to its usage as precursor during the samples moulding. The particle size distribution was performed by mechanical sieving and sedimentation (showing that the termite soil contained 50% of soil) in accordance with the BS 1377:2. The moisture content, Atterberg limits and specific gravity were performed on the soil. Table 4.1 shows the different properties of the soil. Electron Dispersive Spectroscopy EDX was used to determine the elemental composition of the termite mound.

Table 4.1. Termite's soil physical and chemical characteristics

Chemical composition	Mineral content	Particle size distribution	Atterberg limits	Specific gravity	Bulk density
SiO_2 51.26% Al_2O_3 23.89% Fe_2O_3 21.80% Others 3.05%	Quartz Kaolin	Clay 48% Sand 34% Silt 18%	Plastic Limit 30.17% Liquid Limit 17.9% Plasticity Index 12.2% Linear Shrinkage 6.5%	2.61	1.49 g/cm^3

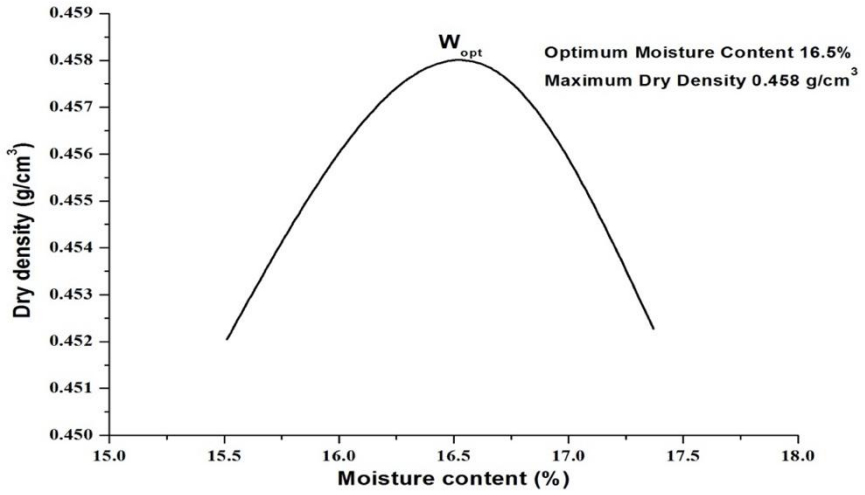

Figure 4.1. Dry density vs moisture content of termite mound soil

Potassium alum (KOH) or potash was obtained from, FCT-Abuja, Nigeria. The potash was obtained in the form of coarse grains with a whitish color. This was grounded to powder in a laboratory mechanical grinder. Its chemical composition was determined with EDX analysis the results showed that this potash is from the potassium sulfate group. The KOH was used due to its availability, its low cost, environmental-friendliness and performances. Thus, it was used in its natural occurrence as potash. Additionally, previous study showed that the use of NaOH as a chemical activating agent in natural pozzolan delayed the formation of and resulted in greater deformations for the samples [21]. It's noteworthy to recall that the TMS has been previously classified as natural pozzolona

The mixtures were prepared with 1, 3 and 5wt% of the activator and 15wt% of water. The precursor and activator were dry mixed in a laboratory mixer for 5 min before adding water at room temperature (27℃) and mixed for additional 5 min before pouring the paste into moulds of dimensions 50 x 50 x 50mm. The alkali activated termites' soil (AATS) was produced by one-part mix technique because of the similarity of the process in manufacturing earthen masonry units. Compaction technique was adopted for the production of the specimens. Studies have shown that the moulding techniques affects greatly the mechanical behavior[22], compaction technique uses the optimum moisture content which results in closely packed soil, hence improved performances [23], [24]. This technique allows to have more closely packed samples by reducing the voids within the

samples. Based on previous studies, the optimal activation concentration was investigated by preparing three proportions of the alkali activator 1%, 3% and 5% [25].

In this study, two initial curing temperatures (ICT) were adopted to determine the effect of the ICT variation on the specimen's micro and macro-structural behavior. Previous studies showed the effect of the initial curing temperature and the curing regime on the alkali activation process [26]. Subsequently, the first series was initially cured at 60°C while the second was initially cured at 105°C.

The Optimization of curing regime was obtained by subjecting the specimens into different environment. The first series was left unsealed in the laboratory environment at room temperature, contrary to the second series that was sealed inside plastic bags. While the last series was oven dried at 60°C for the curing period. Three different days, 7, 15 and 90 days, were considered for the curing period. Table 4.2 summarizes the details of the different set of specimens produced during this investigation. However, some specimens have not been tested without initial curing temperature (ICT) because of their workability. The specimens were losing their shapes as soon as demolded. While they were still wet after 7days of curing in the laboratory environment (27 ºC) without ICT. Thus, they couldn't be handled for mechanical testing as they tend to deform elastically when loaded under compression.

Table 4.2. Details of specimen's production.

	Room Temperature				Oven dried	
Designation	RTU1	RTU2	RTS1	RTS2	OD1	OD2
Initial Curing Temperature (°C)	105	60	105	60	105	60
Curing Regime	unsealed	unsealed	sealed	sealed	60	60

Thus, three (3) curing conditions were tested for the specimens each at two (2) different ICT making six curing tests. Those six curing tests namely are the unsealed room temperature cured specimens (initially cured at ICT1 & ICT2), sealed room temperature cured specimens (initially cured at ICT1 & ICT2) and oven dried specimens (initially cured at ICT1 & ICT2).

b. Characterizations

i. Physical properties

The specific gravity and bulk density of the samples were determined before and after alkali activation to access the effect of the Alkali activation on these properties. Furthermore, the pH for the different specimens under different curing regimes was evaluated to retrieve the effect of the potash on the termite soil at the different percent activation (1%, 3% and 5%) and different curing regime. In addition, the apparent porosity was examined on the activated and non-activated specimens to determine the role of the alkaline activation on the pores. Equation (2) was used to determine the apparent porosity. The dimensional stability analysis was performed based on the linear shrinkage; it is a way of quantifying the amount of shrinkage likely to be experienced by the material in dry conditions. The analysis was performed with the equation (1), it was performed before and after alkali activation to assess the behavior of the specimens under dry conditions, it determines the moisture content below which the material ceases to shrink. It's relevant to the condition of shrinkage due to drying. The dimensional stability was also investigated in wetting conditions by performing the water absorption analysis it's relevant to the condition of the materials' expansion due to wetting. The analysis allows identifying the behavior of the material when saturated.

$$Ls = 1 - \frac{Ld}{L0} \quad (1)$$

$$AP = 1 - \frac{Bulk\ Density}{Particle\ Density} \quad (2)$$

$$Water\ absorption\ (\%) = \frac{Mwet - Mdry}{Mdry} \times 100 \quad (3)$$

ii. X-Ray Diffraction (XRD) analysis

To determine the different minerals in the specimens and their respective transformations, X-ray Diffraction (XRD) was performed on the specimens after 15days. The analysis was achieved using an X-ray Diffractometer model ARL'XTRA (Thermo Scientific, Switzerland) with range of 10-70˚ (2θ) at 0.02˚ 2θ steps integrated at the rate of 4.0s per step. The patterns were processed using Match Software.

iii. Microstructure observation

The morphology and microstructure of the termite's soil (TS) and alkali activated termite's soil (AATS) were examined with the aid of Scanning Electron Microscopy-Energy

Dispersive Spectroscopy (SEM-EDX) to examine the repercussions of the chemical stabilization on the microstructure and morphology of the TS. Thus, the analysis was carried for all the specimens. The analysis was carried in a Carl Zeiss Model EVO LS10 instrumented with an EDX system that can detect elements between Sodium and Uranium. Prior to the analysis the specimens were coated with gold, to ease the imaging of the specimen's superficial appearances.

iv. Fourier Transform Infra-Red (FTIR) spectroscopy

To examine the type of bonds existing between the different elements of the Termite Soil (TS) and the Alkali Activated Termite Soil (AATS), Fourier Transform Infra-Red (FTIR) was carried on the different specimens. The analysis was conducted with a Thermo Scientific Nicolet iS5 FTIR system (Thermo Scientific, USA). The powder form of the different specimen was mixed with Potassium Bromate (KBr) in a ratio of 5:1 separately for each specimen. The software Know it all Bio-Rad was used to analyze the data obtained.

v. Mechanical properties

The mechanical properties examined was the uniaxial compression strength carried on a Universal testing machine Model 4002 & UTM7001 (Utest, Ankara, Turkey) at a loading rate of 0.6 kN/s. The specimens were tested after 7, 15 and 90 days for all the sets of specimens. The specimens from the different curing modes were oven dry for 24 h before testing. The compressive strengths were obtained from equation (4), prior to the testing the real dimensions of the specimens were estimated using Vernier calipers.

$$\sigma c = \frac{Fi}{Ai} \tag{4}$$

Where σc is the compressive strength in MPa, F_i is the applied load in N, and A_i is the cross-sectional area in mm^2. During loading the specimens deformed and failed differently hence the deformed specimens were analyzed with SEM to understand the bonds breakage. The software Origin was used to analyze the data and determine the different variations observed in the mechanical behavior.

3. Results and Discussions

a. From microstructural to macroscopic behavior

i. Macroscopic behavior

The micro and macro-structural behavior of construction materials affects greatly their properties, therefore it's important to link the two from the SEM to Photo images. Photos of the different sets of specimens were taken directly after demolding as shown in **Error! Reference source not found.**. The specimens initially cured at 105°C expanded beyond the mould, however that expansion wasn't considerable. The remaining specimens did not show any noticeable shrinkage or expansion. **Error! Reference source not found.**. b shows the difference in color that was very noticeable with the variation of activation level; at 1wt% of potash the specimens were dark in complexion while they are lighter at 3wt% but they become darker when the activator increased to 5wt%. The effect of the curing regime was considerable in terms of the sealing; the specimens that were sealed exhibited smooth surface with no cracks (**Error! Reference source not found.**. d) but were still wet at 15 days contrary to the unsealed specimens which exhibited significant surface cracks in **Error! Reference source not found.**. a. However, specimens initially cured at higher temperature (105°C) presented remarkable surface cracks while specimens initially cured at low temperature displayed smooth surface (60°C) as shown in **Error! Reference source not found.**. c&d indicating the effect of the ICT on the crack's initiation.


a
a
b
b
c
c
d
d


5%
KOH
3%
KOH
1%
KOH

c)

d)

Figure 4.2 a) Specimen with different curing regime at 3% of potash, b) Different percent of the activator: 1%, 3% and 5%, c) Noticeable cracks observed for the samples initially cured, d) Smooth surface exhibited by specimens initially cured at 60^{O}C.

ii. Microstructural examination.

The SEM images show that the specimens cured at high temperature RTU1 (**Error! Reference source not found.**.a) presented some surface cracks and pores (**Error! Reference source not found.**.e) which are generated by the shrinkage during the curing process. A possible explanation is that the reaction rate is slow as it can be seen from the low Si/Al ratio displayed by the specimens during the curing process. A flocculation within the particles was triggered by the activator resulting in shrinkage cracks around the external surface of the specimens. Meanwhile, the specimens with greater Si/Al=1.91 exhibited more spherulitic new phases filling the pore spaces by binding the particles as shown in Figure 4.3.b indicating the transformation of the matrix from irregular shapes to spherulite. In addition to the difference in Si/Al ratio, slight compositional differences were noticed between the specimens. Slaty et al. reported the same phenomenon in the alkaline activation of kaolinitic clay with NaOH [27]. The relict cracks detected in Figure 4.3.f can be the result of the unreacted termite soil indicating a lower dissolution rate of the termite soil and potash. Trace of iron oxide phases present in the EDX results could possibly play a role in the color change after curing of the specimens at high temperature (105°C) as perceived in the macroscopic observations in Figure 4.7. The Si/Al ratio varied from 2.29 to 3.19 for the specimens containing 1wt% of activator, while the Si/Al ratio varied from 1.23 to 1.63 and 1.32 to 1.99 for 3wt% and 5wt% potash respectively. That reveals the insignificant contribution in Silicon and Aluminum content by the potash activator. In all cases, the specimens initially cured at high temperature displayed higher Si/Al ratio in the 4 curing regimes contrary to the sealed specimens where the highest Si/Al ratio was displayed by the initially low temperature cured specimens. This can be explained by the composition and chemical reactions taking place within the sealed environment. Criado et al. (2008) observed that this parameter played an essential role in the kinetics, the structure and the composition of the initial gel formed [28] thus the mechanical behavior noticed.

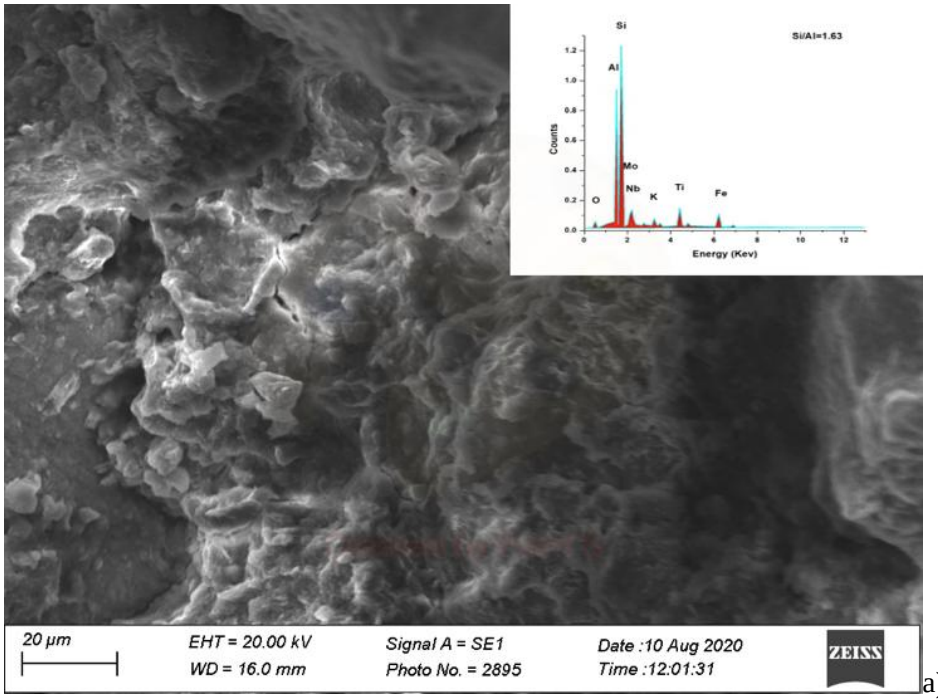
Si
Si/Al=1.63
Al
Mo
Nb
K
Ti
Fe
O
Counts
Energy (Kev)
20 µm
EHT = 20.00 kV
WD = 16.0 mm
Signal A = SE1
Photo No. = 2895
Date :10 Aug 2020
Time :12:01:31
ZEISS

a)

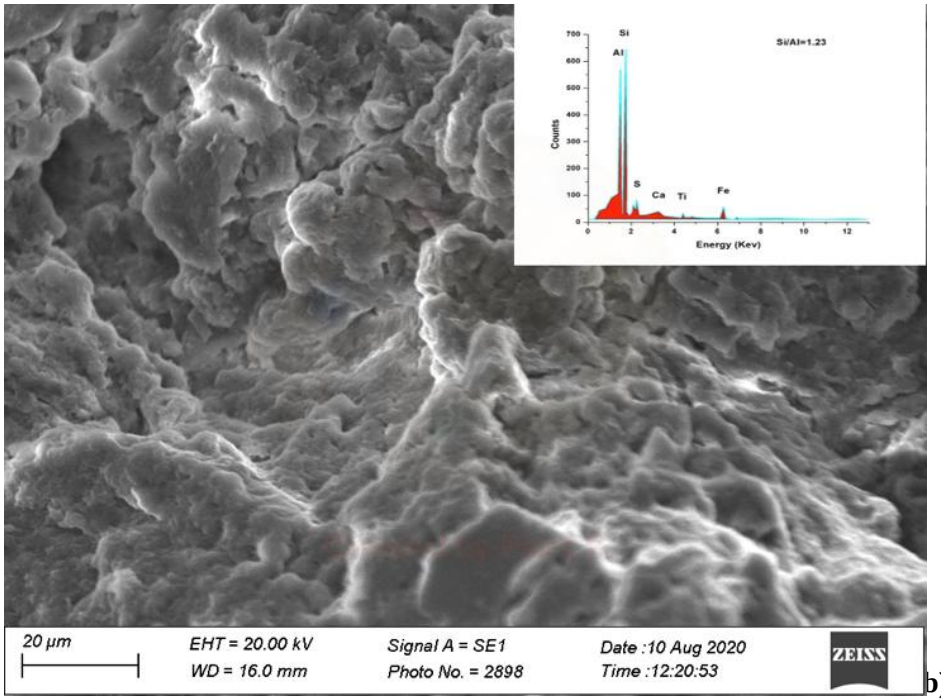
Si
Si/Al=1.23
Al
S
Ca
Ti
Fe
Counts
Energy (Kev)
20 µm
EHT = 20.00 kV
WD = 16.0 mm
Signal A = SE1
Photo No. = 2898
Date :10 Aug 2020
Time :12:20:53
ZEISS

b)

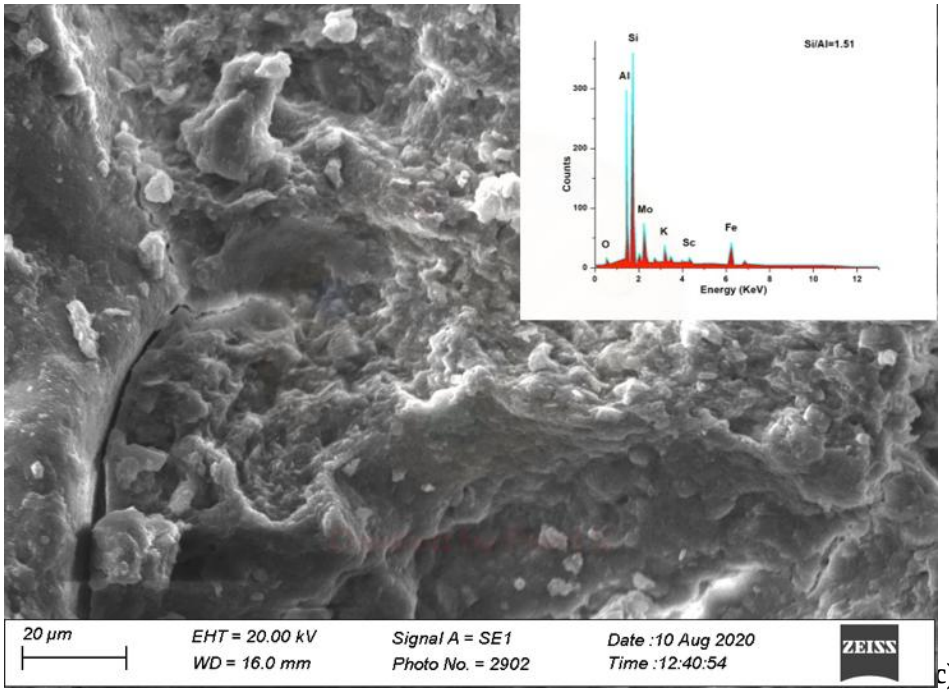
Si
Al
Mo
K
Sc
Fe
O
Si/Al=1.51
Counts
Energy (KeV)
20 µm
EHT = 20.00 kV
WD = 16.0 mm
Signal A = SE1
Photo No. = 2902
Date :10 Aug 2020
Time :12:40:54
ZEISS

c)

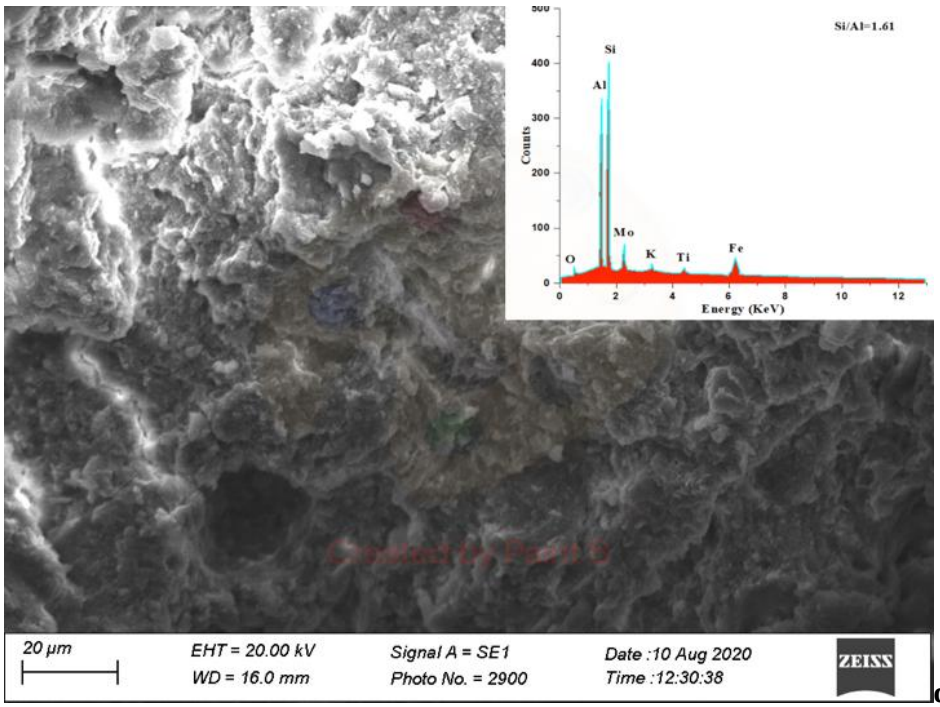
Si
Al
Mo
K
Ti
Fe
O
Si/Al=1.61
Counts
Energy (KeV)
20 µm
EHT = 20.00 kV
WD = 16.0 mm
Signal A = SE1
Photo No. = 2900
Date :10 Aug 2020
Time :12:30:38
ZEISS

d)

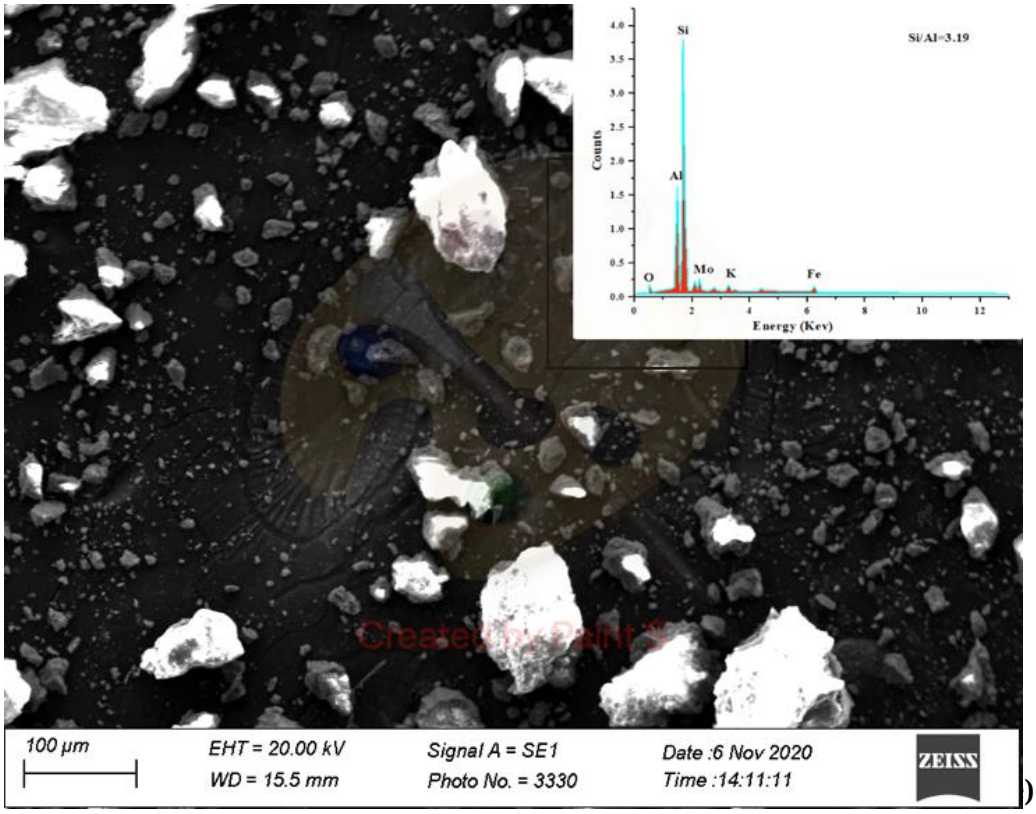
Si
Si/Al=3.19
Al
Mo
K
Fe
O
Counts
Energy (Kev)
100 µm
EHT = 20.00 kV
WD = 15.5 mm
Signal A = SE1
Photo No. = 3330
Date :6 Nov 2020
Time :14:11:11
ZEISS

)

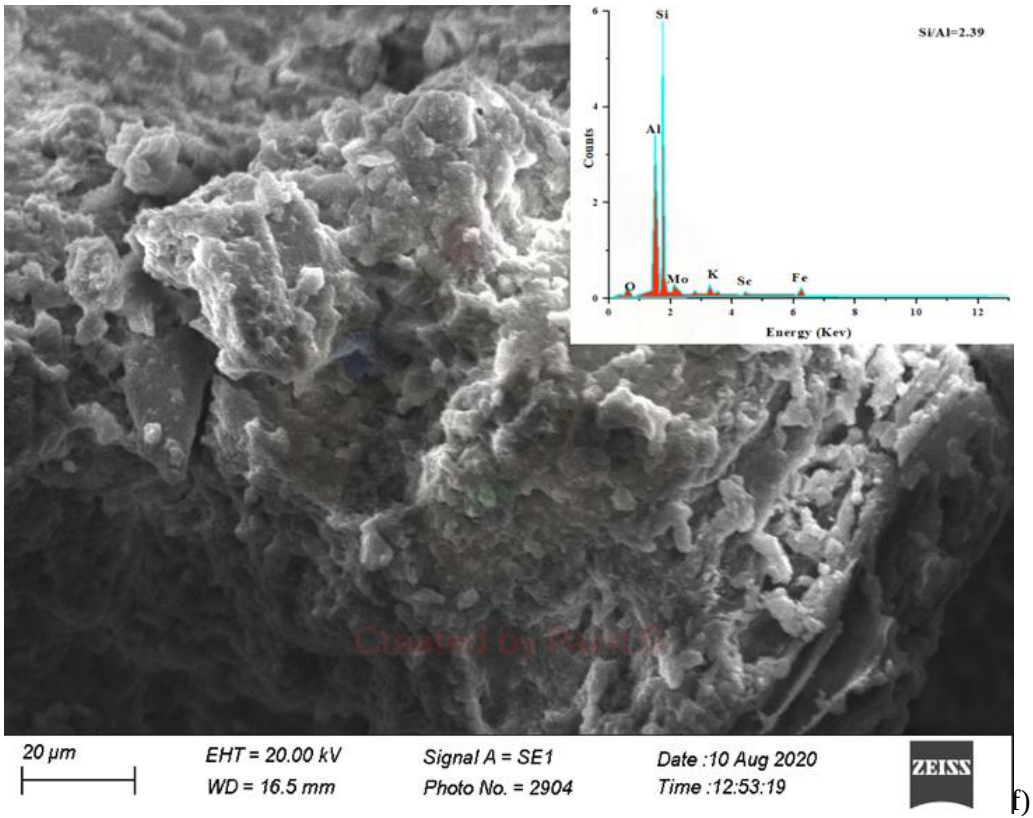
Si
Si/Al=2.39
Al
Mo
K
Sc
Fe
O
Counts
Energy (Kev)
20 µm
EHT = 20.00 kV
WD = 16.5 mm
Signal A = SE1
Photo No. = 2904
Date :10 Aug 2020
Time :12:53:19
ZEISS

f)

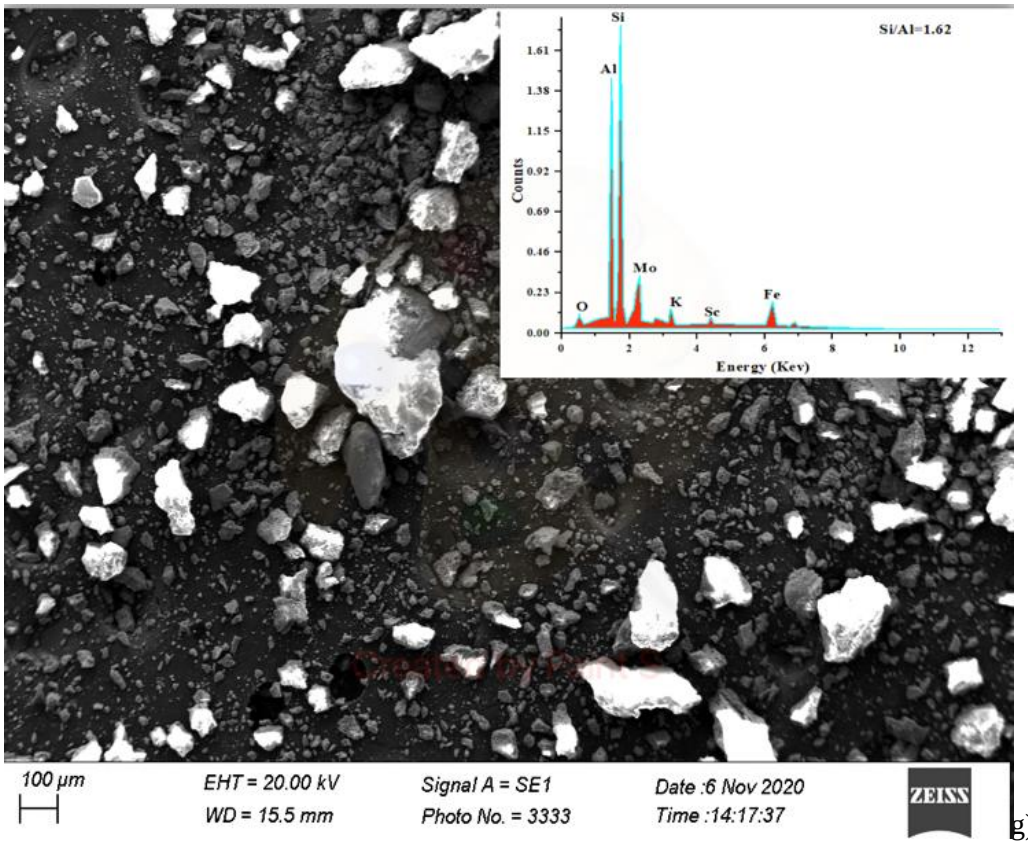
Si
Al
Mo
K
Sc
Fe
O
Si/Al=1.62
Counts
Energy (Kev)
100 µm
EHT = 20.00 kV
WD = 15.5 mm
Signal A = SE1
Photo No. = 3333
Date :6 Nov 2020
Time :14:17:37
ZEISS

g)

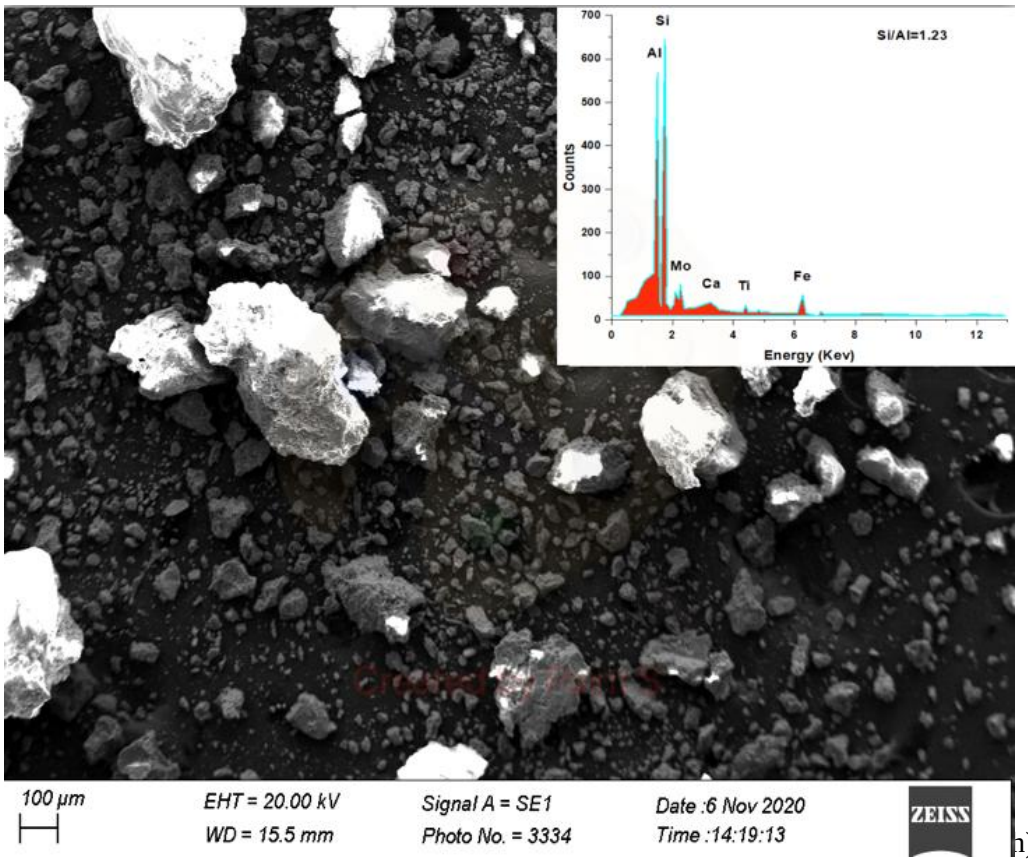
Si
Al
Mo
Ca
Ti
Fe
Si/Al=1.23
Counts
Energy (Kev)
100 µm
EHT = 20.00 kV
WD = 15.5 mm
Signal A = SE1
Photo No. = 3334
Date :6 Nov 2020
Time :14:19:13
ZEISS

h)

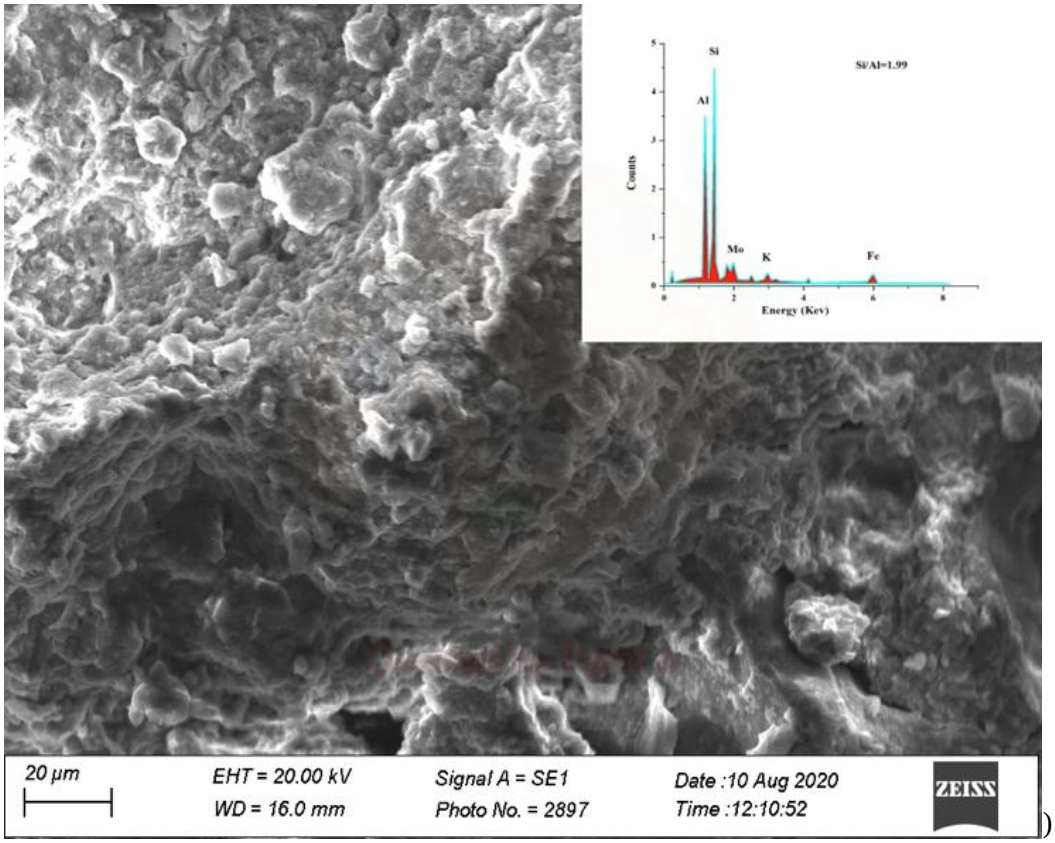
Si
Al
Mo
K
Fe
Si/Al=1.99
Counts
Energy (Kev)
20 µm
EHT = 20.00 kV
WD = 16.0 mm
Signal A = SE1
Photo No. = 2897
Date :10 Aug 2020
Time :12:10:52
ZEISS

)

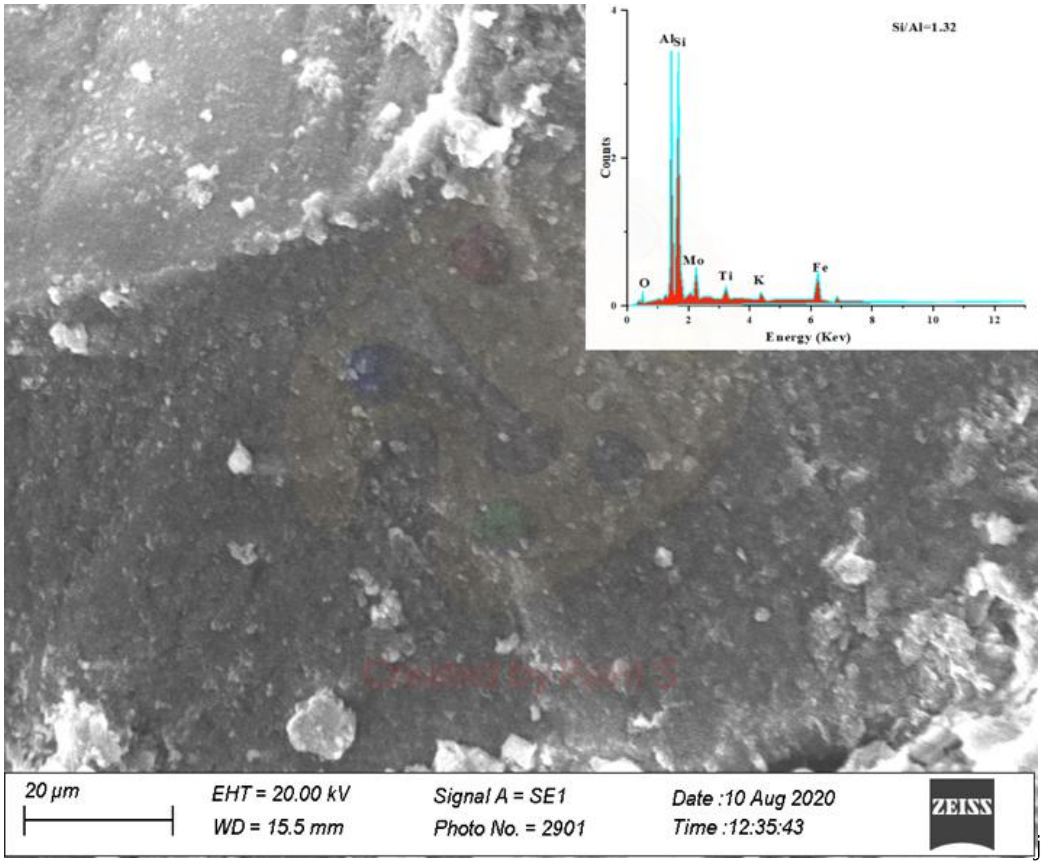
Al
Si
Mo
Ti
K
Fe
O
Si/Al=1.32
Counts
Energy (Kev)
20 µm
EHT = 20.00 kV
WD = 15.5 mm
Signal A = SE1
Photo No. = 2901
Date :10 Aug 2020
Time :12:35:43
ZEISS

j)

Figure 4.3 morphology of different specimens with chemical content micrographs of a) RTU1 b) RTU2, c) OD2, d) OD1 at 3wt% of potash. Of specimens with 1wt%: e) RTU2, f) RTS2, g) OD2 and specimens with 5wt% h) RTU2, i) RTS2 and j) OD2. With RT: Room Temperature curing

iii. Molecular bonding (FTIR)

Figure 4.4 shows the results of the FTIR analyses performed on all the specimens at 15days. Sharp peaks attributed to Si-OH were located at 3619 cm^{-1} to 3695 cm^{-1} for all the specimens with the exception of RTU2 and RTS2 at 1wt%. In these specimens the formation of new peaks was observed at 3854 cm^{-1} attributed to the Si-OH revealing the significant displacement of the band. Broad peaks assigned to the stretching -OH were observed around 3430 cm^{-1} in all the specimens with a band shift reaching values of ± 20 cm^{-1}, shift values are characteristic of aluminosilicate network formation[29]. Contrary to the specimens OD2 at 1wt% in which higher wavenumbers was evidenced around 3850 cm^{-1} and 3479 cm^{-1}. In any case, all the specimens presented broad peaks attributed to bending H-O-H around 1650 cm^{-1} with very slight shift values ranging ± 15 cm^{-1}. The main peaks located around 1090 and 500 cm^{-1} characterize the silicate structure with the assigned vibration of Si/Al-O and S-S stretching bond respectively reflecting the formation of amorphous aluminosilicate gel [30]. For the different curing regimes, the displacement of the different vibrations group is very imperceptible (Figure 4.4 a, b & c), whereas the change in intensity is remarkable for the different activation level (Figure 4.4 d). At 1wt% activator the FTIR spectrum is dominated by 1035cm^{-1} assigned to the vibration of Si/Al-O but with weaker intensity than in the specimens with 3wt% and 5wt%. However, 3wt% the peaks assigned to the stretching -OH were intense around 3430 cm^{-1} and the band assigned to the vibration of Si/Al-O reveal the formation of bond by the ring vibration of Si-O[30]

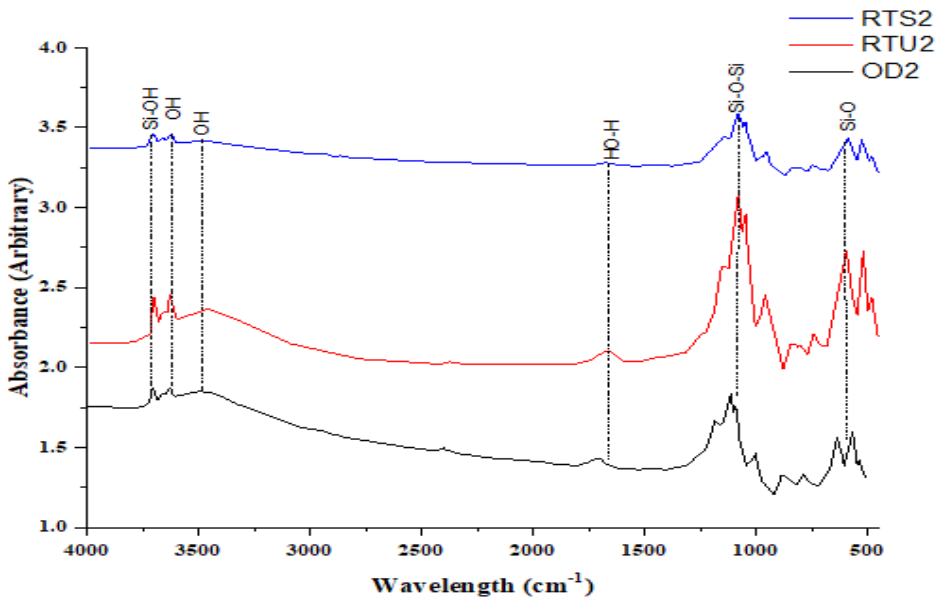
RTS2
RTU2
OD2
Si-OH
OH
OH
HO-H
Si-O-Si
Si-O
Absorbance (Arbitrary)
Wavelength (cm-1)

)

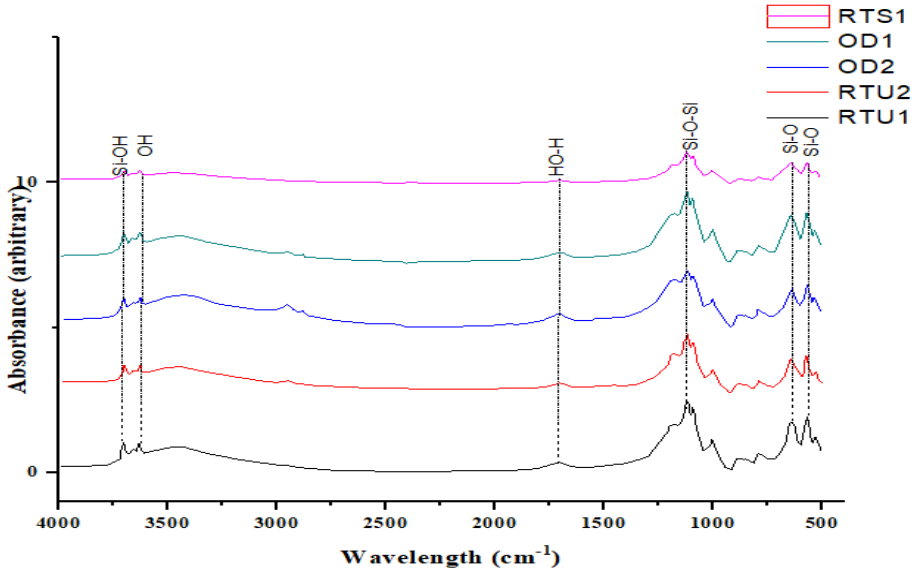
RTS1
OD1
OD2
RTU2
RTU1
Si-OH
OH
HO-H
Si-O-Si
Si-O
Si-O
Absorbance (arbitrary)
Wavelength (cm-1)

)

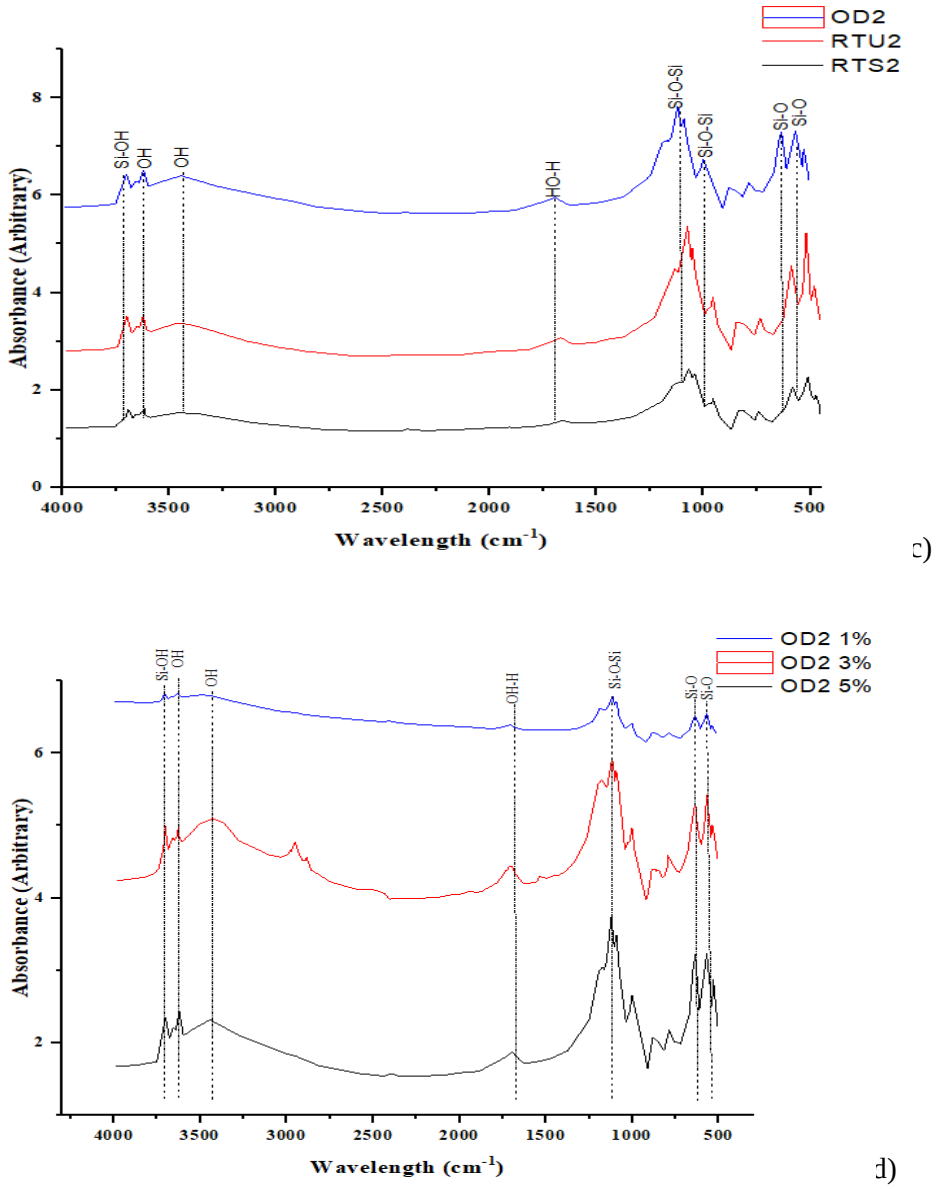

Figure 4.4 FTIR pattern for: a) specimens with 1wt% Potash, b) specimens with 3wt% Potash, c) specimens with 5wt% Potash and d) specimens at optimum curing regime for all the activation level

iv. Transformation of present minerals (XRD)

XRD patterns of the AATS for the different activation level are presented in Figure 4.5, they represent the different transformation by the minerals. The diffraction patterns showed that there is an appreciable transformation of the AATS with different activation level. The crystalline phases detected around $2\Theta = 21.5^{\circ}$ and $2\Theta = 26.5^{\circ}$ were transformed from quartz-kaolin to kaolin and from quartz to quartz-kaolin respectively from 1wt% to 3wt% and 5wt% potash.

At 3wt% of potash, Calcite ($CaCO_3$) [31] was detected at 2Θ = 29.5˚ while it was inexistent at 1wt% of potash (Figure 4.5.a &b), meanwhile the formation of Sylvite (KCl) [32] was observed for 5wt% potash around 2Θ = 27.5˚(Figure 4.5Figure 4.5c). In any case, at 1wt% activation the crystalline phases are mainly quartz and kaolin while at 3wt% quartz and kaolin peaks showed higher intensity than other activation levels, this reveals the higher dissolution reactivity of the termite soil precursor in the alkaline environment at that level. Additionally, formation of Calcite at 3wt% was observed then it was transformed into Sylvite at 5wt% activation. These phase transformation can be attributed to the potassium induction made by the activator and the formation of gel. The formation of calcite is related to the rapid dissolving of Ca obtained in the precursor in the alkaline solution and the precipitation of $Ca(OH)_2$ finally transforming into calcite [31]. While the formation of sylvite can be explained by the sulfate dependent oxidation taking place during the alkali activation of termite's soil [33]. Both calcite and sylvite are evaporite minerals. Thus, some of the quartz and kaolin remained unaltered during the activation revealing lower dissolution reaction between the remained quartz and kaolin with the activator. But calcite exhibits retrograde solubility (it becomes less soluble in water as the temperature increases)[34].

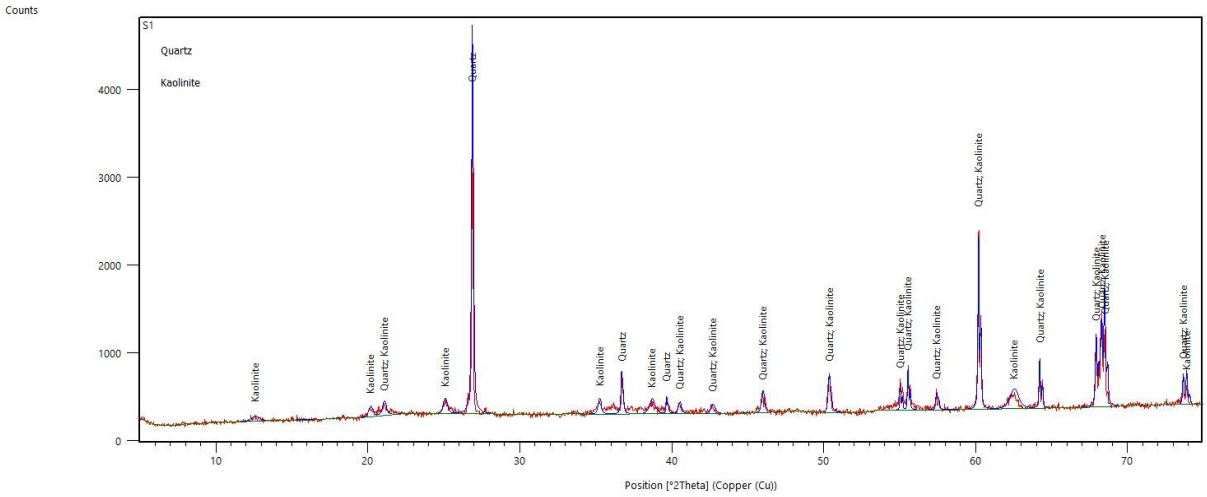

a)

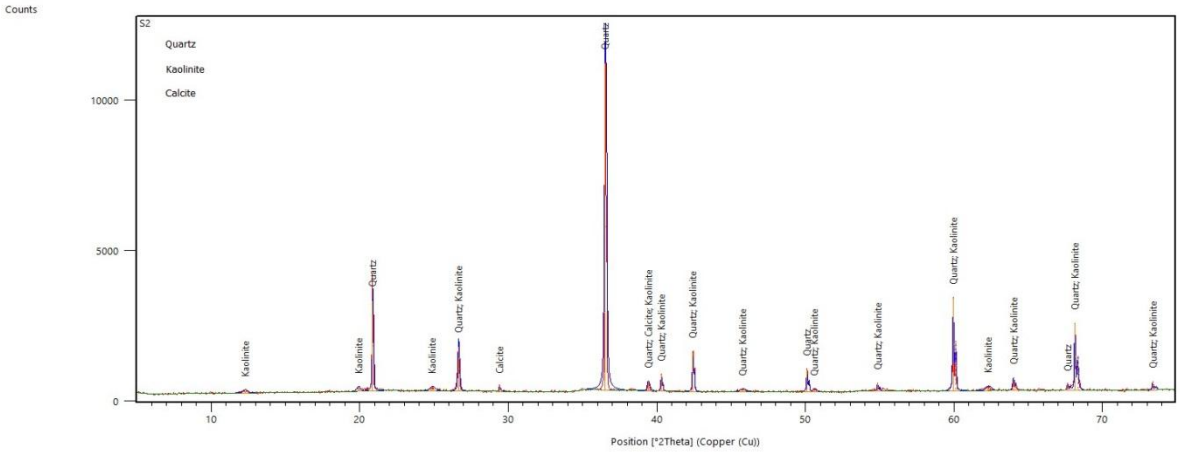

b)

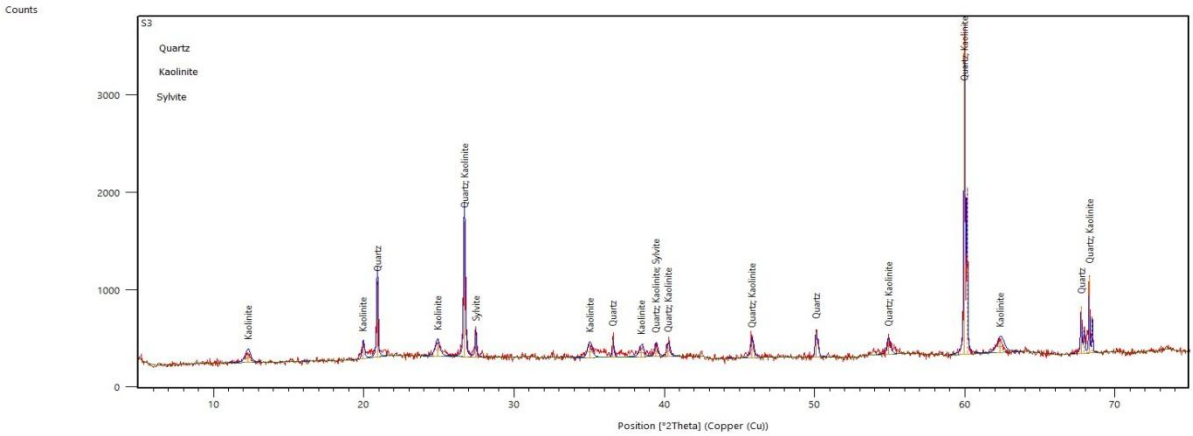

c)

Figure 4.5. XRD patterns for Alkali Activated Termite's Soil (AATS) at: a) 1wt% activator, b) 3wt% activator and c) 5wt% activator

b. Dimensional stability of the Alkali Activated Termite's Soil (AATS).

The linear shrinkage presented in Figure 4.6.a illustrates the behavior of the TS and AATS for the specimens. It was noticed that the shrinkage of both the TS and AATS were not really considerable in spite that the AATS showed less shrinkage. A possible explanation is that the alkaline reaction has induced some flocculation among the particles confirming the microstructural observations. Prud'homme et al. (2010) showed that the oxidation of silica during the alkali activation may produce hydrogen gas [35] inducing particles flocculation. That same reaction may have generated more pores within the specimens. Thereby, the specimens cured initially at low temperature under room temperature showed less sensitivity to water (Figure 4.6.c) compared to oven dried (Figure 4.6.d and Figure 4.6.d)

this is in accordance with the shrinkage mechanism investigated by Hailong Ye [36]. Ye et al. have established the correlation between the relative humidity and Shrinkage, as the viscous deformations occurring at high relative humidity triggered by the rearrangement of particles[37] contributes to the general shrinkage [36][37]. In our study, the specimens initially cured at high temperature showed more sensitivity to water (Figure 4.6.b).

The effect of the alkaline activation on the water absorbability of the specimens are summarized in Figure 4.7.a. Sealed, and room temperature cured specimens showed lower water absorption rate revealing more dense specimens. While the effect of the Alkaline activation on some physical properties (bulk density, specific gravity and apparent porosity) is shown in in Figure 4.7.b.

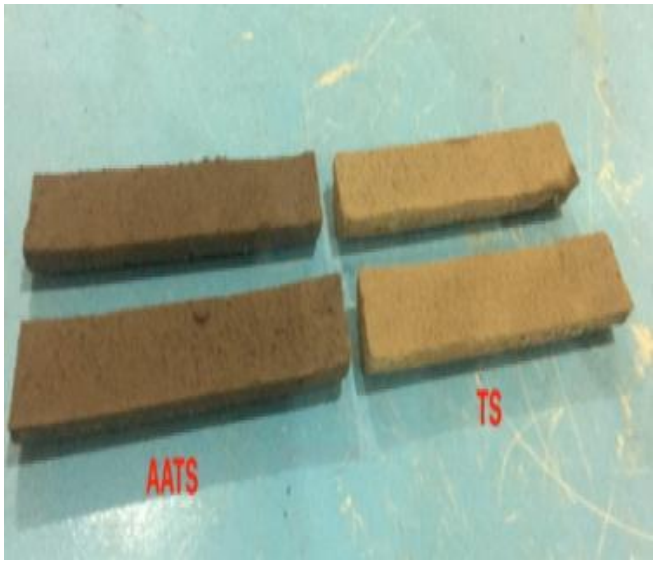

)

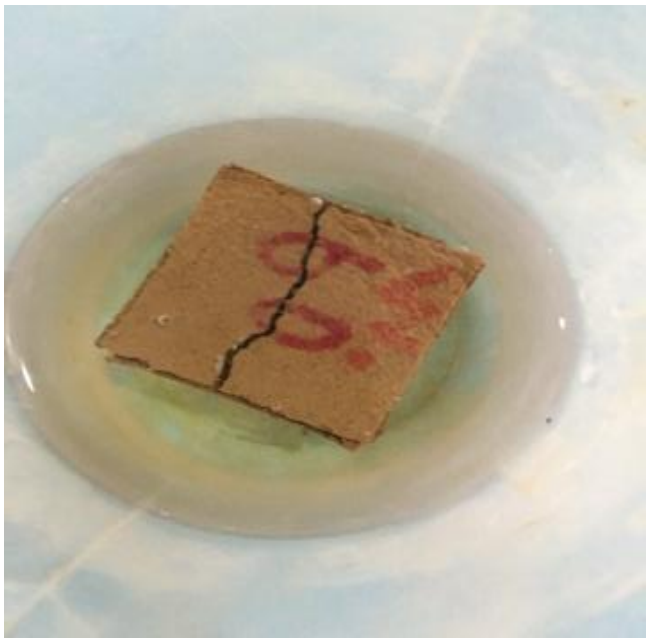

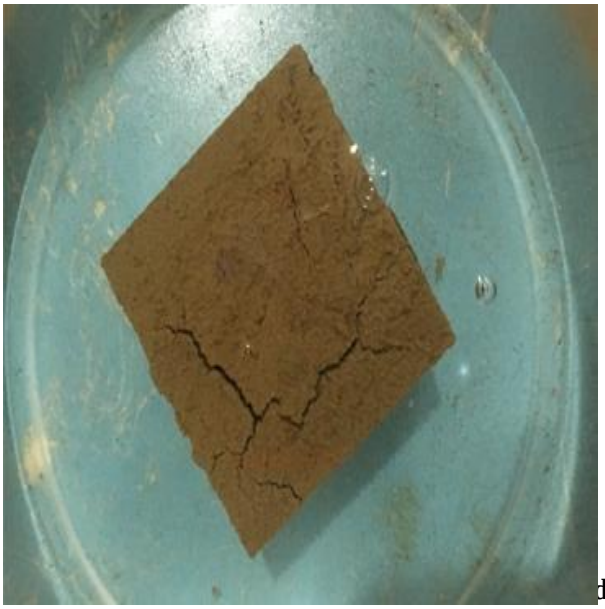

d)

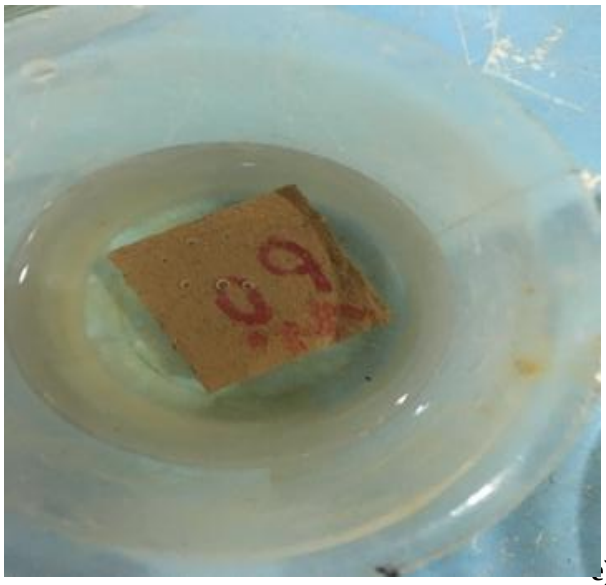

e)

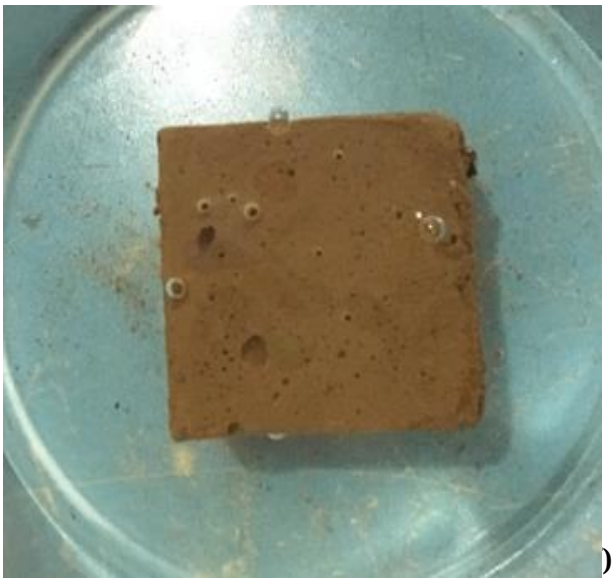

)

g)

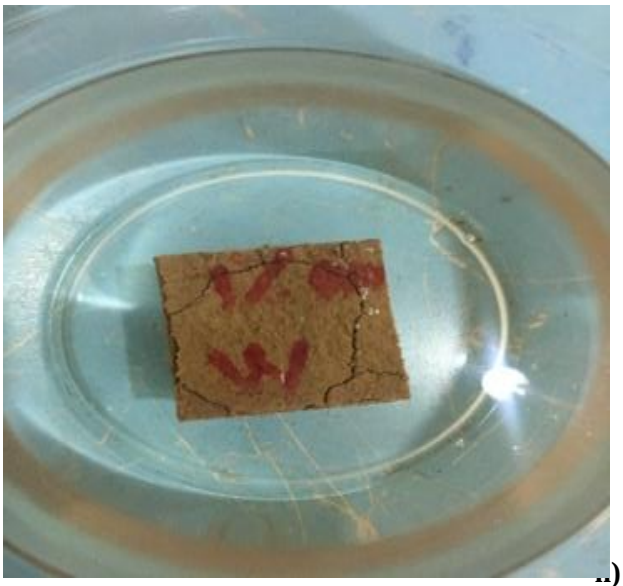

h)

Figure 4.6. a) Linear shrinkage of TS and AATS, b) saturated RTU1 specimens, c)saturated RTU2 specimens. d) saturated OD1 specimens. e) saturated OD2 specimens, f) saturated RTS1 specimens, g) specimens activated at 5% Alum, f) specimens activated at 1% Alum. With RT: Room Temperature curing, OD: Oven- Dried curing, U: Unsealed specimens, S: Sealed specimens,1: Initial curing temperature of 105°C, 2: Initial curing temperature of 60°C

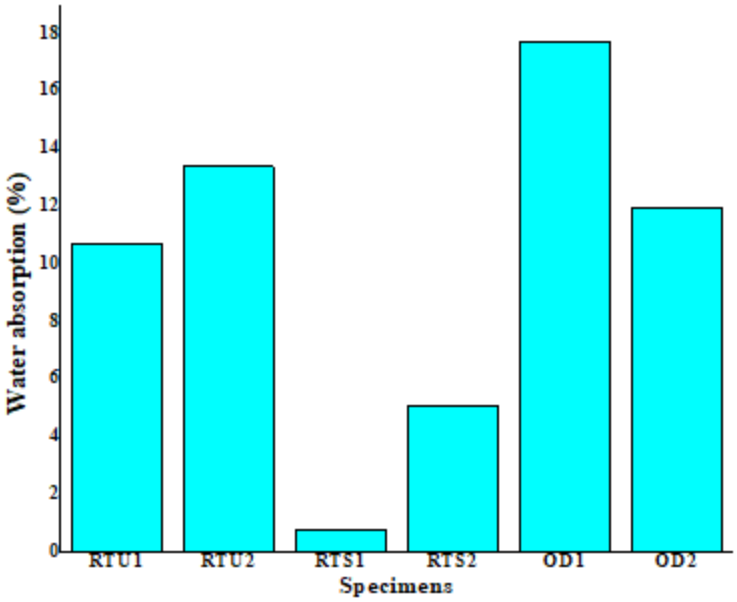

Figure 4.7. Water absorption of the specimens under different curing regime.

Table 4.3. Influences of the alkaline activation on the physical properties

Physical Properties / Specimens	Linear Shrinkage (%)	Bulk Density(g/cm^3)	Apparent porosity (%)	Specific gravity
*TS	6.7	1.47	41.9	2.61
[1]AATS	4.8	1.49	43.5	2.69

*TS: termite soil, [1]AATS: Alkali Activated Termite's soil

c. Influences of the alkaline activation on the soil's pH

The pH is a useful indicator of the AATS behaviour. The most critical role of the alkaline activator in an alkali-activated material is to dissolve the aluminosilicate and accelerate the reaction, which is obtained by generating a high pH [28]. Additionally, the effect of the pH on the activation of the TS is highly dependent upon the potash composition, since the solubility of silica and alumina increases causing the silicate to develop a greater mechanical strength. The alkaline nature of the potash affects the pH of the TS by increasing it or decreasing it depending on the ICT and curing regime. The consumption of alkalinity indicates that the formation of bonds and strengthening of the TS are occurring. The variation of the pH was slightly significant for the specimens with the same activator content for all curing regimes. That indicates that the curing regime affects the pH at a very insignificant level for the AATS. However, specimens initially cured at lower temperature displayed higher pH reveals the effect of the ICT on the specimen's alkalinity. Consequently, the potash reacted with the TS particles to cause the soil particles to flocculate into finer grain (as observed earlier in the SEM micrographs) or coarser grains [27]. When there are no significant reactions taking place between the activator and the soil that suggest that the soil remained intact.

d. Mechanical behavior of the AATS

The compressive strength of all the specimens at the age of 7, 15 and 90 days for the different activation levels and different curing regimes are presented in Figure 4.8. From the compressive strength results it can be noticed that at the early age of 7 days the specimens cured at lower temperature presented higher compressive strength than specimens initially cured at high temperature. The same trend was observed for the age of 15days with exception of the specimens that were oven-cured at 60°C revealing the

optimum initial curing temperature for the AATS. During testing the specimens failed by formation of oblique cracks which grew until separation of the specimens into 2 or more pieces. However, the innermost part of the sepcimens was less subjected to the deformation and it resisted until critical loading before failing. A possible explanation is that during the curing process, the existing calcite experienced a regressive solubility [38] due to the effect of curing temperature. The compressive strength has increased as the temperature increased. In any case, the highest compressive strength was attained by the specimens containing 3wt% activator under oven-dry regime revealing the optimum activation percent. Long curing times give origin to the formation of silica-rich products [28], allowing satisfactory formation of the potassuim aluminosilicate gel. Hence, favoring the development of the material's final resistances. The material owes its good mechanical performance primarily to the sodium aluminosilicate gel[39]. The standard deviation is so high in some cases because of the significant variation among the set of specimens tested for the compressive strength. Meanwhile, it is low for the sets where the variations among the specimens tested is not very significant (low), but the two closest results out of the tree have been considered to remediate to the high standard deviation.

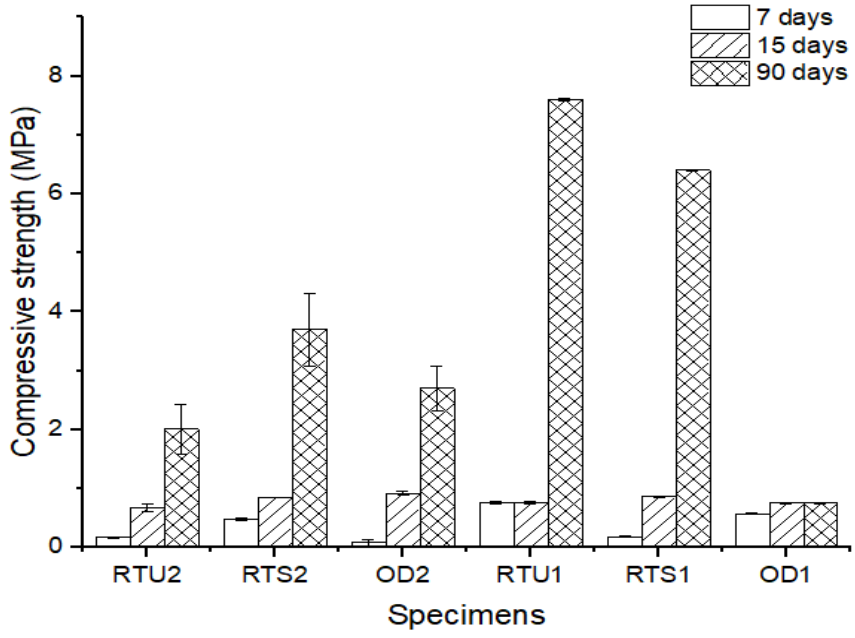

a)

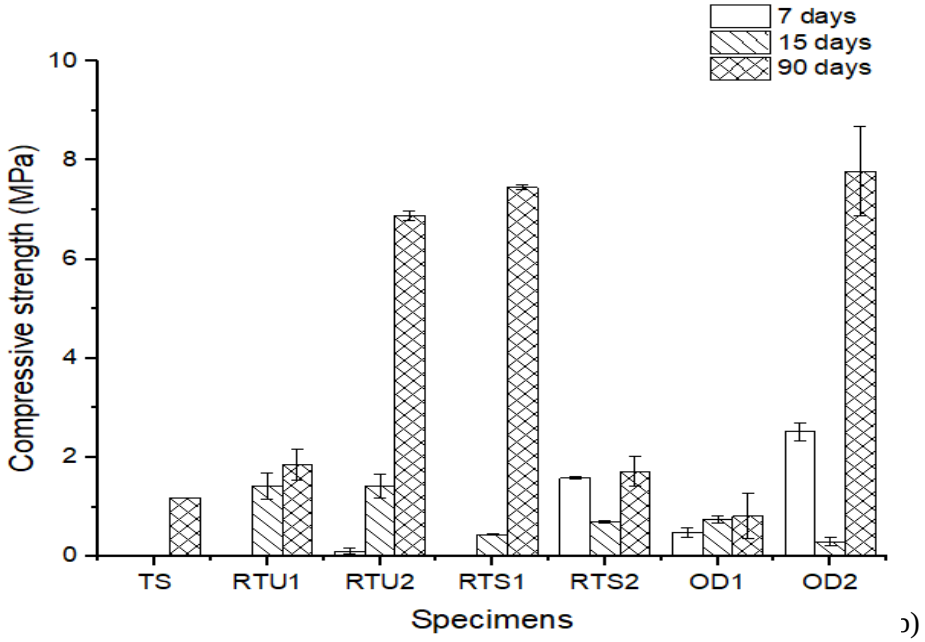

ɔ)

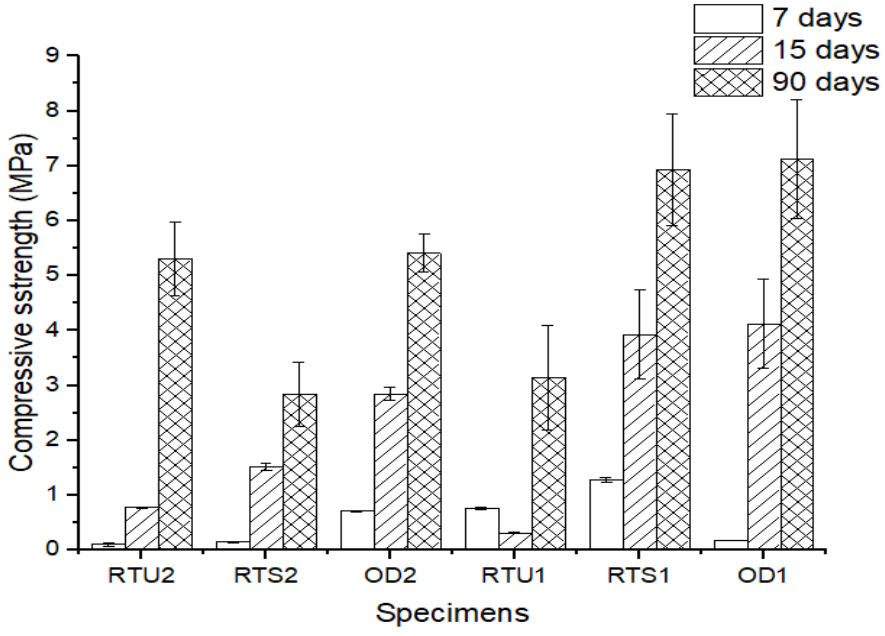

ɔ)

Figure 4.8. Compressive strength at 7,15 and 90 days for: a) 1wt% activation, b) 3wt% activation, c) 3wt% activation with RT: Room Temperature curing, OD: Oven- Dried curing, U: Unsealed specimens, S: Sealed specimens,1: Initial curing temperature of 105°C, 2: Initial curing temperature of 60°C.

4. Conclusions

The propitious experimental results obtained from this investigation can be used to produce AATS for sustainable and eco-friendly masonry units. Indeed, alkaline activation is a key component technique for a green and sustainable global future in construction materials.

This article reported the special effect of the activation concentration, initial curing temperature and curing regimes on the elemental, micro- and macrostructural behavior of AATS. The main findings of the study are summarized as follows:

- The alkaline activation favored reduction of linear shrinkage of the specimens. As the activation concentration increases, the linear shrinkage of the AATS decreases.
- The optimum ICT was 60°C as it favored dimensional stability by improving water sensitivity in dry and wet conditions. Also, by the impressive mechanical behavior displayed by the specimens initially cured at that low temperature. Although, the dissolution of alumina and silica from natural aluminosilicates require higher temperature.
- From the microstructural, elemental and compositional analyses, it can be concluded that the formation of phases is engendered by the dissolution of the potash. Thus, these phases are probably K-aluminosilicate gels responsible for the observed bindings.
- The ideal activation concentration for the compressive strength is 3wt%. In any case, the compressive strength does not increase proportionally with the activator concentration, whereas the highest compressive was obtained for 3wt% of the Potash.
- The highest compressive strength attained by the AATS in this study is 7.79MPa which is higher than the minimum required compressive strength by the ASTM C129 for nonload-bearing masonry units is (3.45 MPa)[40]. Therefore, a potential application of the AATS in construction is non-load-bearing masonry units.

Considering the availability of aluminosilicate globally and TMS in the sub-Saharan region particularly, this study shows that the alkaline activation can be an environmental-friendly technique to process the termite mound soil into a valuable construction material. Consequently, the results will contribute to the development of sustainable materials in construction from waste (the termite soil is considered as waste). The results are valuable for Sub-Saharan and regions where the high energy embodied materials are not affordable and where those natural materials are available (termite soil). The development of that technology represents an important opportunity to transform the natural waste into valuable, renewable and sustainable construction materials to preserve the ecosystem from greenhouses gas emission.

References

[1] N. Y. Jadhav, “Green Energy and Technology Green and Smart Buildings Advanced Technology Options.” [Online]. Available: http://www.springer.com/series/8059.

[2] N. Y. Jadhav, *Green Energy and Technology Green and Smart Buildings Advanced Technology Options*. .

[3] N. Afeez, S. A. Adeshina, A. Inci, and M. M. Boukar, *2019 15th International Conference on Electronics, Computer and Computation (ICECCO). "A framework for Poultry weather control with IoT in sub-Saharan Africa, "*. IEEE, 2019.

[4] United Nations Statistics Division (UNSD) and Division of the Department of Economic and Social Affairs (DESA)., “Make cities and human settlements inclusive, safe, resilient and sustainable.”

[5] R. K. Kandasami, R. M. Borges, and T. G. Murthy, “Effect of biocementation on the strength and stability of termite mounds,” *Environmental Geotechnics*, vol. 3, no. 2, pp. 99–113, Apr. 2016, doi: 10.1680/jenge.15.00036.

[6] M. L. and B. V. P. Jouquet, “jouquet2002,” *Insectes soc.*, vol. 49, pp. 1–7, 2002.

[7] D. E. Pomeroy, “This content downloaded from 128.184.220.23 on Fri,” 1978. [Online]. Available: http://www.jstor.orgURL:http://www.jstor.org/stable/2402920http://www.jstor.org/page/info/about/policies/terms.jsp.

[8] I. L. Ackerman, W. G. Teixeira, S. J. Riha, J. Lehmann, and E. C. M. Fernandes, “The impact of mound-building termites on surface soil properties in a secondary forest of Central Amazonia,” *Applied Soil Ecology*, vol. 37, no. 3, pp. 267–276, Nov. 2007, doi: 10.1016/j.apsoil.2007.08.005.

[9] M. K. Idris, M. M. Boukar, and S. A. Adeshina, “Analysis of bad roads using smart phone,” Dec. 2019, doi: 10.1109/ICECCO48375.2019.9043286.

[10] B. Jean-Pierre *et al.*, “Spatial distribution and Density of termite mounds in a protected habitat in the south of Cote d’Ivoire: case of national floristic center (CNF) of UFHB of Abidjan,” vol. 11, no. 3, 2015.

[11] A. U. Elinwa, “Experimental characterization of Portland cement-calcined soldier-ant mound clay cement mortar and concrete,” *Construction and Building Materials*, vol. 20, no. 9, pp. 754–760, Nov. 2006, doi: 10.1016/j.conbuildmat.2005.01.053.

[12] B. A. Akinyemi, A. Bamidele, and A. Oluwanifemi, “Influence of water repellent chemical additive and different curing regimes on dimensional stability and strength of earth bricks from termite mound-clay,” *Heliyon*, vol. 5, p. e01182, 2019, doi: 10.1016/j.heliyon.2019.

[13] R. M. Gandia, A. A. R. Corrêa, F. C. Gomes, D. B. Marin, and L. S. Santana, “Physical, mechanical and thermal behavior of adobe stabilized with ‘synthetic termite saliva,’” *Engenharia Agricola*, vol. 39, no. 2, pp. 139–149, Mar. 2019, doi: 10.1590/1809-4430-Eng.Agric.v39n2p139-149/2019.

[14] R. K. Dhir, G. S. Ghataora, and C. J. Lynn, “Geotechnical Applications,” in *Sustainable Construction Materials*, Elsevier, 2017, pp. 185–207.

[15] J. L. Provis, “Alkali-activated materials,” *Cement and Concrete Research*, vol. 114. Elsevier Ltd, pp. 40–48, Dec. 01, 2018, doi: 10.1016/j.cemconres.2017.02.009.

[16] J. L. Provis and J. S. J. van Deventer, “RILEM State-of-the-Art Reports State-of-the-Art Report, RILEM TC 224-AAM.” [Online]. Available: http://www.springer.com/series/8780.

[17] J. L. Provis and J. S. J. van Deventer, “RILEM State-of-the-Art Reports State-of-the-Art Report, RILEM TC 224-AAM.” [Online]. Available: http://www.springer.com/series/8780.

[18] B. C. McLellan, R. P. Williams, J. Lay, A. van Riessen, and G. D. Corder, “Costs and carbon emissions for geopolymer pastes in comparison to ordinary portland cement,” *Journal of Cleaner Production*, vol. 19, no. 9–10, pp. 1080–1090, Jun. 2011, doi: 10.1016/j.jclepro.2011.02.010.

[19] P. N. Lemougna, U. F. C. Melo, E. Kamseu, and A. B. Tchamba, “Laterite based stabilized products for sustainable building applications in tropical countries: Review and prospects for the case of Cameroon,” *Sustainability*, vol. 3, no. 1. pp. 293–305, Jan. 2011, doi: 10.3390/su3010293.

[20] Hans Kuhl, “Slag cement and process of making the same. United States patent office,” New York, Oct. 1908.

[21] M. Falah, R. Obenaus-Emler, P. Kinnunen, and M. Illikainen, “Effects of Activator Properties and Curing Conditions on Alkali-Activation of Low-Alumina Mine Tailings,” *Waste and Biomass Valorization*, vol. 11, no. 9, pp. 5027–5039, Sep. 2020, doi: 10.1007/s12649-019-00781-z.

[22] E. B. Ojo, K. Mustapha, R. S. Teixeira, and H. Savastano, “Development of unfired earthen building materials using muscovite rich soils and alkali activators,” *Case Studies in Construction Materials*, vol. 11, Dec. 2019, doi: 10.1016/j.cscm.2019.e00262.

[23] Q. B. Bui, J. C. Morel, S. Hans, and P. Walker, “Effect of moisture content on the mechanical characteristics of rammed earth,” *Construction and Building Materials*, vol. 54, pp. 163–169, Mar. 2014, doi: 10.1016/j.conbuildmat.2013.12.067.

[24] A. W. Bruno, D. Gallipoli, C. Perlot, and J. Mendes, “Effect of very high compaction pressures on the physical and mechanical properties of earthen materials.”

[25] L. Reig, L. Soriano, M. v. Borrachero, J. Monzó, and J. Payá, “Influence of the activator concentration and calcium hydroxide addition on the properties of alkali-activated porcelain stoneware,” *Construction and Building Materials*, vol. 63, pp. 214–222, Jul. 2014, doi: 10.1016/j.conbuildmat.2014.04.023.

[26] S. Ahmari, L. Zhang, and J. Zhang, “Effects of activator type/concentration and curing temperature on alkali-activated binder based on copper mine tailings,” *Journal of Materials Science*, vol. 47, no. 16, pp. 5933–5945, Aug. 2012, doi: 10.1007/s10853-012-6497-9.

[27] F. Slaty, H. Khoury, J. Wastiels, and H. Rahier, “Characterization of alkali activated kaolinitic clay,” *Applied Clay Science*, vol. 75–76, pp. 120–125, May 2013, doi: 10.1016/j.clay.2013.02.005.

[28] M. Criado, A. Fernández-Jiménez, A. G. de la Torre, M. A. G. Aranda, and A. Palomo, “An XRD study of the effect of the SiO2/Na2O ratio on the alkali activation of fly ash,” *Cement and Concrete Research*, vol. 37, no. 5. pp. 671–679, May 2007, doi: 10.1016/j.cemconres.2007.01.013.

[29] “76.FT-IR study of early stages of alkali activated materials based on pyroclastic deposits (Mt. Etna, Sicily, Italy) using two different alkaline solutions.”

[30] L. N. Tchadjié *et al.*, “Potential of using granite waste as raw material for geopolymer synthesis,” *Ceramics International*, vol. 42, no. 2, pp. 3046–3055, 2016, doi: 10.1016/j.ceramint.2015.10.091.

[31] P. T. Staudigel and P. K. Swart, “Isotopic behavior during the aragonite-calcite transition: Implications for sample preparation and proxy interpretation,” *Chemical Geology*, vol. 442, pp. 130–138, Nov. 2016, doi: 10.1016/j.chemgeo.2016.09.013.

[32] S. M. MacKenzie and J. W. Barnes, “COMPOSITIONAL SIMILARITIES AND DISTINCTIONS BETWEEN TITAN’S EVAPORITIC TERRAINS,” *The Astrophysical Journal*, vol. 821, no. 1, p. 17, Apr. 2016, doi: 10.3847/0004-637x/821/1/17.

[33] G. B. P. M. Claudio Finocchiaroa, “FT-IR study of early stages of alkali activated materials based on pyroclastic deposits (Mt. Etna, Sicily, Italy) using two different alkaline solutions,” *Construction and Building Materials* , vol. 262, 2020, doi: https://doi.org/10.1016/j.conbuildmat.2020.120095.

[34] J. W. Morse, R. S. Arvidson, and A. Lüttge, “Calcium carbonate formation and dissolution,” *Chemical Reviews*, vol. 107, no. 2. pp. 342–381, Feb. 2007, doi: 10.1021/cr050358j.

[35] E. Prud’homme *et al.*, “Silica fume as porogent agent in geo-materials at low temperature,” *Journal of the European Ceramic Society*, vol. 30, no. 7, pp. 1641–1648, May 2010, doi: 10.1016/j.jeurceramsoc.2010.01.014.

[36] H. Ye, C. Cartwright, F. Rajabipour, and A. Radlińska, “Understanding the drying shrinkage performance of alkali-activated slag mortars,” *Cement and Concrete Composites*, vol. 76, pp. 13–24, Feb. 2017, doi: 10.1016/j.cemconcomp.2016.11.010.

[37] H. Ye and A. Radlińska, “Shrinkage mechanisms of alkali-activated slag,” *Cement and Concrete Research*, vol. 88, pp. 126–135, Oct. 2016, doi: 10.1016/j.cemconres.2016.07.001.

[38] H. Drake *et al.*, “Extreme 13 C depletion of carbonates formed during oxidation of biogenic methane in fractured granite,” *Nature Communications*, vol. 6, May 2015, doi: 10.1038/ncomms8020.

[39] M. Torres-Carrasco and F. Puertas, “Alkaline activation of different aluminosilicates as an alternative to Portland cement: alkali activated cements or geopolymers La activación alcalina de diferentes aluminosilicatos como una alternativa al Cemento Portland: cementos activados alcalinamente o geopolímeros,” 2017. [Online]. Available: www.ricuc.cl.

[40] American Society for Testing Materials C129. Non load-bearing Masonry, “ASTM C129.”

5.0 Chapter Five: Machine Learning approaches for prediction of the compressive strength of alkali activated termite mound soil

1. Introduction

Over the last decade, a global shift has been noticed in the field of construction. The requirements are oriented in terms of eco-friendliness, renewability, cost, availability, reliability and sustainability for construction materials. These requirements are driven by the ecosystem protection's concerns to reduce CO_2 emission and use wastes for repairing, upgrading and constructing [1]. Most of the research effort are directed towards innovating empirical and traditional materials for construction through modern and sustainable technologies, thus the interest in earth-based materials [1]–[3]. Earth-based materials have long been used empirically as a construction material, among them the termite mound clay [4]. TMS is the soil obtained from the anthill [5]–[14]; it is spread abundantly around the tropics [15] but considered as waste[16]–[22]. Additionally, in the construction field experimental tasks are time consuming, very expensive and some properties cannot be easily modelled due to the complex relationship between the mechanical properties and the constituents.

In order to minimize the experimental tasks and increase accuracy of data, researchers focused on the use Artificial Intelligence (AI) models which are similar to human brain[23] and capable of solving very complex variables [24][25]. Machine Learning (ML) is a subset of AI used to anticipate and evaluate various properties of construction materials. Hence, ML approaches have gained a lot of interest in construction applications to predict the structural behavior of different elements. In addition, data processing indicated high efficiency performance because the outputs can be predicted using the inputs without knowing their correlations [26]. ML models consist of computer algorithms capable of generating (anticipating) patterns and hypotheses through a provided dataset for future values. They have been proven to be effective in saving time, cost, their ability to satisfy the requirements of various design codes, standards [27] and future applications. ML techniques can accurately predict behavior of materials [28] although the relationships between the input and output are nonlinear [27] or not easily modeled [29]. In the prediction of concrete behavior, Artificial Neural Networks (ANN), support vector

machines (SVM), decision trees, and evolutionary algorithms (EA) are the four mainly used models [27].

In Naderpour's et al. (2018) research they utilized the Back-propagation artificial neural networks (ANN) to predict the compressive strength of recycled aggregate concrete (RAC). They obtained very accurate regression values for the training, validation and testing of 0.903, 0.89 and 0.829 respectively [29]. Meanwhile, the study carried by Chopra et al (2016), utilized ANN methods to examine comparatively the compressive strength of concrete. Their [29] study was a comparative examination of the ANN and the genetic programming (GP) to ascertain and compare the accuracy of both techniques in the prediction of the compressive strength of concrete [30]. Aref et al. (2018) investigated the use of natural pozolonna from syria in concrete. They explored the strength and durability of Syrian volcanic scoria and predicted the mechanical behavior using ANN and multiple linear regression (MLR). From the models they used, they found out that the ANN displayed higher accuracy. They concluded by highlighting the contribution of the volcanic scoria in reduction of the concrete's permeability and its effect on durability-related properties too [31]. Whereas, Chithra et al. (2016) carried out a comparative study between ANN and MLR for predicting the compressive strength of concretes containing nanosilica and copper slag [24].

Perk et al. (2019) predicted concrete's strength using support vector machine (SVM) and ANN models. In their prediction they correlated wave velocities to the mechanical properties, meaning that they used three types of ultrasonic velocities as input parameters. The SVM models resulted in more accurate results due to the over-fitting issues observed in ANN models [32]. In Bonifácio work's the prediction of the mechanical properties of light weight aggregate concrete (LWAC) was examined through the use of SVM and Finite Elements (FEM) models. Both models efficiently predicted the mechanical properties of the LWAC but the SVM displayed slightly better performance with lower average error [33]. Lu et al. (2013) investigated the important parameters to be considered when using the SVM models as they control the tradeoff between under-fitting and over-fitting. They emphasized on the advantage of using SVM models for small size of sample set. Hence, efficient learning from a limited number of samples that is very important in shortening the materials developments cycle [34]. Yuantian's (2020) study used six different ML algorithms, among which SVM, to develop hybrid technique in

estimating the compressive strength of jet grouting composite. They compared the different techniques based on their accuracy and concluded that SVM models performed better [26].

The work carried out by Obianyo et al (2020), utilized Multivariate models namely linear regression, nonlinear regression and mixed models. The multivariate models were used to predict the compressive strength of lateritic soil stabilized with agro-waste. They selected 3 independent variables to elucidate their effect on the compressive strength. They concluded that the linear models performed better than nonlinear, meanwhile the mixed models performed better than the two previous [35]. Sadrmomtazi (2013) used regression to model the compressive strength of expanded polystyrene concrete. They found that the regression model can be ideally used to assess the durability of the expanded polystyrene concrete [36]. The simple logistic regression is a common classification technique and is a useful method for solving the binary classification problem. Another category of classification is multinomial classification, which handles the issues where multiple classes are present in the target variable.

This study intends to develop ANN, SVM and LR models to predict the mechanical behavior of alkali activated termite soil bricks. In this study, six inputs characteristics namely Si/Al, Initial curing temperature, activator concentration, water absorption, curing regime and weight were used to predict the compressive strength. Si/Al in alkali activated materials is a key component that control the particles binding, thus commands mechanical behavior (macrostructure). The initial curing temperature controls the period of the chemical reactions taking place, while the curing regime determines the route of the chemical reactions during the curing period. Water absorption determines partially the dimensional integrity of the Alkali Activated termite soil (AATS). Additionally, the variation of these characteristics facilitates the prediction of the optimal compressive strength. ANN, SVM and LR models application can be divided into training, validation, and testing. The training set is used to train the models. Validation data provides evaluation of the models fit on the training data to prevent the models over fitting and also to stop the training when the error increases. The models are finally applied on the experimental data to predict the compressive strength of the alkaline activated termite soil (AATS).

The training and testing data for ANN, SVM and LR model's development were prepared from experimental primary data sets carried out during this investigation. To the author's

knowledge, most of the papers using ML approaches uses secondary data (data from previous published literatures). Therefore, the current study uses primary data to facilitate reproducibility. Direct comparison with existing literature on TMS was not made due to the inexistence of published literature in the prediction of termite soil performances using ML techniques. Subsequently, this study represents a premiere in the use of ML techniques to predict the behavior/performances of unconventional construction materials such as termite mound soil.

2. Materials and Methods

In this study the termite soil (TS) was collected from a construction site in Abuja, Nigeria. The anthills were spread in the region, without any utilization and were about to be demolished due to their location in that construction field. The anthill was deserted by the ants and the hills age ranged from 5 to 15 years old. The physical properties of the anthills differed from one to the other, their height varied from 50cm to 2m while their mineralogical composition didn't vary significantly. The soil was obtained by breaking down the hills, grinding and sieving the soil into finer particles. X-ray Fluorescence (XRF) analysis was conducted using Thermo Scientific Epsilon Spectrometer to access the mineral composition of the TS. Furthermore, Electron Dispersive Spectroscopy (EDX) was used to obtain its chemical composition and Fourier Transform Infra-Red analysis was used to detect the molecular bounding existing between the particles.

Table 5.1. Physical properties of the termite soil (TS) and natural occurring Alum

Atterberg Limits	Particle size	Color	Moisture content	Density	Specific Gravity
Liquid Limit (33.51%) Plastic Limit (22.75%) Plasticity Index (10.76)	Clay (40%) Sand (38%) Silt (22%)	TS (brown) Alum (whitish)	3.5%	0.395g/cm^3	2.59

Natural occurring Alum mineral was used as alkaline activator. The Alum was obtained from a local district market at a very insignificant price. The activator was used at different concentration level 1wt%, 3wt% and 5wt% based on previous study [2]. A chemical analysis and PH determination were performed on the natural occurring Alum.

During the bricks production, the powder form of the soil and the natural Alum were mixed with a laboratory mechanical mixer for 5min before addition of potable water as specified in the BS1377-2 [37]. The paste was poured into metallic mould of 50mm x 50mm x 50mm before being oven-dried for 24h prior to demoulding. The produced bricks were subjected to different curing environment, from room temperature to oven-dry, for a curing period of 7, 14 and 58 days. To predict accurately the compressive strength of the Alkali Activated Termite Soil (AATS) six independent variables were used X_1, X_2, X_3, X_4, X_5 and X_6 denoting activator concentration, Si/Al, initial curing temperature, water absorption, weight and curing regime respectively.

Table 5.2. Details of the experimental input datasets

Si/Al	Percent activation	ICT (C)	Curing Temp (C)	Wa (%)	Weight (kg)	Strength (Mpa)
1.85	0.03	105	27	10.68	0.191	0
1.91	0.03	60	27	13.36	0.189	0.1076
1.43	0.03	105	27	0.74	1.86	0
1.57	0.03	60	27	5.09	1.87	1.5796
1.72	0.03	105	60	17.73	0.185	0.5264
1.83	0.03	60	60	11.91	0.183	2.516
1.85	0.03	105	27	10.86	0.191	0
1.91	0.03	60	27	13.33	0.189	0.6084
1.43	0.03	105	27	0.71	1.86	0
1.57	0.03	60	27	4.88	1.87	2.7144
1.72	0.03	105	60	17.07	0.185	0.246
1.83	0.03	60	60	11.09	0.183	2.252
1.85	0.03	105	27	10.52	0.191	1.4156
1.91	0.03	60	27	13.28	0.189	1.42
1.43	0.03	105	27	0.79	1.86	0.4488
1.57	0.03	60	27	5.03	1.87	0.7076
1.72	0.03	105	60	18.01	0.185	0.588
1.83	0.03	60	60	12.58	0.183	0.1944
1.85	0.03	105	27	10.48	0.191	0.05184
1.91	0.03	60	27	13.55	0.189	2.3132
1.43	0.03	105	27	0.82	1.86	0.696
1.57	0.03	60	27	5.99	1.87	0.6688
1.72	0.03	105	60	18.25	0.185	0.48
1.83	0.03	60	60	12.05	0.183	0.0876
1.31	0.05	105	60	1.49	0.189	3.215
1.35	0.05	60	27	2.53	1.86	3.431
1.99	0.05	105	27	2.45	1.87	0.78

1.62	0.05	60	27	0.04	0.185	1.512
1.31	0.05	105	60	1.51	0.183	4.628
1.99	0.05	60	27	1.89	0.189	0.612
1.62	0.05	105	27	0.13	1.86	1.416
2.39	0.01	60	60	10.2	1.87	1.98
3.19	0.01	105	27	1.58	0.185	0.668
2.29	0.01	60	27	0.56	1.87	0.844
2.39	0.01	105	60	9.98	0.185	2.147
3.19	0.01	60	27	1.74	0.183	0.58
2.29	0.01	105	27	0.57	0.191	0.839

a. Artificial Neural Network (ANN)

The ANN operates by emulating the functionality of the neurons in human brain. A commonly used ANN is the multilayer perceptron (MLP). MLP is comprised of an input layer, one or more hidden layer and an output layer of computation node. The ANN are associated with weights which are adjusted during training to minimize classification error. It can learn a non-linear function approximator for either classification or regression. It is different from logistic regression, in that between the input and the output layer, there can be one or more non-linear layers, called hidden layers. The advantages of MLP are:

- Capability to learn non-linear models.
- Capability to learn models in real-time (on-line learning).

b. Support Vector Machine (SVM)

SVM is a type of machine learning algorithm that was developed by Vapnik (1998) [38]. SVM are a set of supervised learning methods used for classification, regression and outlier's detection. Due to the robust performance of SVM when dealing with noisy and sparse data, it has become a system of choice in many machine learning applications. SVM performs classification by separating data using a hyper-plane that is farthest from them (termed as 'the maximal margin hyper-plane'). The method of support sector classification can be extended to solve regression problems. This method is called support sector regression (SVR). The model produced by support vector classification (as described above) depends only on a subset of the training data, because the cost function for building the model does not care about training points that lie beyond the margin. Analogously, the model produced by SVR depends only on a subset of the training data, because the cost

function ignores samples whose prediction is close to their target. The advantages of support vector machines are:

- Effective in high dimensional spaces, high speed, possibility for continuous re-training with new information.
- Still effective in cases where number of dimensions is greater than the number of samples.
- Uses a subset of training points in the decision function (called support vectors), so it is also, memory efficient.

Versatile: different Kernel functions can be specified for the decision function. Common kernels are provided, but it is also possible to specify custom kernels.

c. Linear Regression (LR)

Linear Regression is one of the simplest and commonly used ML algorithms for two-class classification. It is easy to implement and can be used as the baseline for any binary classification problem. LR describes and estimates the relationship between one dependent binary variable and independent variables. It is a predictive algorithm using independent variables to predict the dependent variable [39]. The advantage of LR is that the model finds the two parameters that minimize the error between predictions and the true regression targets on the training set.

d. Regression Analysis

Regression is the measure of the average relationship between two or more variables in terms of the original units of the data. It also attempts to establish the nature of the relationship between variables that is to study the functional relationship between the variables and thereby provide a mechanism for prediction, or forecasting. A scatter diagram can be used to show the relationship between two variables. Regression analysis is used to:

- Predict the value of a dependent variable based on the value of at least one independent variable.
- Explain the impact of changes in an independent variable (the variable used to explain the dependent variable) on the dependent variable (the variable we wish to predict or explain).

e. Metrics

The performance of the models can be appraised by various validation methods. In this study, the validation methods used are namely the coefficient of determination (R^2) and root mean square (RMSE). These validation methods have been used to examine the prediction's accuracy, subsequently the R^2 is used to correlate the inputs and outputs [40]. If its value is close to 1, this indicates that a good fitting of the model while the value close to 0 indicates a bad fitting of the model [41] additionally the RMSE is used to evaluate the error that emerged during the training, testing and validating. The R^2 and RMSE were calculated as described in Wassim 's work [27].

f. Experimental Setup

The experiment was implemented in Python 2.7.12. The hardware configuration used for the implementation environment was Intel Core (TM) i5-4790 CPU, 3.60 GHz and 4GB RAM. The parameters used for the SVM is shown in Table 3. For ANN and LR the default parameters were used.

Table 5.3. Parameter settings for SVM

Parameter	value
Kernel	linear
C	1

3. Results and Discussions

Figure 5.1 shows the results of the models developed to predict the compressive strength. These results demonstrate that the testing, training and validation of all the three (3) models were successful. However, the results of the statistical measures (Figure 5.2) reveal that the SVM exhibited the highest R^2 (70%). Low R2 and RMSE of 63% and 0.7 respectively were displayed by the ANN. Meanwhile, LR displayed R^2 and RMSE of 26% and 0.95 respectively. Moreover, results obtained from the LR in terms of R^2 differed significantly from the ANN and SVM models indicating the weak correlation between the input and output given by the model. The highest R^2 was obtained from the SVM model pointing out the accuracy of the model in establishing the interdependence between the

input and compressive strength of the AATS. These results align with the previous work carried out by Chou et al., in their study they found out that the SVM displayed the best performance over ANN and MR [47]. In addition, the RMSE displayed by all the models indicates the insignificance of the errors arose from the prediction models during the training. However, LR exhibited RMSE of 0.95 indicating the near inexistence of errors during the training. Furthermore, SVM and ANN also displayed RMSE higher than 0.5 (0.6 and 0.7 respectively).

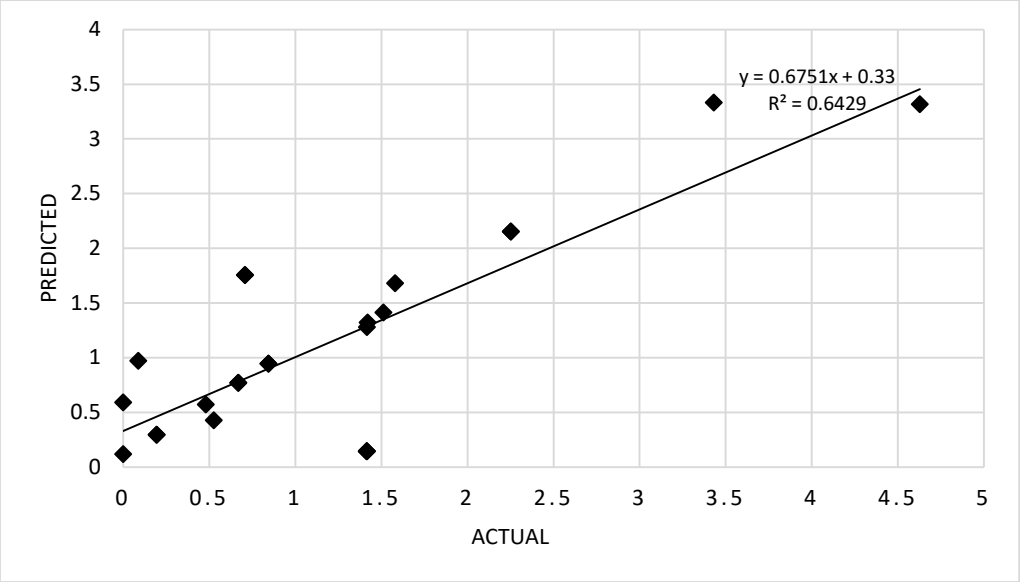

a)

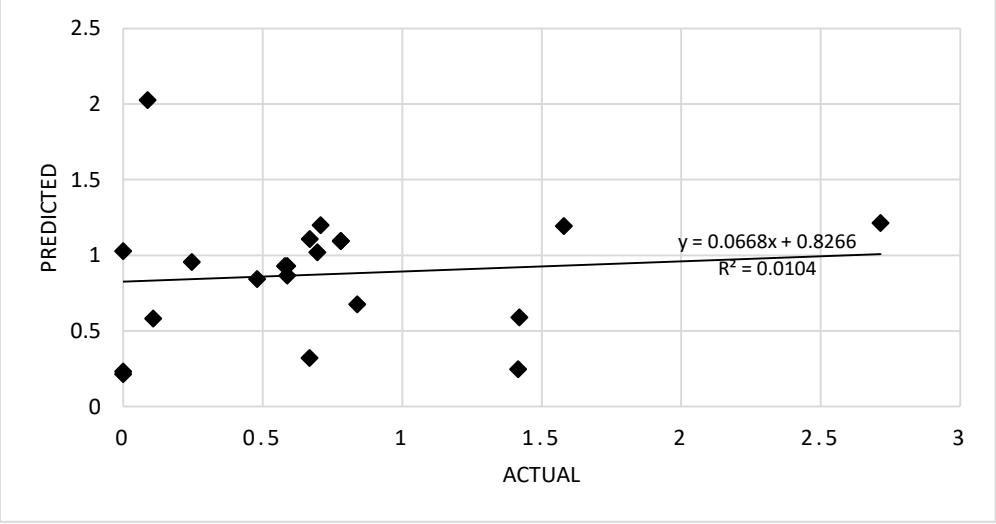

b)

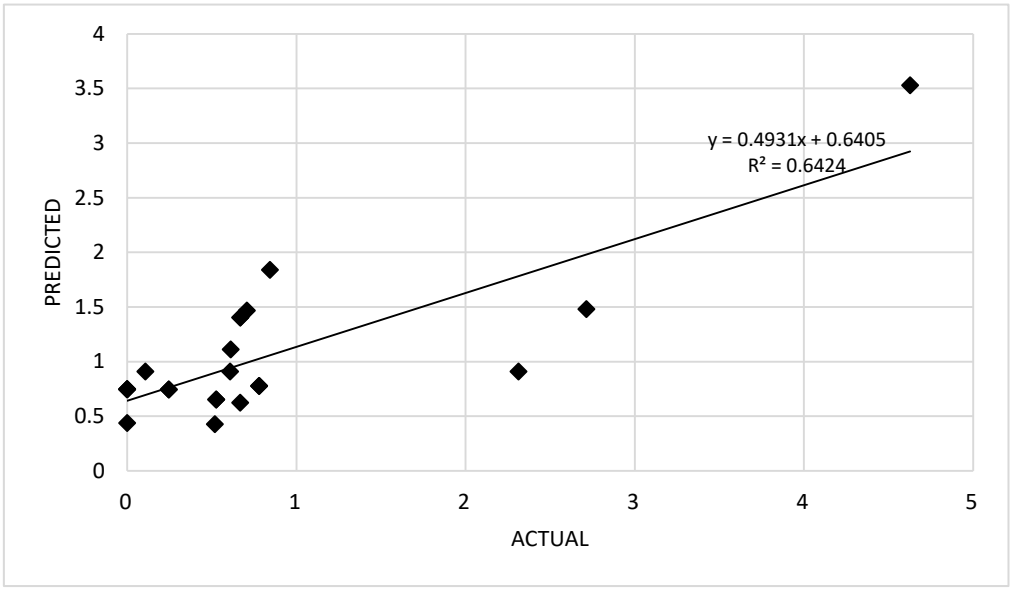

c)

Figure 5.1. Predicted values vs actual values from the models: a) SVM, b) LR and c) ANN

The results of the comparison of residuals in compressive strength from the prediction models are seen in **Error! Reference source not found.**. The difference was examined between the predicted and actual values, it can be deducted that the LR model exhibited good performance as the difference in the values was very insignificant, followed by the SVM and ANN. This indicates the linear nature of the relationship existing between the input parameters and the compressive strength of the AATS.

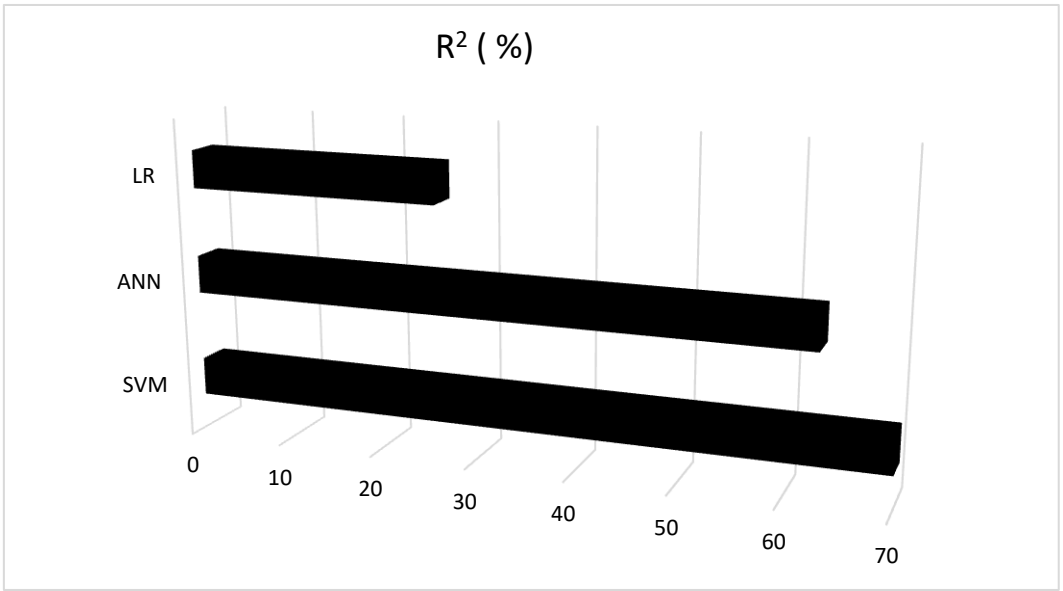

a)

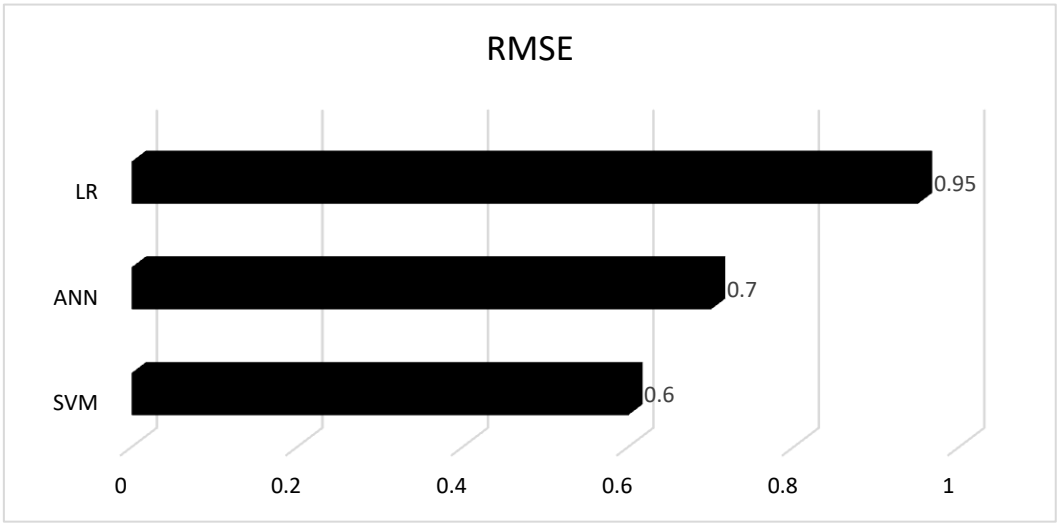

b)

Figure 5.2 a) Coefficient of determination of the various models, b) RMSE of the various models

4. Discussions

Analysis of the result shows that SVM algorithms demonstrated a superior performance in terms of both R^2 score and RMSE. This result stems from the fact that SVM has a robust performance relative to ANN and LR because SVM employs the maximal margin hyper plane in predicting the correlation between the features (ICT, curing temp, weight etc.) and the compressive strength of the AATS. In addition, SVM only uses a subset of training points which are highly correlated with the dependent variable (Strength) in the decision function (called support vectors), consequently SVM is capable of eliminating noise which may hamper the prediction result and therefore only the attributes that are highly linked with the AATS strength will be employed for prediction. ANN performs relatively poorly because with ANN different random weight initializations can lead to different validation accuracy. Also, ANN requires tuning a number of hyper parameters such as the number of hidden neurons, layers, and iterations. The Linear regression has the lowest performs in terms of both R^2 score and RMSE because the coefficient estimates for LR rely on the interdependence of the features. When features are correlated and the columns of the design matrix X have an approximate linear dependence, the design matrix becomes close to singular and as a result, the least-squares estimate becomes highly sensitive to random errors in the observed target, producing a large variance which could result in high RMSE and low coefficient of determination (R^2).

Additionally, the statistical values displayed by each model corroborate that the prediction of AATS compressive strength with SVM model is singularly accurate. This is inconsistent with results obtained from the prediction of volcanic scoria-based concrete [31]. However, the result from the present study aligns with the results obtained using SVM in the prediction of light weight aggregate concrete (LWAC)[33]. Nonetheless, due to the inexistence of literature on the prediction of AATS compressive, the results can't be compared appropriately because of the difference in the materials used. Henceforth, the comparison was made with similar materials such as the scoria used in the previous reference. The resemblance of the scoria with the termite soil is that both materials are classified as natural pozzolanas. Furthermore, it's worth recalling that the various statistical measures and results obtained peaked the importance and effect of the input parameters on the compressive strength.

5. Conclusions

In this aspect of the work, the applicability of the SVM, ANN and LR for the prediction of alkali activated termite soil's compressive strength were explored. It was demonstrated that the developed models were successfully trained and validated based on the experimental dataset. The three models developed were compared based on their accuracy. The following focal conclusions can be drawn:

- Termite mound soil is an unconventional earth-based material, classified as natural pozzolanas. Its activation through natural occurring alum is aimed to produce eco-friendly and locally available construction materials. Subsequently, the novelty of these materials makes the application of ML techniques a useful tool to appraise their properties with variation of constituents.

- The correlation between the input parameters and the output feature displayed by the coefficient of determination R^2 (70%, 63% and 26%) indicates that the three models are suitable for modeling the compressive strength of AATS dataset.

- SVM model displayed the higher coefficient of determination (70%) and a root mean square of (0.6). These values indicate the accuracy of the model in predicting the compressive strength of the AATS based on the given input parameters. The results obtained from the SVM model were close to the experimental values.

- ANN exhibited the second-best performance with a coefficient of determination of 63% and a root mean square of 0.7.
- LR demonstrated the lower accuracy with a coefficient of determination of 26% and a root mean square of 0.95. A lower mean square error is desirable a high RMSE signifies higher error. Therefore, SVM and ANN performs better since they have low RMSE compared to LR.

The higher accuracy and suitability of the SVM model made it most desirable than the ANN and LR methods in the prediction of AATS compressive strength. In addition to the high accuracy, the usage of SVM model contributes to reduce time consuming laboratory experiments resulting in the reduction of the general cost and time during the properties' investigations. The regression analysis showed that all studied parameters in this work have considerable effects on the properties of the AATS. However, more analysis can be performed in future investigations to determine the most influential parameter.

For future work the applicability of the ML methods can be used to assess the properties of new unconventional materials with questionable features such as new mixture constituents. In addition, the experiment was conducted with small scale data. In future research it is recommended to expand the data scale in order the examine the performance of the algorithms with large scale data in the domain.

References

[1] J. L. Provis and J. S. J. van Deventer, "RILEM State-of-the-Art Reports State-of-the-Art Report, RILEM TC 224-AAM." [Online]. Available: http://www.springer.com/series/8780.

[2] M. Falah, R. Obenaus-Emler, P. Kinnunen, and M. Illikainen, "Effects of Activator Properties and Curing Conditions on Alkali-Activation of Low-Alumina Mine Tailings," Waste and Biomass Valorization, vol. 11, no. 9, pp. 5027–5039, Sep. 2020, doi: 10.1007/s12649-019-00781-z.

[3] Z. Zhang, H. Wang, X. Yao, and Y. Zhu, "Effects of halloysite in kaolin on the formation and properties of geopolymers," Cement and Concrete Composites, vol. 34, no. 5, pp. 709–715, May 2012, doi: 10.1016/j.cemconcomp.2012.02.003.

[4] E. B. Ojo, K. Mustapha, R. S. Teixeira, and H. Savastano, “Development of unfired earthen building materials using muscovite rich soils and alkali activators,” Case Studies in Construction Materials, vol. 11, Dec. 2019, doi: 10.1016/j.cscm.2019.e00262.

[5] A. J. Dhembare, “Physico-chemical properties of termite mound soil,” 2013. [Online]. Available: www.scholarsresearchlibrary.com.

[6] T. Nwakonobi, C. Anyanwu, and L. Tyav, “Effects of rice husk ash and termite hill types on the physical and mechanical properties of burnt termite clay bricks for rural housing,” Global Journal of Pure and Applied Sciences, vol. 20, no. 1, p. 57, 2015, doi: 10.4314/gjpas.v20i1.9.

[7] N. Anigbogu, “Properties of compressed earth bricks stabilized with termite mound material,” 2000. [Online]. Available: http://www.researchgate.net/publication/235910056.

[8] R. K. Kandasami, R. M. Borges, and T. G. Murthy, “Effect of biocementation on the strength and stability of termite mounds,” Environmental Geotechnics, vol. 3, no. 2, pp. 99–113, Apr. 2016, doi: 10.1680/jenge.15.00036.

[9] B. A. Akinyemi, T. E. Omoniyi, and M. O. Adeyemo, “Prospects of coir fibre as reinforcement in termite mound clay bricks,” Acta Technologica Agriculturae, vol. 19, no. 3, pp. 57–62, Sep. 2016, doi: 10.1515/ata-2016-0013.

[10] R. M. Gandia, A. A. R. Corrêa, F. C. Gomes, D. B. Marin, and L. S. Santana, “Physical, mechanical and thermal behavior of adobe stabilized with ‘synthetic termite saliva,’” Engenharia Agricola, vol. 39, no. 2, pp. 139–149, Mar. 2019, doi: 10.1590/1809-4430-Eng.Agric.v39n2p139-149/2019.

[11] A. A. R. Corrêa, L. Bufalino, T. de Paula Protásio, M. X. Ribeiro, D. Wisky, and L. M. Mendes, “Evaluation of mechanical properties of adobe chemically stabilized with ‘synthetic termite saliva,’” in Key Engineering Materials, 2014, vol. 600, pp. 150–155, doi: 10.4028/www.scientific.net/KEM.600.150.

[12] B. B. Mujinya et al., “Clay composition and properties in termite mounds of the lubumbashi area, D.R. congo,” Geoderma, vol. 192, no. 1, pp. 304–315, 2013, doi: 10.1016/j.geoderma.2012.08.010.

[13] Y. Millogo, M. Hajjaji, and J. C. Morel, “Physical properties, microstructure and mineralogy of termite mound material considered as construction materials,” Applied Clay Science, vol. 52, no. 1–2, pp. 160–164, 2011, doi: 10.1016/j.clay.2011.02.016.

[14] O. B. Faria, R. A. G. Battistelle, and C. Neves, “Influence of the addition of ‘synthetic termite saliva’ in the compressive strength and water absorption of compacted soil-cement,” Ambiente Construído, vol. 16, no. 3, pp. 127–136, Sep. 2016, doi: 10.1590/s1678-86212016000300096.

[15] A. A. Mahamat, N. Linda Bih, O. Ayeni, P. Azikiwe Onwualu, H. Savastano, and W. Oluwole Soboyejo, “Development of Sustainable and Eco-Friendly Materials from Termite Hill Soil Stabilized with Cement for Low-Cost Housing in Chad,” Buildings, vol. 11, no. 3, p. 86, Feb. 2021, doi: 10.3390/buildings11030086.

[16] P. Jouquet, S. Traoré, C. Choosai, C. Hartmann, and D. Bignell, “Influence of termites on ecosystem functioning. Ecosystem services provided by termites,” European Journal of Soil Biology, vol. 47, no. 4, pp. 215–222, Jul. 2011, doi: 10.1016/j.ejsobi.2011.05.005.

[17] A. K. Ganguli, S. Kumar, A. Baruah, and S. Vaidya, “Nanocrystalline silica from termite mounds,” Current Science, vol. 106, no. 1, pp. 83–88, 2014.

[18] A. van Huis, “Cultural significance of termites in sub-Saharan Africa,” Journal of Ethnobiology and Ethnomedicine, vol. 13, no. 1, Jan. 2017, doi: 10.1186/s13002-017-0137-z.

[19] D. E. Pomeroy, “The Distribution and Abundance of Large Termite Mounds in Uganda,” 1977.

[20] I. L. Ackerman, W. G. Teixeira, S. J. Riha, J. Lehmann, and E. C. M. Fernandes, “The impact of mound-building termites on surface soil properties in a secondary forest of Central Amazonia,” Applied Soil Ecology, vol. 37, no. 3, pp. 267–276, Nov. 2007, doi: 10.1016/j.apsoil.2007.08.005.

[21] T. S. Sarcinelli et al., “Chemical, physical and micromorphological properties of termite mounds and adjacent soils along a toposequence in Zona da Mata, Minas Gerais State, Brazil,” Catena, vol. 76, no. 2, pp. 107–113, 2009, doi: 10.1016/j.catena.2008.10.001.

[22] B. Jean-Pierre et al., “Spatial distribution and Density of termite mounds in a protected habitat in the south of Cote d’Ivoire: case of national floristic center (CNF) of UFHB of Abidjan,” vol. 11, no. 3, 2015.

[23] R. Özcan, T. Malas, O. Yilmaz, Turgut Özal Üniversitesi, Ėl aralyk Atatürk-Ala Too universiteti, and Süleyman Demirel Üniversitesi, 2013 International Conference on Electronics, Computer and Computation (ICECCO) : International Conference : November 7-8, 2013 : Ankara, Turkey. .

[24] S. Chithra, S. R. R. S. Kumar, K. Chinnaraju, and F. Alfin Ashmita, “A comparative study on the compressive strength prediction models for High Performance Concrete containing nano silica and copper slag using regression analysis and Artificial Neural Networks,” Construction and Building Materials, vol. 114, pp. 528–535, 2016, doi: 10.1016/j.conbuildmat.2016.03.214.

[25] Institute of Electrical and Electronics Engineers and Nile University, 2019 15th International Conference on Electronics, Computer and Computation (ICECCO). .

[26] Y. Sun, G. Li, and J. Zhang, “Developing hybrid machine learning models for estimating the unconfined compressive strength of jet grouting composite: A comparative study,” Applied Sciences (Switzerland), vol. 10, no. 5, pp. 1–14, 2020, doi: 10.3390/app10051612.

[27] W. ben Chaabene, M. Flah, and M. L. Nehdi, “Machine learning prediction of mechanical properties of concrete: Critical review,” Construction and Building Materials, vol. 260, p. 119889, 2020, doi: 10.1016/j.conbuildmat.2020.119889.

[28] M. K. Idris, M. M. Boukar, and S. A. Adeshina, “Analysis of bad roads using smart phone,” Dec. 2019, doi: 10.1109/ICECCO48375.2019.9043286.

[29] H. Naderpour, A. H. Rafiean, and P. Fakharian, “Compressive strength prediction of environmentally friendly concrete using artificial neural networks,” Journal of Building Engineering, vol. 16, no. January, pp. 213–219, 2018, doi: 10.1016/j.jobe.2018.01.007.

[30] P. Chopra, R. K. Sharma, and M. Kumar, “Prediction of Compressive Strength of Concrete Using Artificial Neural Network and Genetic Programming,” Advances in Materials Science and Engineering, vol. 2016, 2016, doi: 10.1155/2016/7648467.

[31] A. M. Al-Swaidani and W. T. Khwies, “Applicability of Artificial Neural Networks to Predict Mechanical and Permeability Properties of Volcanic Scoria-Based Concrete,” Advances in Civil Engineering, vol. 2018, no. i, 2018, doi: 10.1155/2018/5207962.

[32] J. Y. Park, Y. G. Yoon, and T. K. Oh, “Prediction of concrete strength with P-, S-, R-wave velocities by support vector machine (SVM) and artificial neural network (ANN),” Applied Sciences (Switzerland), vol. 9, no. 19, Oct. 2019, doi: 10.3390/app9194053.

[33] A. L. Bonifácio, J. C. Mendes, M. C. R. Farage, F. S. Barbosa, C. B. Barbosa, and A. L. Beaucour, “Application of support vector machine and finite element method to predict the mechanical properties of concrete,” Latin American Journal of Solids and Structures, vol. 16, no. 7 CILAMCE 2018, Jul. 2019, doi: 10.1590/1679-78255297.

[34] W. C. Lu, X. B. Ji, M. J. Li, L. Liu, B. H. Yue, and L. M. Zhang, “Using support vector machine for materials design,” Advances in Manufacturing, vol. 1, no. 2, pp. 151–159, 2013, doi: 10.1007/s40436-013-0025-2.

[35] I. I. Obianyo et al., “Multivariate regression models for predicting the compressive strength of bone ash stabilized lateritic soil for sustainable building,” Construction and Building Materials, vol. 263, p. 120677, 2020, doi: 10.1016/j.conbuildmat.2020.120677.

[36] A. Sadrmomtazi, J. Sobhani, and M. A. Mirgozar, “Modeling compressive strength of EPS lightweight concrete using regression, neural network and ANFIS,” Construction and Building Materials, vol. 42, pp. 205–216, 2013, doi: 10.1016/j.conbuildmat.2013.01.016.

[37] British Standards Institution., British Standard methods of test for soils for civil engineering purposes. British Standards Institution, 1990.

[38] V. Vapnik, “3 THE SUPPORT VECTOR METHOD OF FUNCTION ESTIMATION,” 1998.

[39] R. Khandelwal, “Quick and Easy Explanation of Logistic Regression A simple explanation of Logistic Regression, why we need it, how to evaluate its performance and build a multi-class classification using Logistic Regression in python.”

[40] D. Tien Bui, N. D. Hoang, and V. H. Nhu, “A swarm intelligence-based machine learning approach for predicting soil shear strength for road construction: a case study at

Trung Luong National Expressway Project (Vietnam)," Engineering with Computers, vol. 35, no. 3, pp. 955–965, Jul. 2019, doi: 10.1007/s00366-018-0643-1.

[41] H. Anysz, Ł. Brzozowski, W. Kretowicz, and P. Narloch, "Feature importance of stabilised rammed earth components affecting the compressive strength calculated with explainable artificial intelligence tools," Materials, vol. 13, no. 10, May 2020, doi: 10.3390/ma13102317.

[42] J.-S. Chou, C.-K. Chiu, M. Farfoura, and I. Al-Taharwa, "Optimizing the Prediction Accuracy of Concrete Compressive Strength Based on a Comparison of Data-Mining Techniques," Journal of Computing in Civil Engineering, vol. 25, no. 3, pp. 242–253, May 2011, doi: 10.1061/(asce)cp.1943-5487.0000088.

6.0 Chapter Six: Effect of Borassus fruit natural fiber reinforcement on one-part alkali activated termite mound soil-based bio-composite's compressive strength in the early curing stages

1. Introduction

Ecological concerns about the ecosystem degradation have trigger off interest to produce green materials. The green materials production's motto is met by the natural fibers, they can be obtained from plant, animal or mineral [1]. Natural fibers from plants origin are known as vegetables fibers, the global interest is turned towards the vegetable's fibers because of their availability, bio-degradability, eco-friendliness, low cost, low density, high specific mechanical properties (better stiffness, high modulus and strength), light weight, low energy consumption during extraction and they are sourced from renewables materials (3). They are sourced from renewable materials that are largely abundant globally. Vegetable fibers can be classified as bast or stem fibers, Leaf fibers, seed or fruit fibers, grass fibers and bark fabrics [2]. The fibers are used as reinforcement to remedy shrinkage, dimensional un-stability, air voids existence [3].

On the other hand, Alkali activated binders have gained a lot of attention too as 'green' alternative to ordinary Portland cement (OPC). This technology is based on the dissolution of aluminosilicate in the presence of alkaline activator[4]. The alkali activation process involves alkali solutions (two-part alkali activated binders) or solid alkali source (one-part alkali activated binders) [5]. The use of two-part alkali activation process is corrosive, difficult and not user-friendly [6]. Meanwhile, one-part alkali activation process requires solid alkali source with the aluminosilicate precursor and water [7]. During this process, the dry ingredients are mixed together before addition of water. This is similar to the preparation of OPC and it enables better cast-in-situ features which are among the main requirement in the construction field[8]. During the mixture chemical reactions [9] take place, among which the dissolution of the aluminosilicate precursor activated by the alkaline source followed by polycondensation and formation of amorphous network [10].

An investigation carried out by Obi Reddy et Al, studied the coarse and fine borassus fruit fibers, the composition of the natural fibers indicates the presence of alpha-cellulose, hemicellulose, and lignin. They changed chemically the natural fibers through Alkali treatment and showed that the maximum stress and the modulus of the fine fibers where

higher than those of the coarse fibers. The increase in percentage of elongation at break was not very noticeable in the case of coarse fibers after alkali treatment. Thus, the alkali treatment contributed to enhancing the strength of the fiber [11]. While L. Boopathi et al. treated the Borassus fiber with NaOH solution at different concentration. They found out that the alkali treatment improved the density values of the Borassus fruit fibers. Subsequently, due to the impurity's removal from the fibers surface with the aid of the alkali treatment. However, the alkali treatment caused the fiber to swell, to remove the hemicellulose and other impurities from the fiber surface and the micro fibrils of cellulose remained unaffected due to the alkali treatment. Hence, the removal of the impurities improved the mechanical properties of the fibers and the fiber-matrix adhesiveness in diverse composites applications. The noticeable cleaner surface and the pores on the fiber surface were detected after alkali treatment, therefore the addition of pores caused by removal of fatty substances increased the bonding characteristics of the fibers [2]. However, Sudhakara et al., studied Borassus fruit fiber alkali treated on maleated polypropylene. The composite achieved more tensile strength, modulus, flexural strength, modulus and impact strength. Partially green Borassus fiber reinforced polyester composites was reported to have high tensile, flexural and impact properties of the composites. These fibers were found to be higher than that of` the matrix and increased with fiber content, conforming the reinforcing action of the fibers. The density of these composites was found to decrease with fiber content[12] .

The main objective of this chapter is to extract, characterize and treat the natural fibers from the borassus fruit. The characterizations made on the natural fibers are morphological to improve the hygroscopicity and mechanical properties. It is noteworthy to recall that Borassus aethiopium trees are renewables with high potential growth rate, eco-friendly and abundantly available in the landscape. They represent an economical source if properly processed and used as reinforcement in green sustainable composites.

2. Materials and Methods

a. Extraction of the natural fiber

The Borassus fruit fibers were extracted from matured fruits. These matured borassus fruits were collected in Jabi, Federal Capital Territory Nigeria. The fruits were sliced vertically into many pieces, then boiled in tap water at 80°C for 30min. Two types of fibers were

obtained: fine and coarse fibers. The fibers were dispersed from the fruit nut edge to edge with the coarse fibers mostly near the shell and the fine fibers close to the nut. The shell of the fruit was constituted of an assembly of coarse fibers that tend to separate after the water treatment. Both, fine and coarse fibers were washed under running water to wash off the juice-like material from the fruit before being oven dried for 72h at 80°C.

Table 6.1.a) complete borassus fruit, and b) wet and dry extracted fibers from a fruit.

b. Physical and hygroscopic properties

i. Morphology

The Scanning Electron Microscope (SEM) technique was used to measure the diameter of the Borassus fruit natural fibers (BNF). The analysis was carried in a large range of fibers (50-100μm) and the mean long and short diameters were kept for this study. The analysis was carried on the natural fibers before and after chemical treatment to ascertain the effect of the chemical treatment on the fiber's morphology and microstructure. The microscopic analysis was made with a CARL ZEISS instrument, model EVO40 EP implemented with an EDX system. Additionally, the Energy Dispersive Spectroscopy (EDX) technique was employed to identify the chemical elements present in the fibers before and after chemical treatment to determine the effect of the chemical treatment on the chemical composition of the fibers.

ii. Hygroscopic swelling

The water absorption and the hygroscopic swelling needs to be investigated carefully as it predicts the hydrophilic behavior of the fibers. The water absorption affects greatly the volume change of the fibers inside the matrix leading to internal stresses or when the trapped water evaporates this can create interstices within the matrix. The hygroscopic swelling examination was conducted on the Borassus Natural Fibers. The various fibers were subjected to humidity by the use of hygroscopic salts solutions of KOH and NaCl which generate a Relative Humidity of 8% and 75% respectively at fixed temperature of 23°C. The fibers were kept in a hermetically closed glass boxes with controlled humidity and an optical microscopic was used to measure the diameter's change during water absorption.

c. Bio-composite production

In the preparation chronology, the bio-composite was obtained by mixing the precursor, the natural fibers and 3wt% of Potassuim Carbonate as alkaline activator. The Potassium Carbonate was dissolved into the required amount of distilled water and the solution was allowed to cool for few minutes given the exothermic nature of the dissolution. The natural fibers were added to the mixture at 0.75wt% then mixed for 5 min in a laboratory mixer before being transferred to a dynamic Zwick press to be compressed at 2 MPa with a maximum force of 12.8 KN at a displacement rate of 100N/mm. The bio-composite containing 1wt% of Borassus fruit natural fiber had very low workability as the fibers tend to stick to the moulds' inner side favoring cracks in the samples during demoulding. Consequently, specimens with 1wt% of fibers concentration were not considered for the mechanical characterizations

a)


b)

Table 6.2. a) Freshly demoulded samples. b) samples after mechanical failure

d. Mechanical properties

The compressive and three-point bending tests were conducted as described in Abdollahnejad's work [6]. However, in the present study the specimens were evaluated under compression deformation on a hydraulic universal testing machine.

3. Results and Discussions

i. Physico-hygroscopic behavior of the natural Borassus fruit fiber

From the diameter and length distribution examination, it was observed that the natural fibers diameter was uniform throughout the length hence the average was considered. The average values of the diameter distribution indicated that the majority of fibers existed around 150µm, whereas the length distribution showed that the average values of fibers length were 15cm. The natural fibers exhibited a multi-cellular structure with very porous surface. Additionally, to the surface pores the fibers contained some impurities as seen in **Error! Reference source not found.**. In the case of the natural fibers obtained from the palmyra leaf, the average diameter was 320µm [11]. To improve the natural Borassus fruit fiber, chemical treatment can potentially remedy to the high surficial porosity. Previous study shown that the benzoylchloride treatment had a very efficient result in weight loss ((29%) while alkali treatment was of 23%) [14].

The exposure of the borassus fruit natural fiber to various media has indicated that there was not any noticeable swelling. The unaltered diameters displayed by the borassus fruit natural fiber can be explained by the negligible depth of the surficial pores. These pores provide lower humidity sensitivity of the fibers therefore higher resistance to humidity penetration.

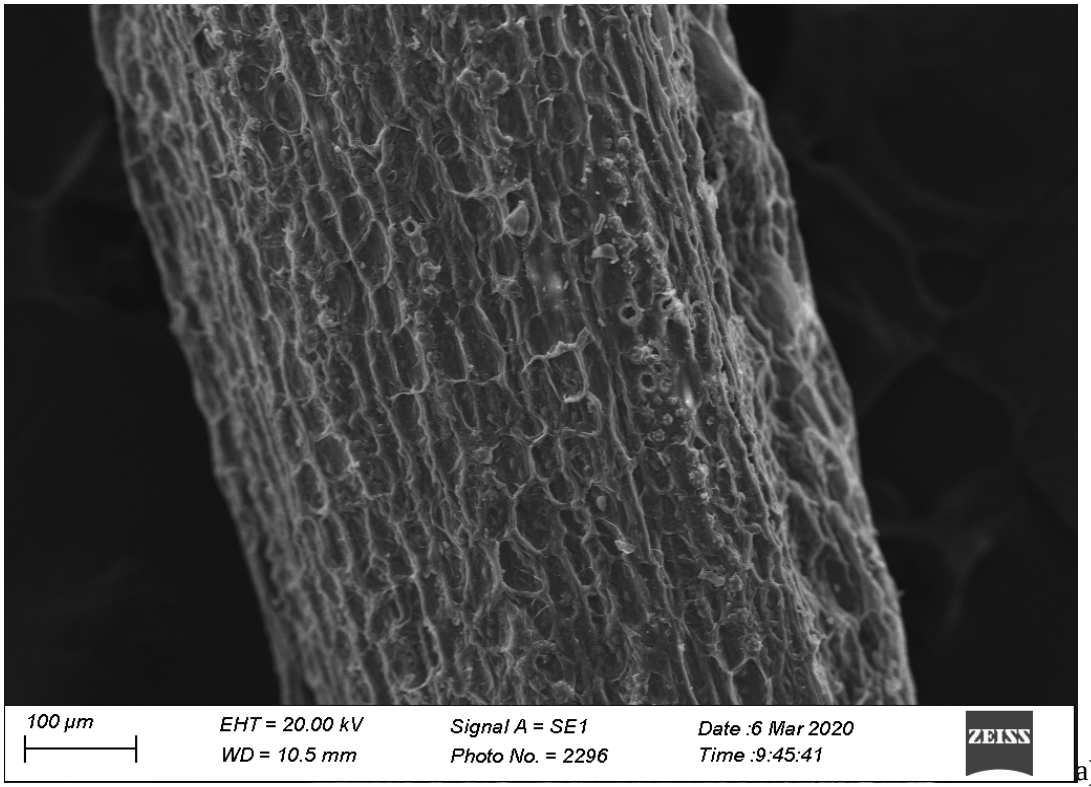
100 µm
EHT = 20.00 kV
WD = 10.5 mm
Signal A = SE1
Photo No. = 2296
Date :6 Mar 2020
Time :9:45:41
ZEISS

a)

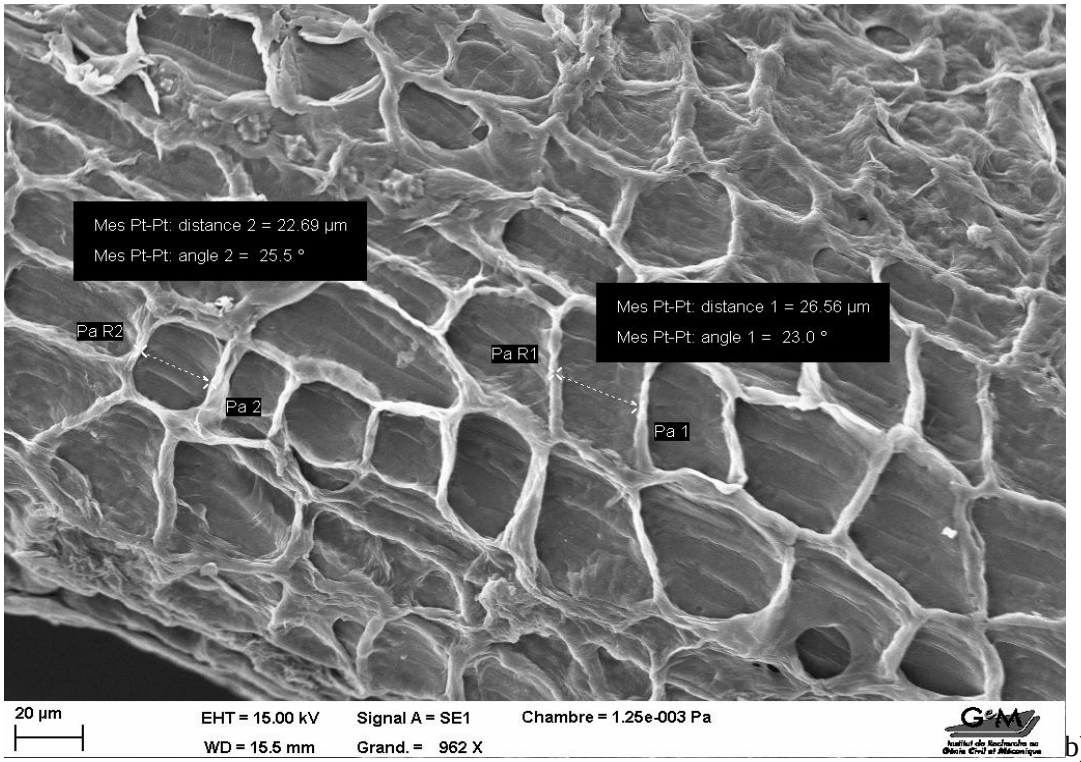
Mes Pt-Pt: distance 2 = 22.69 µm
Mes Pt-Pt: angle 2 = 25.5 °
Mes Pt-Pt: distance 1 = 26.56 µm
Mes Pt-Pt: angle 1 = 23.0 °
Pa R2
Pa 2
Pa R1
Pa 1
20 µm
EHT = 15.00 kV
WD = 15.5 mm
Signal A = SE1
Grand. = 962 X
Chambre = 1.25e-003 Pa
b)

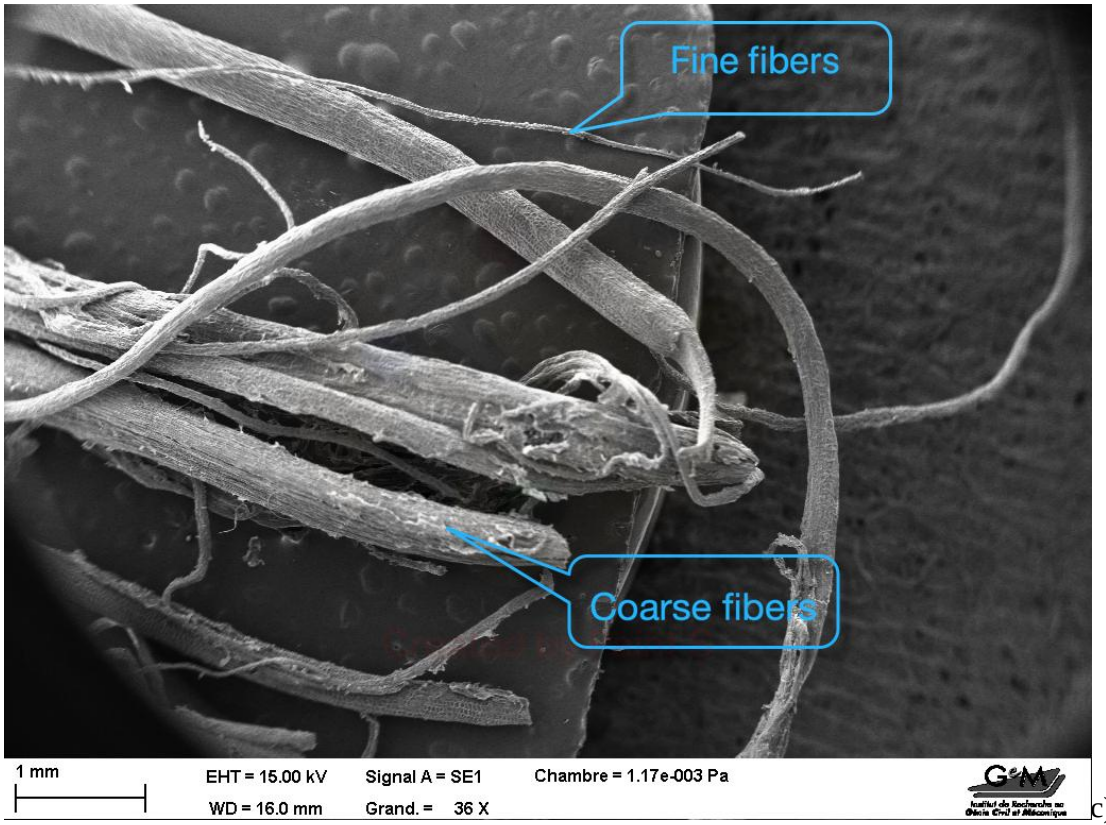

c)

Table 6.3. SEM graph of: a) a single borassus fruit natural fiber, b) magnified view on the superficial pores, c) extracted fine and coarse fibers

ii. Effect of the natural Borassus fruit fiber on the bio-composite mechanical properties

The inclusion of the natural Borassus fruit fiber increased the existence of air voids. This influenced synchronously the compressive strength positively as the natural fibers limited the crack's propagation. The compressive strength was recorded around 8MPa for the plain samples without any fiber reinforcement[15]. Moreover, an increase was noticed with the inclusion of natural fibers. The maximum compressive was displayed by the samples containing 0.75wt% of natural fiber. However, during the compression deformations loading the sample failed by disintegration of the outer sides, indicating the weak bond between the matrix and the reinforcement in that region[16]. Nonetheless, during loading initiation of cracks were notice from the lateral sides of the sample and even after failure the fibers held together the outer side from falling into pieces. This confirms previous investigations in which the authors recommended Borassus fiber application in

construction as reinforcement [17]. The central part displayed more resistance during the compression loading, as the part was still stable after failure. At failure, the samples presented cracks throughout the central part, but the fiber limited the propagation and growth of the cracks[18]. The maximum compressive strength displayed by the bio-composite could be explained by the rough surface of the natural Borassus fruit fibers, which provides a strong bond at the fiber/matrix interfaces.

In the samples containing the natural fibers the compressive strength increased proportionally with the curing period. Therefore, the compressive strength is expected to increase at the late curing ages. In similar investigation, the effect of the inclusion of palm date fibers at 0.05% presented the best compressive strength [19]. In another investigation, where Pulverized TMS was used, the tensile properties increased with curing days following the trend of the compressive strength [20].

The chemical bond is the first mechanism to be activated during strengthening. During this initial phase, the fiber and matrix deformations are fully compatible, in such a way that the bond of the fiber/matrix interface does not suffer any damage. Outer surface of the bio-composite didn’t display high resistance to loading. This can be explained by weak densification occurring at the wall-side of the bio-composite [21]. However, the good mechanical performances displayed by the samples cannot be attributed to the fiber reinforcement only. The mechanical compaction densified the samples, by increasing the adhesion of the fibers to the termite mound soil matrix. Moreover, the compaction generated the consolidation of the fibers to the matrix as displayed by the sample’s failure mode.

However, the addition of date palm fibers was previously studied. It was reported that the addition of the date palm fiber had an adverse effect on compressive and tensile strength of compressed earth block, which lead the author not to recommend the use of date palm fibers based on its strength[19]. Furthermore, residual unreacted materials can explain the compressive strength trend noticed here. Although, there is no definitive and accurate method for quantitatively determining the amount of unreacted material in a particular specimen.

a)

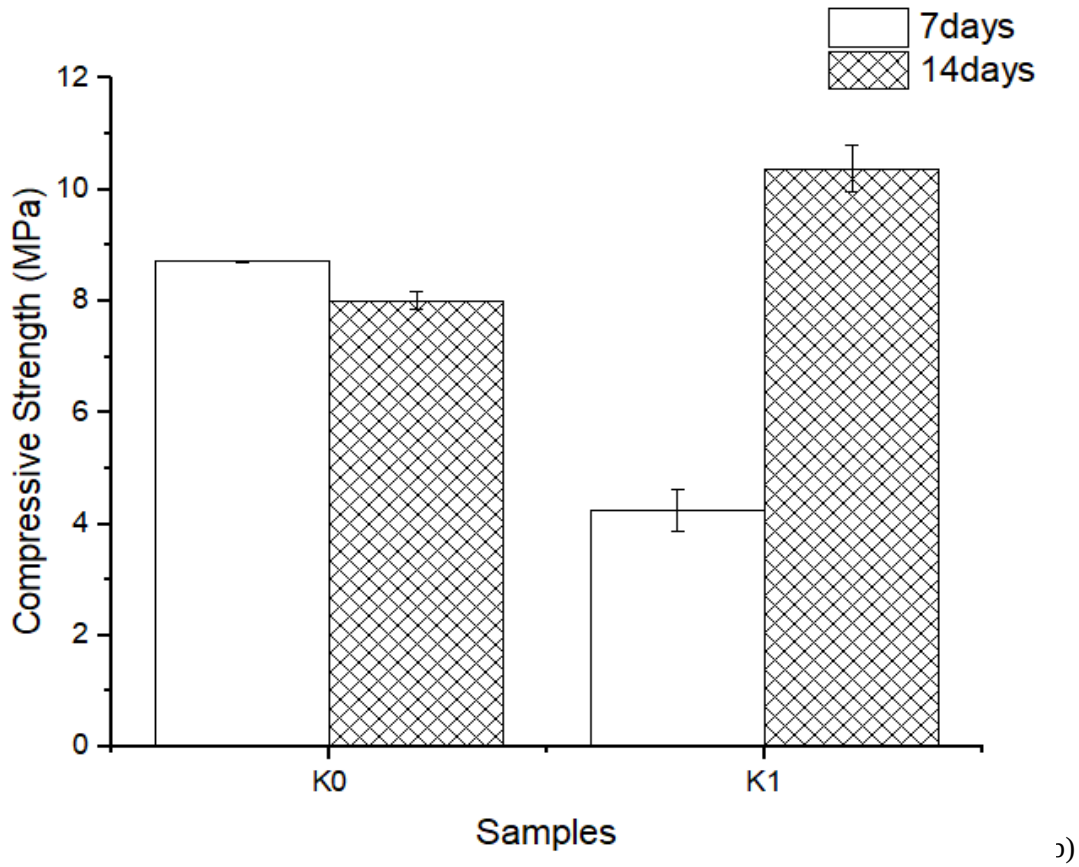

ɔ)

Table 6.4.a) Sample's failure under compression deformation and b) Compressive strength of plain and reinforced samples

4. Conclusions

This chapter presented the feasibility of natural fiber reinforcement in one-part alkali activated termite mound soil matrix. The examination was carried out in terms of compressive and flexural strengths. As expected, the fibers reinforcement has impacted positively the mechanical properties and overall stability of the bio-composite. Focal conclusions extrapolated from the study are presented beneath:

- Borassus fruit natural fibers displayed a very porous surface, however these pores didn't affect its hygroscopic properties. This can be explained by the negligible depth and size of the pores.
- Practicability of one part alkali activated termite mound soil was examine in terms of compressive strength only. From these results, the process can be used as an optimization technique for TMS
- Natural Fiber reinforcement impacted positively the compressive strength as a change was noticed in the early ageing period and there was a noticeable difference in the unreinforced and reinforced samples. Henceforth, inclusion of Borassus fruit natural fibers has affected the compressive strength by acting as a crack propagations obstructor.
- The mechanical compaction affected greatly the mechanical properties of unreinforced and reinforced alkali activated TMS. Subsequently, it is considered to be an effective technique to improve the mechanical properties of the TMS.

This investigation has shown the potential use of the Borassus fruit natural as fiber reinforcement in construction. This is aimed to develop renewable construction materials from agro-waste. The results can be implemented in regions where the materials are abundantly available for eco-friendly, low cost and sustainable housing.

References

[1] K. Ramanaiah, A. v Ratna Prasad, K. Hema, and C. Reddy, "Effect of Fiber Loading on Mechanical Properties of Borassus Seed Shoot Fiber Reinforced Polyester Composites," *J. Mater. Environ. Sci*, vol. 3, no. 3, pp. 374–378, 2012.

[2] L. Boopathi, P. S. Sampath, and K. Mylsamy, “Investigation of physical, chemical and mechanical properties of raw and alkali treated Borassus fruit fiber,” *Composites Part B: Engineering*, vol. 43, no. 8, pp. 3044–3052, Dec. 2012, doi: 10.1016/j.compositesb.2012.05.002.

[3] A. Karozou, S. Konopisi, E. Pavlidou, and M. Stefanidou, “Long-term behavior and durability of alkali-activated clay mortars,” *Materials*, vol. 13, no. 17, Sep. 2020, doi: 10.3390/MA13173790.

[4] J. L. Provis, “Alkali-activated materials,” *Cement and Concrete Research*, vol. 114. Elsevier Ltd, pp. 40–48, Dec. 01, 2018, doi: 10.1016/j.cemconres.2017.02.009.

[5] J. L. Provis, A. Palomo, and C. Shi, “Advances in understanding alkali-activated materials,” *Cement and Concrete Research*, vol. 78. Elsevier Ltd, pp. 110–125, Dec. 01, 2015, doi: 10.1016/j.cemconres.2015.04.013.

[6] Z. Abdollahnejad, M. Mastali, T. Luukkonen, P. Kinnunen, and M. Illikainen, “Fiber-reinforced one-part alkali-activated slag/ceramic binders,” *Ceramics International*, vol. 44, no. 8, pp. 8963–8976, Jun. 2018, doi: 10.1016/j.ceramint.2018.02.097.

[7] F. Slaty, H. Khoury, J. Wastiels, and H. Rahier, “Characterization of alkali activated kaolinitic clay,” *Applied Clay Science*, vol. 75–76, pp. 120–125, May 2013, doi: 10.1016/j.clay.2013.02.005.

[8] J. L. Provis and J. S. J. van Deventer, “RILEM State-of-the-Art Reports State-of-the-Art Report, RILEM TC 224-AAM.” [Online]. Available: http://www.springer.com/series/8780.

[9] L. Mateus, M. do R. Veiga, and J. de Brito, “In situ characterization of rammed earth wall renders,” *International Journal of Architectural Heritage*, vol. 9, no. 4, pp. 430–442, Jan. 2015, doi: 10.1080/15583058.2013.798714.

[10] “76.FT-IR study of early stages of alkali activated materials based on pyroclastic deposits (Mt. Etna, Sicily, Italy) using two different alkaline solutions.”

[11] P. Sudhakara *et al.*, “Studies on Borassus fruit fiber and its composites with Polypropylene,” *Composites Research*, vol. 26, no. 1, pp. 48–53, Feb. 2013, doi: 10.7234/kscm.2013.26.1.48.

[12] P. Sudhakara *et al.*, “Studies on Borassus fruit fiber and its composites with Polypropylene,” *Composites Research*, vol. 26, no. 1, pp. 48–53, Feb. 2013, doi: 10.7234/kscm.2013.26.1.48.

[13] R. Illampas, I. Ioannou, and D. C. Charmpis, “Adobe bricks under compression: Experimental investigation and derivation of stress-strain equation,” *Construction and Building Materials*, vol. 53, pp. 83–90, Feb. 2014, doi: 10.1016/j.conbuildmat.2013.11.103.

[14] N. Srinivasababu, J. S. Kumar, and K. V. K. Reddy, “Manufacturing and Characterization of Long Palmyra Palm/Borassus Flabellifer Petiole Fibre Reinforced Polyester Composites,” *Procedia Technology*, vol. 14, pp. 252–259, 2014, doi: 10.1016/j.protcy.2014.08.033.

[15] P. Duxson, J. L. Provis, G. C. Lukey, S. W. Mallicoat, W. M. Kriven, and J. S. J. van Deventer, “Understanding the relationship between geopolymer composition, microstructure and mechanical properties,” *Colloids and Surfaces A: Physicochemical and Engineering Aspects*, vol. 269, no. 1–3, pp. 47–58, Nov. 2005, doi: 10.1016/j.colsurfa.2005.06.060.

[16] M. Criado, A. Fernández-Jiménez, A. G. de la Torre, M. A. G. Aranda, and A. Palomo, “An XRD study of the effect of the SiO2/Na2O ratio on the alkali activation of fly ash,” *Cement and Concrete Research*, vol. 37, no. 5. pp. 671–679, May 2007, doi: 10.1016/j.cemconres.2007.01.013.

[17] A. Megalingam, M. Kumar, B. Sriram, K. Jeevanantham, and P. Ram Vishnu, “Borassus fruit fiber reinforced composite: A review,” *Materials Today: Proceedings*, Mar. 2020, doi: 10.1016/j.matpr.2020.02.750.

[18] O. Wasfi and M. Imbabi, “Experimental evaluation of the properties of lightweight breathable concretes,” *Advances in Applied Ceramics*, vol. 116, no. 4, pp. 225–229, May 2017, doi: 10.1080/17436753.2017.1288372.

[19] B. Taallah, A. Guettala, S. Guettala, and A. Kriker, “Mechanical properties and hygroscopicity behavior of compressed earth block filled by date palm fibers,” *Construction and Building Materials*, vol. 59, pp. 161–168, Mar. 2014, doi: 10.1016/j.conbuildmat.2014.02.058.

[20] C. A. Fapohunda and D. D. Daramola, “Experimental study of some structural properties of concrete with fine aggregates replaced partially by pulverized termite mound (PTM),” *Journal of King Saud University - Engineering Sciences*, 2019, doi: 10.1016/j.jksues.2019.05.005.

[21] A. W. Bruno, D. Gallipoli, C. Perlot, and J. Mendes, “Effect of very high compaction pressures on the physical and mechanical properties of earthen materials.”

7.0 Chapter Seven: Summary and Concluding remarks

a. Main conclusions in response to the proposed objectives

In response to the proposed objectives in chapter one, the thesis has explicitly presented a clear understanding of the TMS properties (microstructural and macrostructural). It has also examined the effect of selected factors on \ examined properties of the alkali activated TMS. The study evaluated the effect of fiber content on the bulk properties of compacted alkali activated termite mound soil. One of the proposed objectives related to the use of Artificial Intelligence techniques for predictions the performances of the composite was attained. Thus, the study has distinctly succeeded in attaining the proposed objectives. Nevertheless, scaling up to the industrial level the result of this study is a point that will be achieved gradually.

b. Summary and concluding remarks

This thesis investigated and reported the development of sustainable, low cost and eco-friendly construction materials from termite mound soil. The techniques used to design the materials are alkali activation of the TMS with natural fiber reinforcement additionally to the manufacturing process which is the mechanical compaction.

This thesis is composed of seven chapters. Chapter one focused on the introduction of the problems related with the use of conventional construction materials in terms of green gas emission and cost. Resulting in the choice of the earth-based materials as a remediation to the predicted problems. Chapter two emphasized on previous related work carried out by researchers in the construction field in addition to a brief introduction of the TMS as a potential construction material. Finally, concise descriptions of the various methods used during this study were presented in this section. Chapter three presented the results of cement stabilization (5, 10, 15 and 20wt%) on the structural and mechanical properties (compressive/flexural strengths and fracture toughness) of abandoned TMS. From the results obtained in this chapter the stabilized TMS displayed the highest mechanical properties over the non-stabilized TMS. Besides displaying good mechanical properties, locally available at no cost, renewable and an eco-friendly material, the TMS will contribute to lower the cost of housing. Chapter four examined the feasibility of optimizing the mechanical behavior and dimensional stability of TMS through alkaline activation. The raw aluminosilicate TMS was used without any pre-thermal treatment and natural

occurring potash was used as the alkaline activator. Results from this chapter showed that the optimal initial curing temperature was 60℃ for the oven-dry regime at 3wt% activator with optimal mechanical performances. This implies that the alkali stabilized TMS can be used as masonry elements predominantly submitted to compression. Chapter five explored the use of three (3) Machine Learning (ML) techniques to predict the properties of the alkali activated termite mound soil with factors such as activator concentration, Si/Al, initial curing temperature, water absorption, weight and curing regime were used as input parameters due to their significant effect in the compressive strength. All the machine learning models used in this study were successful to predict the compressive strength. Chapter six inspected the mechanical properties of the Borassus fruit natural fiber reinforced one-part alkali activated TMS-based bio-composite. In this chapter the effect of the fiber's reinforcement on the mechanical properties of the bio-composite were assessed. Lastly, Chapter seven presented a brief summary, suggestions for future work and the contribution to knowledge of this investigation. This chapter has highlighted the advantage of TMS and Borassus fruit natural fiber in the construction field for low cost, sustainable and eco-friendly materials.

c. Suggestions for future work

This thesis can be divided into many parts to appraise the variables considered in each part. The first part of this thesis examined the used of TMS with cement as stabilizer. Despite that, there is the need to perform experimental examinations using affordable stabilizer such as agro-waste-based stabilisers. The stabilisers can be produced from local materials available that are considered as waste. These wastes could be improved through some treatments before being used as stabilizer with the TMS. The waste-based stabilisers can be used at various replacement levels.

The second and third part of the thesis explored the use of natural alkali activator for the TMS and predicted its properties through Machine Learning techniques. Still, synthetic alkaline sources can be used to obtain significant results because of their processed properties. The synthetic alkali activator can be used at various percentages under various curing conditions.

The fourth part of the thesis focused on the bio-composite obtained from one part alkali activation of TMS Borassus fruit natural fiber reinforced through compaction process.

Anyway, other manufacturing processes can be used in addition to the compaction. Furthermore, the study didn't investigate the durability of the various materials used in addition to their degradation when submitted to erosion or sunlight, thus these characteristics can be investigated in future.

d. Contribution to knowledge

The following focal points have been highlighted as the major contribution to the existing knowledge:

- Correlation between the microstructure of the TMS and its mechanical properties.
- The feasibility of one-part alkali activation and cement stabilisation as the binding mechanisms of compacted termite mound soil construction materials.
- The study has demonstrated the effect of water exposure on the dimensional stability and integrity of the samples.
- The study has presented the fibers reinforcements' effect on the mechanical properties of the bio-composite.
- The study has explored the use of Borassus fruit natural fiber in the construction field.
- Strengthening and toughness apported by the mechanical compaction of the samples.
- The predictions of compressive strength through machine learning techniques based on factors affecting it.

The repercussions of the results are analyzed for potential applications of the Alkaline Activation techniques as an environmental-friendly approach to obtain renewable and sustainable building materials at low cost with low energy consumption and efficient replicability in most of the regions.